Designing and developing a novel, in vitro model to enable comparative assessment of regenerative endodontic scaffold materials

Thesis submitted in accordance with the requirements of the University of Liverpool for the degree of Doctor of Dental Science in Endodontics by

Nicholas Neil Longridge

21st November 2019

Abstract

Introduction

Regenerative Endodontic Procedures (REPs) are endodontic treatment strategies for managing teeth with immature root apices. Despite well reported clinical outcomes for these procedures, the role and influence of tissue scaffolds within this discipline requires greater investigation. Biological hydrogels are frequently used due to their high water content and analogous chemical composition to dental pulp. Variation in the chemical composition of hydrogels, along with tuneable mechanical characteristics and functionalisation can influence the phenotypic differentiation of local progenitor cells. Greater understanding of the interactions between progenitor cells and tissue scaffolds are required.

Objectives

Design and develop an in vitro model to enable comparative assessment of biological hydrogels for regenerative endodontic applications.

Methodology

Root canal analogues of varying diameters were designed using Materialise©3matic software and additively manufactured within a surrounding model - the 'Culture Button Well' (CBW) - by stereolithography using a Kulzer© caraprint4.0. Medical grade, type-1 bovine collagen (6mg/ml) and gelatin from porcine skin (5% w/v) were used to produce three-dimensional cylindrical hydrogels within the CBW. Triple negative, human adenocarcinoma cells (MDA-MB-231) were fixed and seeded within the hydrogel cylinders and visualised within the CBW using a spinning disc confocal scanning laser microscope (Zeiss spinning disc axio-observer Z1). Invasion assays were attempted using L929 mouse fibroblasts and MDA-MB-231 cells that were seeded independently onto the upper compartment of the CBW, which contained 6mg/ml collagen hydrogels. Dulbecco's modified eagles medium (DMEM) with 10% fetal calf serum and epidermal growth factor were used as chemoattractant within the lower compartment. Chemically cross-linked gelatin cryogel discs were fabricated and L929 mouse fibroblasts were seeded onto the surface and cultured in DMEM for 7 days.

Results

Fixed and pre-seeded cells could be visualised within collagen hydrogels within the CBW without removal of the gels. Cells seeded onto the upper surface of collagen hydrogels demonstrated cell survival and growth at 3 days, but no invasion into the collagen hydrogels

was recorded. Cells seeded onto macroporous gelatin cryogels demonstrated cell migration into the gels at 7 days.

Conclusions

The CBW presents a novel, additively manufactured in vitro model to enable investigation of cell migration in 3D. The CBW can be produced quickly via multiple additive manufacturing techniques. The CBW can be modified to enable hydrogels with different dimensions and characteristics to be comparatively assessed. Macroporous gelatin cryogels demonstrated good cell migration into the scaffolds at 7 days and further investigation of the pore size and interconnectivity of scaffolds on cell migration in REPs are required.

Acknowledgments

Over the last three years, I have gained a huge amount of insight into the trials and tribulations associated with lab-based research. The opportunity to complete this project has been simultaneously rewarding and frustrating in equal measure, but on reflection, it is an experience that I would start again without question. I suppose that statement alone suggests that the last three years have been "successful", in that I don't wish to wash my hands of research and that my curiosity to learn is even more alive.

Research itself has gained a new perspective within my mind. In some ways, I consider it one of the most selfless tasks a clinician can involve themselves in. Who wouldn't want to have outcomes that improve the care of their patients and others worldwide? Whilst at the same time, it remains one of the most selfish aspects of my career, as I indulge my own curiosity in late nights in the labs or in the books – often with marginal gains. Without doubt, I therefore have to start my acknowledgements by thanking my wife, Sarah. Since starting the doctorate project, we've had our first child (Ruby - August 2017) and now our second (Joshua - October 2019), we've moved house, then moved out of our house to refurbish it, and I've also published my first book, which has taken an irresponsible amount of time out of being a father and husband. As always Sarah has supported me and provided for our family and for this I shall be eternally grateful. I'll prospectively thank my daughter, Ruby, so should she ever dust this off my shelf, she'll know that I appreciated her not being too difficult for her mum whilst I was "at work". I hope that the books, papers and journals she frequently discovers in our study produces a curious mind and that the chaotic set-up she sees encourages them both to be more organised.

Professionally, I owe my progression, both clinically and academically, to the support and guidance of Professors Fadi Jarad and Sondos Albadri. Throughout my time at Liverpool they have advised, encouraged and supported me from lowly student to clinical lecturer and I would not be where I am without them. Often occupying the role of life coach over supervisor, they have shown faith in me that I often lacked myself and have frequently picked me up when some of the plates have stopped spinning. This support has been mirrored by my supervisor Professor John Hunt, who encouraged me to dream big in the beginning and remained optimistic throughout my project despite frequent set-backs. I wish John all the best with his own project in Nottingham and I look forward to visiting when complete and hopefully continuing our work together. I'd also like to extend my gratitude to Dr Kevin Hamill who was willing to step in and support my final year in the lab when things really needed a big push. Talking biology with Kevin really helped me to formalise my laboratory goals and helped push the project from an engineering concept into biological

results. Again, I hope to strengthen our research links with Kevin and his group to enable our research output to grow in the future.

Without doubt I would not be submitting this project in its current format without the help and guidance of Dr Lee Troughton and Dr Eve Rogers, both of which gave up immeasurable amounts of laboratory time to support my cell culture and material trials, and didn't laugh too hard or ignore me when I asked silly questions (there were a lot!). I'd like to thank Dr I-Ning Lee for her help with staining protocols and Dr Tobias Zech for his help and advice with the confocal microscopy. Further laboratory assistance was provided by Mr Lee Cooper, Dr Nick Rhodes, Dr Joni Roachdown, Professor Van t' Hof, Dr Gemma Charlesworth and Dr Pallavi Deshpande. I'd like to thank Kevin Mathew from Materialise for his training in CAD/CAM technologies and Associate Professor Hal Duncan for guiding me in the right direction with cell migration assays back in 2017, as well as Professor Callum Youngson for the professional career and CV support whilst I have been otherwise distracted by 3D printing and cell culture. Finally, I'd like to thank the National Institute of Health Research for funding my academic clinical fellowship and offering opportunities for further academic progression.

Table of Contents

List of Figures

List of Tables

List of abbreviations

2D – Two Dimensions

3D – Three Dimensions

3DP – Three Dimensional Printing

AM – Additive manufacturing

BSA – Bovine serum albumin

BM-MSCs – Bone marrow mesenchymal stem cells

CAD/CAM – Computer aided design/Computer aided manufacture

CBCT – Cone beam computed tomography

CBW – Culture button well

CT – Computed tomography

DAMT - Dentine associated mineralised tissue

DAP – Double antibiotic paste

DFSCs – Dental follicle stem cells

DISCs - Dental Implant Stem Cells

DLP – Digital light processing/projection

DMEM – Dulbecco's modified eagles media

DMSO - Dimethyl sulphoxide

DNA – Deoxyribonucleic acid

DPSCs – Dental pulp stem cells

ECM – Extracellular matrix

EDCI - 1-(3-Dimethylaminopropyl)-3-ethylcarbodiimide HCl

EDTA - Ethylene-diamine-tetra-acetic acid

EGF – Epidermal growth factor

ET – Endodontic treatment

FCS – Fetal Calf Serum

FDA – U.S. Food and Drug Administration

FDM – Fused deposition modelling

FEM – Finite element methods

G-CSF – Granulocyte-colony stimulating factor

GFP – Green fluorescent protein

GFSCs - Gingival Fibroblastic Stem Cells

GP – Gutta percha

IACD - Institute of Aging and Chronic Diseases

LOM – Laminated object manufacturing

MJP – Multi-jet printing

MSCs – Mesenchymal stem cells

MRI – Magnetic resonance imaging

MTA – Mineral trioxide aggregate

NFLMP - Non-frozen liquid micro-phase

NHS – N-Hydroxysuccinimide

PARL – Periapical radiolucency

PBS – Phosphate buffered saline

PDC – Pulp dentine complex

PDLSCs – Periodontal ligament stem cells

PDMS - polydimethylsiloxane

PEN - Penicillin

PFA – Paraformaldehyde

PRF – Platelet rich fibrin

PVS - Polyvinylsiloxane

Re-RCT – Root canal retreatment

RCT – Root canal treatment

REPs – Regenerative endodontic procedures

RP – Rapid prototyping

RPM – Revolutions per minute

SCAP – Stem cells of the apical papilla

SDF-1 - Stromal Cell-Derived Factor-1

SFF – Solid freeform fabrication

SHED – Stem cells from human exfoliated deciduous teeth

SLA – Stereolithography apparatus

SLM – Selective laser melting

SLS – Selective laser sintering

STREP - Streptomycin

TAP – Triple antibiotic paste

TGF-β – Transforming growth factor beta

UV – Ultraviolet

VEGF – Vascular endothelial growth factor

1 Introduction

1.1 Trauma and Dental Caries

Trauma and dental caries are two common dental conditions that result in the loss of tooth substance. Frequently, these conditions require remedial restorative treatment to restore function, relieve symptoms and protect the underlying dental pulp. Whilst evidence exists to show a reduction in the prevalence of dental caries (Watt et al., 2013), the most recent UK Adult Dental Health Survey showed that 31% of dentate adults had evidence of coronal or root caries (White et al., 2011). Unfortunately, dental caries is a dynamic and often progressive process that can result in pulpal necrosis, leaving a non-vital, infected root canal space. Dental trauma is also prevalent within the population (Andreasen et al., 1995), especially in children (Forsberg and Tedestam, 1990, Krasner and Rankow, 1995). Whilst the stage of root development can influence the survival of the injured pulp (Ebeleseder et al., 1998), frequently dental trauma results in a significant, acute insult to the pulp that once again may lead to complete or partial pulpal necrosis (Andreasen, 2001). Loss of pulp vitality and vascularity can have significant consequences for patients, including pain, sepsis, tooth fracture and potentially tooth loss. Currently, pulpal necrosis is managed with conventional root canal treatment.

1.2 Conventional Root Canal Treatment

Root canal treatment (RCT), also known as endodontic treatment (ET), is still the treatment of choice for retaining non-vital teeth in which pulpal necrosis has occurred, with high success rates reported widely (de Chevigny et al., 2008, Farzaneh et al., 2004, Salehrabi and Rotstein, 2004, Ng et al., 2011). A systematic review and meta-analysis of over 300,000 teeth showed the prevalence of RCT to be approximately ten percent, which was equivalent to two RCTs per patient (Pak et al., 2012). Of the remaining untreated teeth in this review (271,980), two percent displayed periapical radiolucency (PARL), which is consistent with pulpal necrosis. Alarmingly, up to 78% of RCTs were deemed technically inadequate, suggesting that non-surgical RCT and obturation pose a number of challenges when attempting to achieve an ‘adequate’ technical outcome. Another systematic review by Hamedy et al. highlighted that prevalence of non-surgical RCT and PARL increases with age, with 21% of subjects greater than 65 years of age having had RCT and a further 4% displaying PARL in the absence of RCT (Hamedy et al., 2016).

Gutta percha (GP) remains the gold standard root canal obturation material. However, despite all the proposed benefits of this inert material, bacteria regularly re-infect or re-proliferate within the root canal system with root canal retreatment (Re-RCT) being required. Re-RCT is associated with lower success rates compared to primary RCT (Ng et al., 2011), due to the number of additional challenges and complexities arising from revising the initial RCT. The above research highlights that RCT is a significant issue for patients and health care providers worldwide, as well as being a disease that frequently goes untreated.

1.3 Root Canal Treatment of Teeth with Immature Apices

Obturation of affected teeth with immature apices is challenging to perform due to the large apical diameter and possible reverse taper (Trope, 2010). Traditionally, calcium hydroxide paste (Heithersay, 1975, Vernieks and Messer, 1978) has been used to produce a hard tissue apical barrier in a process referred to as 'apexification' (Rafter, 2005). The high pH of calcium hydroxide makes it antibacterial (El-Meligy and Avery, 2006). The caustic nature of calcium hydroxide produces a mild inflammatory reaction within the apical soft tissues that leads to formation of a mineralised barrier (Rafter, 2005), which then acts as the apical extent of the obturation. More recent methods involve the immediate placement of an apical barrier with a calcium silicate material such as Mineral Trioxide Aggregate (MTA) or Bioceramic putty (e.g. TotalFill Putty®) (Witherspoon and Ham, 2001). Whilst high success rates have been reported for both techniques (Mackie et al., 1988, Witherspoon et al., 2008), the immediate placement of an MTA barrier offers a number of benefits over calcium hydroxide, including; the reduced treatment time and number of appointments, but also the reported improved sealing ability of MTA (Nair et al., 2008). Ultimately, these techniques serve to eradicate infection and improve the prognosis of a compromised tooth, but they do not address the fact that immature teeth are more susceptible to fracture (Kerekes et al., 1980). Furthermore, these techniques do not restore all of the benefits of the natural dental pulp and the pulp-dentine complex (PDC). A more contemporary, biological strategy for managing immature teeth, is to mechanically invoke bleeding into the root canal from the periapical tissues in a process referred to as 'revascularisation', 'revitalisation' or more collectively 'Regenerative Endodontic Procedures'.

1.4 Regenerative Endodontic Procedures and the gaps in the literature

1.4.1 Status Quo and the Rise of Regenerative Endodontic Procedures

Regenerative endodontic procedures (REPs) have emerged as an exciting and progressive discipline within the field of dentistry. Since the concept of revascularisation was introduced

in the 1960's, a huge breadth of research has been directed towards the understanding of pulp biology, the reparative responses to pulp injury, and the potential benefits with its regeneration. Whilst true regeneration of the entire dental pulp has yet to be demonstrated histologically, clinical research continues to support REPs as a potential management strategy for the immature apex. Immature teeth have short roots, thin root canal walls and large apical foramina, which makes them more prone to fracture, more susceptible to mobility through periodontal disease and more difficult to manage with conventional endodontic treatment (Harlamb, 2016, Andreasen et al., 2002). The increases in root length and dentine thickness that have been reported with REPs could improve the prognosis for an immature tooth (Bose et al., 2009, Jeeruphan et al., 2012), which historically would have been subjected to prolonged calcium hydroxide intracanal medicaments in a process called apexification; from which, root fractures were a frequently reported sequelae (Andreasen et al., 2002). As discussed above, a more contemporary management strategy involves the immediate placement of an apical barrier with bioactive calcium silicate cements e.g. MTA. This progression from prolonged apexification with calcium hydroxide to immediate, root-end barrier apexification with bioactive cements served to dramatically reduce the treatment time for young patients. Whilst the barrier method is associated with favourable clinical outcomes, it can be a difficult procedure to perform and achieve optimal technical outcomes due to large apical foramina, which can present with reverse taper anatomy. Furthermore, neither technique described above addresses the issues of short and thin root canal walls, which becomes increasingly relevant during the earliest stages of root development. Patients presenting at these early stages often display extremely short and thin root canal walls whereby extraction and prosthetic replacement may be the only viable management approach. For these reasons, researchers have continued to search for more biological treatment strategies aimed at increasing root length and wall thickness, whilst serving to manage any concomitant infection. Maintenance of pulp vascularity and innervation would also serve further protective functions through: the re-introduction of a positive pulpal pressure, which can reduce desiccation of root dentine and impede bacterial penetration; the presence of pulpal stromal cells and progenitor cells, that deposit tertiary dentine in response to insult; and the reintroduction of pulpal proprioception, a controversial phenomenon that may protect against the effects of excessive occlusal forces.

1.4.2 Pulp regeneration in mature teeth

A logical extrapolation of the successful clinical outcomes associated with immature apices, is to consider the potential for pulp regeneration in mature apices. Mature apices, being fully developed, do not require additional increases in root length and width to improve their long term prognosis. However, the presence of vital pulp tissue and the associated pulpal defence

mechanisms, would confer a number of potentially beneficial characteristics. As a future goal in pulp regeneration, the replacement of the conventional obturation material, GP, with a bioactive alternative serves as a major driving force in this rapidly advancing research field. The challenges associated with failed endodontic treatment and poorly obturated teeth suggest that biological alternatives are a desirable and realistic strategy for improving the oral health of patients and avoiding tooth loss. Furthermore, in broader terms, the tooth and the dental pulp serve as an extremely exciting model for tissue engineering, as the protective outer layers of enamel and dentine reduce the required mechanical characteristics of the biomaterial and as teeth are also removable, ethics considered, an ex vivo model with histological sampling may be feasible.

Despite possible benefits of this strategy, there remains a great dearth of knowledge and research into the presence and role of progenitor cell niches at the apex of mature teeth. Stem cells of the apical papilla (SCAP) are frequently discussed in the literature as a viable stem cell source for cell homing strategies. However, it is not entirely clear what progenitor cells remain following apexogenesis and whether these niches are affected by pulpal necrosis, bacterial invasion and aging. Evidence has emerged to show different histological outcomes when REPs have been performed in partially vital teeth compared with non-vital cases (Shimizu et al., 2012, Shimizu et al., 2013). It is therefore clear that an in vitro model for pulp regeneration could provide a great amount of information regarding how stem cells interact with extracellular matrix (ECM) derivatives and their substitutes.

1.4.3 Tooth Loss and Quality of Life

It is well reported that tooth loss can have psychosocial consequences that have been shown to influence quality of life (Gerritsen et al., 2010). A reduction in chewing efficiency, speech changes and aesthetic concerns are some of the more common issues associated with tooth loss. Dental caries and traumatic dental injuries are common in children and young adults. Therefore, research into REPs stands to benefit a large cohort of patients for a long duration. Health economists have previously attempted to quantify the costs of different restorative strategies for teeth with pulpal necrosis and again tooth preservation through conventional endodontic treatment appears to have distinct cost benefits over extraction and prosthetic replacement. It stands to reason that regenerative treatments that could delay endodontic treatment and recover some inherent pulpal defence would represent good value for money for health services worldwide.

1.4.4 Gaps in the literature

There remains a number of research areas within REPs that would benefit from an optimised and validated in vitro model. Firstly, and most fundamentally, cancer studies would suggest that there is a maximum distance away from a capillary that a mammalian cell can survive. This distance of 100-200μm has been attributed to the maximum diffusion distance of oxygen and is one of the contributing factors in the central necrosis of tumours. This distance is obviously insufficient for pulp regeneration. Beyond this distance, new vessels are required and the processes of angiogenesis and vasculogenesis are necessary (Carmeliet and Jain, 2000). A wealth of literature has discussed a wide range of pro-angiogenic cues as well as the complex interplay between cells, ECM and growth factors (Saberianpour et al., 2018). Whilst this interplay has frequently been considered as a chemical relationship between cells and their growth factors, the mechanical characteristics of the ECM has also been shown to influence cell phenotype (Guilak et al., 2009, Wozniak and Keely, 2005) and in line with the great investment in tissue engineering strategies, understanding these interactions more thoroughly would serve to benefit pulp regeneration and the wider research community.

An in vitro model for REPs would therefore enable greater research into:

- Cell migration into tissue scaffolds including the speed of migration, cell-matrix interactions and cytokine expression.
- Types of biomaterials including the influence of their mechanical properties and topography on cell behaviour.
- Tissue scaffold porosity and porosimetry.
- Effects of cytokines on the migratory behaviour of cells including growth factor gradients.
- Comparative assessment of cell types and co-cultures on cell migration and angiogenesis.
- The influence of scaffold/apical diameter on cell migration.

1.5 Aims and Objectives

The primary aim of this project is to produce an in vitro model for studying cell migration and cell-ECM interactions in tissue scaffolds designed for regenerative endodontic procedures.

This aim was subdivided into four primary objectives:

1. Appraise the literature relating to tissue scaffolds in regenerative endodontic procedures,
2. Design and additively manufacture a series of root canal analogues for in vitro use,
3. Develop a range of biocompatible tissue scaffolds for use in the model,
4. Validate the model design using the tissue scaffolds developed,

Secondary objectives for this study included:

1. Investigate the effect of different growth factor profiles on the speed and depth of cell migration.
2. Investigate different tissue scaffold architecture e.g. porosity and pore size on speed and extent of cell migration.
3. Investigate the effects of altering the mechanical properties of the tissue scaffolds on progenitor cell phenotype.
4. Investigate the effects of scaffold functionalisation on cell migration.

2 Literature Review

2.1 Dentine and the Pulp-Dentine Complex

Dentine is an innervated, mineralised collagen network formed and supported by numerous pulpal cells, most notably odontoblast cells and their processes. Dentine is intricately linked with the underlying dental pulp and together they are commonly referred to as the Pulp-Dentine Complex (PDC). Whilst these two tissues differ in composition, a synergistic relationship exists whereby dentine protects the pulp and the pulp supports dentine. Pashley discussed in detail the 'Dynamics of the Pulp-Dentin Complex' (Pashley, 1996). The organic component makes up 30% of dentine's volume. It is predominantly type I collagen supported by a small percentage of non-collagenous proteins, proteoglycans and phosphoproteins, which induce and direct mineralisation.

The pulpal microcirculation provides oxygen and nutrients to the cells of the PDC and it has been shown to confer protective benefits to the tooth. This includes a high hydrostatic tissue pressure which provides an outward flow of fluid from the dentinal tubules that adds resistance to the passage of pathogens and noxious substances from the external environment into the dental pulp (Nagaoka et al., 1995). This hydrostatic tissue pressure is only maintained by a functional PDC that is lost when the biological dental pulp is replaced with GP i.e. following conventional RCT. Furthermore, preservation of pulpal tissue has been shown to increase the damping ratio of premolar teeth when compared to non-vital and endodontically treated teeth (Ou et al., 2009). This provides greater dissipation of stress during function, which may provide additional resistance to fracture. Fundamentally, the PDC can enable regenerative and reparative processes to occur in response to insults such as caries and trauma, which are key protective events referred to as 'tertiary dentinogenesis'(Sloan, 2015). This can include accelerated deposition of mineral by odontoblasts (reactionary dentine) and recruitment of local progenitor cells from pulpal niches (reparative dentine)(Goldberg et al., 2011, Smith et al., 1995). When pulpal necrosis occurs, these protective processes are lost and there is a greater risk of tooth loss, which is demonstrated by the improved success rates of pulpotomy (partial removal of inflamed pulp tissue) over pulpectomy (complete removal of all pulp tissue) (Taha and Abdelkhader, 2018, Ng et al., 2008). Despite the benefits of a functional PDC being widely acknowledged, the preservation of the natural pulp is frequently unachievable. For this reason, considerable research is being conducted into the production of biological substitutes for the pulp with subsequent regeneration of the PDC being the ultimate, desirable aim. These research topics and treatment strategies are collectively referred to as 'Regenerative Endodontic Procedures' (Diogenes et al., 2013) and can be considered to be a branch of tissue engineering.

2.2 Regenerative Endodontic Procedures

2.2.1 History of REPs

Regenerative Endodontic Procedures (REPs), sometimes referred to as revascularisation or revitalisation, are alternative treatment strategies to conventional RCT that aim to regenerate the dental pulp and PDC. They have been defined as 'biologically based procedures designed to replace damaged structures, including dentin and root structures, as well as cells of the pulp-dentin complex' (Murray et al., 2007). Research conducted over forty years ago identified that periapical stimulation of blood flow into previously devascularised root canal systems led to connective tissue ingrowth (Nygaard-Ostby and Hjortdal, 1971) and since this time countless studies have looked at the various procedural steps involved in regenerating the dental pulp (Albuquerque et al., 2014, Diogenes et al., 2013, Murray et al., 2007, Iwaya et al., 2001). REPs have been shown to support continued root development resulting in apical closure, increased root length and root thickness (Thibodeau et al., 2007, Wang et al., 2010). Histologically, these tissues have been identified in both animal and human studies, as mineralised tissue closely resembling cementum and bone (Wang et al., 2010, Shimizu et al., 2013, Yamauchi et al., 2011a, Yamauchi et al., 2011b), with pulp-like tissue also identified (Shimizu et al., 2012, Albuquerque et al., 2014). The absence of apical infection and the presence of apical papilla or vital apical pulp tissue may be important prognostic factors in these cases (Shimizu et al., 2012, Shimizu et al., 2013).

Incomplete root development remains a significant prognostic factor in trauma management with greater risk of pulpal necrosis in teeth with mature root apices (Andreasen and Pedersen, 1985). The diameter of the apical foramen is therefore considered to be an important prognostic factor for success of REPs, with research from the 1980s demonstrating that spontaneous revascularisation of avulsed incisors only occurred when the apical diameter exceeded 1mm (Kling et al., 1986). Immature apices were radiographically measured between 0.5mm and 5mm within this study.

2.2.2 Requirements for REPs

As with most tissue engineering research, REPs focus on a number of key issues briefly summarised below (Langer and Vacanti, 1993):

1. Mesenchymal Stem Cells.
2. Tissue Scaffolds.
3. Growth factors e.g. Stromal Cell-Derived Factor-1 (SDF-1).

Furthermore, REPs have additional considerations due to the role of pathogens in the demise of the dental pulp in an enclosed microenvironment:

4. Disinfection/Preparation of the Root Canal System.

2.2.3 Cell homing vs cell transplantation

As progenitor cells are required for tissue regeneration, the application or recruitment of these progenitor cells relies upon one of two strategies. The first strategy, cell homing, involves the recruitment of progenitor cells from local stem cell niches. Evidence-based clinical protocols recommended by both the American Association of Endodontists (Diogenes et al., 2013) and European Society of Endodontics (Galler et al., 2016) promote the use of the cell homing strategy. In comparison, cell transplantation techniques extract progenitor cells from alternative sources, such as extracted or stored deciduous teeth, and transplant the cells into the desired site or scaffold. Whilst multiple sources of progenitor cells in the oral tissues have been reported, the potential differentiation profile of each will vary. As such, the resultant tissue profiles that may be possible are likely to be directly linked to the progenitor cell source (Sharpe, 2016). As cell transplantation protocols require an additional source, they have been less widely researched when compared to cell homing strategies, which are already being utilised in current clinical procedures and are therefore less confined by ethical considerations. As such, there continues to be great interest in cell homing strategies, which rely upon appropriate chemical cues to orchestrate cell migration. Of particular interest is the release of dentine matrix components (DMCs) that are sequestered in dentine during tooth development or extracted and added to bioactive tissue scaffolds (Duncan et al., 2018).

2.2.4 Disinfection of the root canal system

The volume of literature detailing the effect of endodontic irrigants and medicaments upon pathogens, dentine and local progenitor cells has been increasing (Trevino et al., 2011, Galler et al., 2011, Ruparel et al., 2012, Essner et al., 2011, Althumairy et al., 2014, Chuensombat et al., 2013, Yassen et al., 2013). This area remains contentious due to the wide range of treatment protocols utilised in published case reports that have reported successful outcomes (Diogenes et al., 2013). However, it has been shown that the traditional use of double or triple antibiotic pastes (DAP/TAP) can significantly affect the cell viability of DPSCs and SCAP (Ruparel et al., 2012). Furthermore, use of TAP has been associated with tooth discolouration (Miller et al., 2012), difficult removal from the canal (Berkhoff et al., 2014) and potential development of antibiotic resistance. Interestingly, calcium hydroxide and metronidazole have displayed fairly positive results in a number of these

studies with regards to stem cell toxicity (Althumairy et al., 2014, Chuensombat et al., 2013, Ruparel et al., 2012). As a result, the European Society of Endodontology position statement on revitalisation procedures recommends the use of sodium hypochlorite irrigation (1-3%) and calcium hydroxide intracanal medicament (Galler et al., 2016). Further research into this area will consolidate the international opinion regarding disinfection protocol. The conventional approach in REPs classifies disinfection of the root canal system as stage one of a two-stage procedure. Stage two involves stimulation of bleeding into the root canal from the periapical tissues with or without the use of an appropriate tissue scaffold. As discussed earlier, the presence of bacteria within the apical tissues is likely to play an important role in the potential for regeneration (Shimizu et al., 2012, Shimizu et al., 2013) and as such the disinfection of teeth where pulpal necrosis has occurred is likely to remain a popular research topic.

2.2.5 Growth factors/Morphogens

The role of growth factors in the recruitment of cells to the site of injury can be demonstrated in the cellular processes associated with wound healing (Velnar et al., 2009). At present, the exact reparative or regenerative processes associated with cell homing in REPs are not fully understood. However, as with wound healing, it is well accepted that the co-ordinated release of growth factors by cells or ECM can influence the resultant cell recruitment and differentiation, which is vital if true pulpal regeneration is to be achieved. Growth factors are sequestered within dentine during tooth development (Duncan et al., 2018). Under pathological circumstances, such as dental caries, demineralisation releases potent chemotactic agents, such as transforming growth factor beta (TGF-β), platelet derived growth factor (PDGF) and vascular endothelial growth factor (VEGF), that contribute to the reparative and reactionary processes of tertiary dentinogenesis (Galler et al., 2011, Smith et al., 1995). The use of ethylene-diamine-tetra-acetic acid (EDTA) as a dentine conditioner during REPs has been studied, with research showing development of dentine associated mineralised tissue (DAMT) (Yamauchi et al., 2011b). Interestingly, hair-like projections from the regenerated DAMT into the demineralised dentine were only evident when EDTA was utilised. Alongside the growth factors above, a wide array of additional cytokines and growth factors deemed ‘mobilisation’ factors have also been reported, due to their strong chemotactic effects including stromal-cell derived factor-1 (SDF-1) and granulocyte-colony stimulating factor (G-CSF)(Duncan et al., 2018), some of which have also been incorporated into tissue scaffolds in current pulp regeneration studies (Albuquerque et al., 2014). Studying the potential sources of these morphogens and the roles they play in cell homing remains an important topic for REPs. Furthermore, the ability to design tissue scaffolds that release cytokines upon degradation, or extract growth factors from dentine is an additional

facet to the complex interactions between the tissue engineering triad of stem cells, morphogens and tissue scaffolds.

2.3 Adult Progenitor cells of the head and neck

2.3.1 Stem/progenitor cell niches and markers

Mesenchymal stem cells (MSCs) like all stem cells are capable of self-renewal and multi-lineage differentiation. They are postnatal stem cells, which despite having less plasticity than embryonic stem cells, are less confined by legal and ethical issues (Murray et al., 2007). MSCs are multi-potent, neural crest derived cells, that can differentiate into the skeletal structures of the body including bone and connective tissue (Caplan, 1991). A number of sources have been identified including a large number in the tissues of the head and neck (Diogenes et al., 2013, Surendran and Sivamurthy, 2015, Liu et al., 2006, Huang et al., 2009, Sharpe, 2016):

- Stem Cells of the Apical Papilla (SCAP).
- Dental Pulp Stem Cells (DPSCs).
- Periodontal Ligament Stem Cells (PDLSCs).
- Stem Cells from Human Exfoliated Deciduous Teeth (SHEDs).
- Dental Follicle Stem Cells (DFSCs).
- Gingival Fibroblastic Stem Cells (GFSCs).
- Dental Implant Stem Cells (DISCs).

These cells are present in each individual and as such can be harvested to produce autologous stem cell populations that can be used for tissue engineering within the same individual with fewer legal, ethical and immunological contra-indications (Murray et al., 2007). Due to the range of cells isolated from different sources, the document ‘minimal criteria for defining multi-potent mesenchymal stem cells’ was published in 2006 (Dominici et al., 2006). According to this criteria, MSCs should:

- Adhere to plastic.
- Express specific surface antigens – CD105, CD73, CD90.
- Tri-lineage in vitro differentiation – Osteoblasts, Adipocytes, Chondroblasts.

The method of isolation has also been identified as an important prognostic factor in regenerative potential (Nakayama et al., 2017) and a large amount remains unknown. Isolating specific MSCs populations can be challenging due to the range of cell markers that are common across stem cell populations. Kawashima discussed ‘candidate markers of DPSCs’ in great detail (Kawashima, 2012). In this paper, a range of common mesenchymal

cell markers were discussed, including STRO-1, CD29, CD73, CD105, CD146. Specific stem cell markers for haematopoietic progenitors are also highlighted including CD34 and CD117. Strategies for isolating DPSCs may include: the dental pulp explant method; antibody-conjugation with cell surface markers detailed above; isolation of dental pulp cells with the highest growth rate; and isolation of cells with the ability to remove fluorescent binding dye through membrane efflux pumps (Kawashima, 2012, Huang et al., 2006).

2.3.2 Dental Pulp Stem Cells and Stem Cells of the Apical Papilla

The specific source of adult progenitor cells has been the source of great interest in REPs. A wide range of MSCs have been identified in the tissues of the head and neck (Sharpe, 2016), many of which are outlined above. Of most significance to REPs are stem cells of the apical papilla (SCAP) and dental pulp stem cells (DPSCs), which can be recruited into the root canal by cell homing strategies. Whilst Bone-marrow mesenchymal stem cells (BMMSCs) and MSCs from the head and neck share similar immunophenotypes (Gronthos et al., 2000), the exact relationship between different populations of MSCs remains unclear. DPSCs and SCAP have shown high levels of dentinogenic/osteogenic differentiation as well as potential neuronal differentiation, but lower adipogenic differentiation (Gronthos et al., 2000). In contrast, BMMSCs have shown osteogenic and adipogenic differentiation (Gronthos et al., 2000), but dentinogenic differentiation has not been identified (Huang et al., 2008). This supports the use of adult progenitor cells that reside most closely to the root canal, with DPSCs found within the central pulp of vital teeth shown to differentiate into both odontoblasts and also endothelial cells, making them ideal cells for pulp tissue regeneration (Cavalcanti et al., 2013). It is becoming apparent that different populations and side-populations of stem cells show greater potential for REPs. Of particular note is the use of side-population DPSCs utilised by Nakashima and Iohara, which includes CD105+ and CD31-/CD146- stem cells (Nakashima and Iohara, 2014). Furthermore, the exact source of DPSCs following tooth injury remains an area of research, with both pericytes and glial cells reported as potential precursors of DPSCs and their post-differentiation cells, odontoblasts (Sharpe, 2016).

2.4 Tissue Scaffolds

2.4.1 Broad classification of tissue scaffolds

Biomaterials have been defined by the European Society of Biomaterials as ‘a material intended to interface with biological systems to evaluate, treat, augment, or replace any tissue, organ or function of the body’ (O'Brien, 2011). With this in mind, tissue scaffolds are biomaterials used to replicate ECM of healthy tissues that have subsequently been damaged

by trauma or disease. Tissue scaffolds, sometimes referred to as cellular scaffolds, can be natural polymers (e.g. collagen), synthetic polymers (e.g. poly-lactic acid), ceramics (e.g. hydroxyapatite) or a composite of two or more materials (Ricapito et al., 2016, O'Brien, 2011). These materials are required for cell attachment, migration and proliferation, but should also enable metabolite and nutrient exchange before biodegrading appropriately as cells produce natural ECM for support (Dhandayuthapani et al., 2011). For this reason, it is essential that tissue scaffolds are porous structures with well interconnected pores (Loh and Choong, 2013). In early animal models, non-porous scaffolds did not encourage osteogenesis (Kuboki et al., 1998) and implant studies have shown that porous scaffolds may provide mechanical benefits over solid surfaces due to interlocking with natural tissues (Story et al., 1998).

2.4.2 Scaffold properties, production and functionalisation

In their simplest form, a tissue scaffold can be visualised as a series of vacant pores within a polymeric structure analogous to a piece of sponge or honeycomb. Tissue scaffolds can be fabricated via a number of different strategies including conventional techniques such as porogen leaching, cryogelation, gas foaming and emulsion freezing (Bencherif et al., 2013). More recent advances in additive manufacturing and extrusion/inkjet technology has provided the foundations for computer aided manufacturing processes such as fused deposition modelling (FDM), stereolithography (SLA), selective laser sintering (SLS) and bioprinting (Woodfield et al., 2004, Duan et al., 2010, Derby, 2012, Vanderburgh et al., 2017). Each fabrication technique will significantly influence the resultant architecture and mechanical structure of the tissue scaffolds including pore size, pore shape, pore volume and interconnectivity, which in turn may have significant effects upon cell behaviour and tissue development (Murphy and O'Brien, 2010, Hollister, 2005, Druecke et al., 2004), especially where vascularised tissues are required (Mehdizadeh et al., 2013, Novosel et al., 2011). Whilst greater porosity may allow for greater cell migration and nutrient exchange, these advantages come at the expense of reduced cell attachment and mechanical rigidity (Murphy and O'Brien, 2010, O'Brien et al., 2007). Therefore, a balance must be achieved between the need for cell space to migrate and ligands for cell attachment. This has driven the investigation into cell and tissue specific scaffold design, with optimisation of the scaffold required for each specific biological function (Karageorgiou and Kaplan, 2005, Mehdizadeh et al., 2013). Scaffolds that display pore sizes of less than 10 microns are considered microporous, whilst those with pore sizes greater than 10 microns are considered macroporous.

Using conventional methods like porogen leaching, the pore size can be controlled through careful sieving of the porogen i.e. salt particles of specified diameter can be pre-measured and used (and removed). However, precise control over the pore size is difficult and a pore size range is normally achieved. By comparison, additive manufacturing strategies may precisely recreate exact pore shapes and sizes, but are restricted by the range of polymeric materials available and by the technology with regard to the smallest pore dimensions achievable (Derby, 2012). Interconnectivity, refers to the degree of communication between subsequent pores and is a fundamental design consideration for tissue engineering, where cell migration and nutrient exchange is pivotal (Murphy et al., 2010). With this concept in mind, cryogelation produces highly interconnected pores due to the contact of adjacent ice crystals during freezing. In contrast, gas foaming involves the addition of gas bubbles to the polymer, which has been associated with fewer interconnected pores, as the thin polymeric lining of each bubble can sometimes remain.

Aside from the influence of various production methods on scaffold architecture, tissue scaffolds can also be pre-seeded with cells or functionalised with growth factors in an attempt to enhance the regenerative capacity of the scaffold. The quest for engineered vascularised tissues has seen a large amount of interest in the incorporation of pro-angiogenic growth factors such as VEGF (Jain et al., 2005) and TGF-β1 (Piva et al., 2014, Lovett et al., 2009, Rouwkema et al., 2008). Functionalisation of scaffolds can also refer to the addition of enzymes or molecules that can increase the binding sites for cells or influence the physical behaviour of the scaffold to make them temperature or pH responsive.

2.4.3 Extracellular matrix and its constituents

ECM represents the non-cellular component of tissues. It is a dynamic structure which supports and modulates cellular activity and is constantly modified and recycled by a number of enzymatic and non-enzymatic processes (Frantz et al., 2010). Whilst collagens are the predominant fibrous proteins (Gordon and Hahn, 2010), the exact composition of ECM is tissue and site specific. Broadly speaking, ECM can be subdivided into interstitial matrix and basement membrane, the latter of which could be considered a specialised ECM structure that predominantly contains collagen type IV and laminin (LeBleu et al., 2007). In contrast, collagen type I is the most abundant interstitial protein. However, the exact composition of each component is varied.

In the context of regenerative endodontic procedures, tissue scaffolds should closely resemble the ECM of the dental pulp, a vascular, loose connective tissue composed primarily of collagen (Type I and III) and ground substance (e.g. glycosaminoglycan) (Goldberg and Smith, 2004). Pulpal necrosis, which can occur in response to dental caries

and trauma, results in the demise of this vascular connective tissue and is the target tissue for regeneration in REPs. It is therefore prudent to investigate possible biomaterials for REPs that can closely resemble dental pulp in terms of topographical architecture, mechanical properties and bioactivity (Chan and Leong, 2008). These materials should be non-cytotoxic with low immunogenicity and should be appropriately biodegradable to allow replacement with endogenously synthesised ECM. It is therefore no surprise that many natural polymers such as collagen, hyaluronic acid, alginate and chitosan have been investigated (Chrepa et al., 2017).

ECM composition has been shown to influence cell behaviour, but the full intricacies of cell-ECM interactions are not fully understood and are currently an area being researched widely (Guilak et al., 2009). Whilst the presence of various chemical molecules within the ECM is likely to have a strong influence upon cell viability and activity, it is also now more widely recognised that the physical composition of the ECM itself will also modulate the attachment and phenotypic differentiation of cells (Guilak et al., 2009, Pek et al., 2010, Engler et al., 2006). For example, cell behaviour has been shown to vary between 2 and 3-dimensional cultures and cell differentiation has been altered by the stiffness of the biomaterial being used (Kisiday et al., 2002, Pek et al., 2010). For this reason, there has been a great amount of interest in tools that enable the study of cell behaviour in 3-dimensions (3D).

2.4.4 Tissue scaffolds in REPs

As previously discussed, the PDC is a biphasic connective tissue with mineralised dentine supported by a central core of unmineralised dental pulp. Whilst there are a number of distinct differences between the two tissue types in terms of cellular content and ECM composition (Goldberg and Smith, 2004), type I collagen is the predominant protein. Natural polymers like collagen are therefore a popular choice of tissue scaffold in REPs. Despite providing the necessary supporting structure for cell attachment and growth, tissue scaffolds alone are inadequate for regenerative processes to occur. For complete pulp regeneration it is clear that the predominant cells of the dental pulp will be required, namely odontoblasts and fibroblasts. These cells can be pre-seeded or encapsulated within the tissue scaffold, or alternatively, progenitor cells or cell precursors that display multi-potency may be recruited into the root canal by cell homing strategies. Whilst a large number of studies have reported the application of tissue scaffolds into root canal systems, fibrin (blood clot) scaffolds remain the most widely used and are produced by deliberate mechanical trauma to the periapical tissues. The fibrin scaffold that results represents a reservoir of cytokines and ECM-proteins that can recruit cells and determine their fate in a process analogous to

general wound healing. Connective tissue in-growth of bone and cementum have been reported along with odontoblast-like cells (Shimizu et al., 2013, Shimizu et al., 2012), but true regeneration is yet to be demonstrated. Where exogenous scaffolds are used, their bioactivity and influence over cell recruitment is likely to be fundamental to success.

Broadly speaking, tissue scaffolds in REPs can be categorised as injectable or pre-fabricated/casted (Piva et al., 2014). The injectable materials are extremely convenient for endodontic practice, which frequently involves applications of irrigants and medicaments through hollow bore, small gauge needles. The most compelling attribute for injectable material technology relates to the ability of these materials to conform to the often highly irregular anatomy of the root canal system with seemingly little mechanical preparation required. However, the injectable nature of materials can restrict the control over the internal-architecture of the resultant tissue scaffold when compared with casted scaffolds, which can be produced based on pre-determined structural requirements e.g. pore size. In contrast, pre-fabricated scaffolds can be produced using conventional fabrication techniques or additive manufacturing that enables more precise control over porosity and interconnectivity. These conventional "casting" techniques, which were outlined earlier include porogen leaching, gas foaming and cryogelation, in which polymeric, macroporous materials are produced with fairly precise architecture. In the case of cryogelation, freezing of the biomaterial to sub-zero temperatures induces crystal formation of the solvent (commonly water), which is subsequently sublimated to leave the porous structure of the polymerised solute.

Alternatively, additive manufacturing (AM), a branch of engineering that is rapidly expanding into the medical sector can be used to fabricate porous tissue scaffolds. The combination of AM strategies with three-dimensional imaging techniques such as cone-beam computed tomography (CBCT) and magnetic resonance imaging (MRI), enables computer-aided segmentation and design tools to produce bespoke, custom-made medical devices from a wide range of materials. Titanium or Titanium/Zirconium Implants used in orthopaedic and cranio-facial applications have historically lead the field in this discipline. However, exciting advances are being made in extrusion technology-based systems such as fused deposition modelling (FDM) and electrospinning; photon-polymerisation techniques such as stereolithography apparatus (SLA) and digital light processing (DLP); and bioprinting technologies including inkjet printing and microextrusion.

Despite these advances, the search for biomimetic ECM substitutes in pulp regeneration has focussed research on more conventional materials (Albuquerque et al., 2014), such as ECM-derivatives like collagen, decellularized pulp (Alqahtani et al., 2018), platelet-rich fibrin

(PRF) (Shivashankar et al., 2012) and combination-scaffolds (Nosrat et al., 2019, Huang et al., 2018). The wide adoption of REPs in clinical practice has enabled a meta-analysis comparing the use of blood clot and platelet concentrates such as PRF, which reported improved outcomes for apical closure at 12 months when PRF was used (Murray, 2018). This suggests that the quest for improved bioactive materials for use in REPs is likely to lead to improvements in outcomes over conventional blood clot revascularisation techniques currently employed. In this scenario, these platelet concentrates that are centrifuged from autologous blood samples, represent a growth factor-laden fibrin clot that has demonstrated good wound healing properties through its chemotactic and angiogenic properties (Naik et al., 2013, Borie et al., 2015). Alternative materials have also been investigated that would not require venepuncture. The majority of these alternative materials are synthetic and ECM-derived tissue scaffolds that represent a group of hydrophilic monomers referred to as 'Hydrogels'.

2.4.5 Hydrogels in Regenerative Endodontic Procedures

The use of numerous biological and biohybrid hydrogels in REPs was documented by Alberqurque et al. (2014) The vast number of hydrogels being studied reflects the rapidly expanding field of research into hydrogels for medical and dental applications (Van Vlierberghe et al., 2011). Peppas et al. defined hydrogels as, "three dimensional, hydrophilic, polymeric networks capable of imbibing large amounts of water or biological fluids" (Peppas et al., 2000). The injectable nature of this group makes them desirable in endodontics, as they can be stored in syringes and applied clinically in the same manner as general endodontic irrigants and medicaments (Murray et al., 2007). In their basic form, these natural materials are considered nanoporous, with a high water content (70-90%) that enables nutrient exchange by diffusion (Ikada, 2006). As a result of their high water content, single network hydrogels are weak with poor mechanical characteristics. As pulp regeneration occurs within the confines of the highly mineralised enamel and dentine, the lack of mechanical resilience may have little effect upon the performance of the hydrogel and may in fact offer distinct advantages due to their ease of application. However, in many tissue engineering applications, mechanical characteristics are fundamental to success, and as such combinations of hydrogel networks or hydrogels produced with multiple cross-linking methods are also widely reported (Ma et al., 2016, Li et al., 2017, Lin et al., 2015).The polymeric structure of hydrogels remain insoluble due to the production of chemical crosslinks or due to physical entanglement of polymeric fibres. Hydrogen bonding and van der Waals interactions have also been identified and discussed in greater detail elsewhere (Peppas et al., 2000, Van Vlierberghe et al., 2011).

The type of crosslinking, physical or chemical, can be used to classify hydrogels, along with numerous other strategies including their chemical structure e.g. peptide-based or their preparation method e.g. self-assembling/pH/temperature (Jonker et al., 2012). Polysaccharide and protein (peptide) hydrogels that have been discussed in a number of detailed reviews (Ricapito et al., 2016, Van Vlierberghe et al., 2011, Jonker et al., 2012), are composed of molecules present in homeostatic, metabolic processes that accounts for their low immunogenicity. In their basic form, protein hydrogels are fabricated from ECM derivatives such as collagen, gelatin and elastin. However, various synthetic peptide and hybrid peptide hydrogels have also been produced and reported in the literature (Jonker et al., 2012, Ricapito et al., 2016). These include self-assembling peptides that have been investigated both with and without progenitor cell encapsulation. Puramatrix™, a commercially available self-assembling peptide, is one such material widely researched that has a high water content (99%) and a fibrous structure with nanopores of 50-200nm scale.

2.4.5.1 Collagen and Gelatin

Collagenous proteins are the most abundant proteins in the human body. It is also the most common protein in the dental pulp, of which type I and III are most frequently encountered (Linde, 1985). Collagen is therefore a popular choice of biomimetic tissue scaffold for cell culture applications (Kreger et al., 2010) and REPs (Albuquerque et al., 2014, Nakashima and Iohara, 2014). Gelatin is a biopolymer produced from collagen. Hydrolytic degradation of collagen produces a polymer that is used in a wide range of pharmaceutical and food applications. As a biological polymer derived from mammalian organisms, it has been widely reported as a suitable biomaterial candidate in tissue engineering applications. Gelatin based hydrogels are highly biocompatible (Lai, 2010, Sung et al., 1999, Ulubayram et al., 2002, Yang et al., 2018) and can be easily modified to influence mechanical structure and biodegradability (Jaipan et al., 2017, Van Vlierberghe, 2016). Chemical cross-linking is required to avoid dissolution in physiological aqueous conditions at 37°C, due to the sol-gel transition temperature of approximately 30°C. A number of potential cross-linking agents have been identified (Liang et al., 2004, Sung et al., 1999, Van Vlierberghe, 2016), which are predominantly water-soluble. Carbodiimides are one chemical group shown to activate carboxylic acid residues on gelatin, which are subsequently attacked by amine groups to form short-range intermolecular crosslinks (Cammarata et al., 2015, Liang et al., 2004).

2.4.6 Tissue scaffold challenges in REPs

Whilst the clinical benefits of REPs are clear, the biological reparative/regenerative processes underlying them are not. Furthermore, whilst biomaterials may serve to improve the outcome or predictability of regenerative procedures, the requirements for any potential

tissue scaffolds are not understood. Whilst injectable technology seems practically and anatomically appropriate, little is available in the literature to compare one material from the next. Furthermore, understanding the effect of pore size and mechanical structure of the scaffold on the resultant cell phenotypes requires investigation. Research in the field of cancer invasion would suggest that hydrogels with pore sizes in the nano or micro scale will require enzymatic degradation for cells to be able to invade, which may restrict the speed of cell recruitment (Paul et al., 2017). In comparison, clinical studies using PRF have reported favourable outcomes for platelet concentrates that display internal pore sizes of less than 1µm when fresh (Li et al., 2014). However, it must be stressed that clinical success is not synonymous with regeneration. The rate of new biological and bio-hybrid material development further serves to complicate this area, as basic research into the material-cell interactions can take several years to perform. Further material considerations such as elastic modulus and scaffold considerations such as porosity and interconnectivity require greater investigation to examine the effects of these parameters on a range of factors including cell migration, cell phenotype differentiation and ECM-production. Tissue/application specific research of the above factors is necessary to understand the requirements for pulpal regeneration.

2.5 Progenitor Cell migration, proliferation and attachment

2.5.1 Cell migration

Cell migration is an imperative process for cell survival, repair and regeneration in many organisms. The critical role of cell migration for complex organisms is evident in a wide range of cellular processes such as gastrulation, neovascularisation, nerve sprouting, immune surveillance and wound healing (Trepat et al., 2012, Vicente-Manzanares et al., 2005). Cell migration has been studied extensively within biological processes and in vitro, as invasion of tissues by migratory cells is a therapeutic target in the prevention and management of cancer. In fact, the mere definitions of these two terms, migration and invasion, are critical when considering the parameters being investigated and the desired result from cell motility. Kramer et al. defined cell invasion as the movement of cells in 3D with the subsequent restructuring of the ECM (Kramer et al., 2013). In contrast, cell migration was defined as the "non-destructive, non-proteolytic movement of cells". Ultimately, in the context of biomaterial research, the differences in the processes discussed within the above definitions are multi-factorial and this will inevitably have significant effects upon the outcome of studies investigating biomaterials in REPs. For example, the use of a non-invasive cell line in a nano-porous biomaterial could yield drastically different results in comparison to a highly migratory cell line seeded onto a macro-porous scaffold, as the ability to reorganise

the biomaterial would be fundamental to invasion. The type of cell and the size of the internal cellular organelles are also critical to cell migration/invasion, as different cells display different patterns of migratory behaviour and large cell nuclei can resist movement through small pore matrices in what has been coined the 'nuclear limit' (Paul et al., 2017). This very simplified example further reinforces the gravity of the challenges faced when assessing different biomaterials with different cell lines in different biomedical applications; as small changes in chemical or physical composition can have a significant impact upon the cell-matrix interactions observed. Furthermore, the primary objective for cell migration/invasion is dependent on the medical applications i.e. in cancer metastasis the primary objective is to impede cell metastasis, whilst for tissue regeneration, rapid cell migration would be desired.

A wealth of information is available on topographical and molecular changes within cells during migration (Pollard and Borisy, 2003, Devreotes and Horwitz, 2015, Nagano, 2012). Studies on cancer metastasis have shown that cells possess a range of migratory techniques to enable movement and invasion of tissues (Paul et al., 2017). Whilst some cells may migrate individually e.g. leukocyte extravasation, some migrate collectively i.e. cell-cell adhesion is maintained e.g. epithelial wound healing. These migratory behaviours are influenced by the physical interactions between the cell and the ECM; the proteolytic activity of cellular enzymes; and a series of complex intracellular pathways (Trepat et al., 2012). The ability of cells to polarize for directional migration is reliant upon internal modulation of the actin cytoskeleton to produce projections like lamellipodia and filopodia (Huttenlocher and Horwitz, 2011, Pollard and Borisy, 2003). Subsequently, focal adhesions and adhesion complexes that connect the intracellular cytoskeleton to the external ECM develop to enable the cell to gain traction (Parsons et al., 2010). The process of cell migration is inherently linked with these cell adhesions, which have been broadly classified as integrin and non-integrin mediated cell-substrate interactions (Huttenlocher and Horwitz, 2011). Integrins are transmembranous receptors composed of αβ-heterodimers with specific ECM-binding profiles, of which the RGD sequence (Arg-Gly-Asp) appears to be the most frequently reported. The assembly and disassembly of these adhesions (adhesion turnover) is cell and ECM dependent, with more migratory cells associated with smaller focal adhesions, whilst sedentary cells on 2-dimensional substrates display larger adhesions (Vicente-Manzanares et al., 2005). Furthermore, some ECM proteins display a greater array and number of integrin binding sites such as the aforementioned RGD motif, which can further influence migration (Trepat et al., 2012).

A large amount of early research into cell adhesion and migration has focussed on fibroblasts (Chen, 1979, Abercrombie et al., 1970), which migrate via a process referred to

as ‘mesenchymal migration’ (Justus et al., 2014, Kramer et al., 2013). Fibroblasts are cells found in abundance in mesenchymal tissues such as dental pulp, where they contribute to the production and regulation of the ECM; most notably the synthesis of collagen. Fibroblasts, like other migratory cells, display a complex actin cytoskeleton that is heavily involved in cell polarity, focal ECM attachments and protrusion (Pollard and Borisy, 2003). Actin polymerisation is a critical cellular process involved in the protrusion of the cell’s leading edge through the associated ECM and it is these features that are characteristic of ‘mesenchymal migration’ (Kramer et al., 2013). The actin rich projections that form at the leading edge of a migratory cell are referred to as lamellipodia, and within these projections, the actin cytoskeleton maintains a dynamic relationship with transmembrane cellular adhesion moieties such as integrins and syndecans. These transmembranous proteins and proteoglycans are interaction points between the advancing cell and the surrounding ECM. As mentioned above, turnover of these adhesion molecules is a contributory factor in the speed of cell migration, whereby smaller molecules can undergo faster assembly and disassembly for highly motile cells (Trepat et al., 2012). Whilst lamellipodia-based migration is well documented, other migration strategies have been reported (Petrie and Yamada, 2012).

2.5.2 Methods of assessing cell migration in vitro

Traditionally, the initial method for assessing cell migration was with 2-dimensional cell culture assays such as the scratch test (Liang et al., 2007). This simple strategy involved artificially creating a gap in an already confluent plate of cells using a standardised piece of laboratory equipment e.g. a P-200ul pipette tip. The cells were subsequently imaged using light or fluorescence microscopy to visualise the migratory behaviour of the cultured cells as they bridge the gap. Fluorescent labelling of target DNA enables further analysis of intracellular molecular up-regulation or suppression. This wound healing assay is similar to the cell exclusion zone assay, in which cells are cultured on tissue culture plastic that is divided by a removable insert. Following removal of the insert, a cell free zone remains into which cell migration can be observed and recorded. This strategy also allows for the addition of ECM protein hydrogels such as collagen or matrigel™ over the monolayer cultures, which enables the restrictive or inductive effects of matrix and/or growth factors to be assessed (Kam et al., 2008). This second strategy, synonymous with the circular invasion assay (circular cell free zone), produces a predefined space for improved consistency and reproducibility.

Alternative methods to assess the effects of chemotactic agents on cell migration include the Boyden chamber or Transwell® migration assay (Boyden, 1962). The Transwell® assay

involves the culturing of cells within a tissue culture plastic insert, the base of which contains a polycarbonate track-etched membrane with pores of specific diameters and densities. The insert can divide a standard culture plate well into upper and lower compartments to enable an array of parameters to be assessed including growth factor profiles or different ECM composition. The transmigration of leucocytes through endothelial monolayers has also been assessed using the Boyden chamber design (Li and Zhu, 1999). As above, the coating of the insert with ECM components enables cell invasion to be assessed in what is termed the transwell® invasion assay (Marshall, 2011). The process of cell migration into or through ECM derivatives enters the realm of 3D cell invasion/migration assays, which more closely resembles cell behaviour in physiological and pathological processes.

2.5.3 Methods of assessing cell migration in 3D

It has been well reported that 2D monolayer cell cultures do not represent the true physiological behaviour of cells (Baker and Chen, 2012, Duval et al., 2017, Vanderburgh et al., 2017). Cell-cell and cell-ECM interactions are drastically different between the two types of culture and these changes alter cell phenotype and gene transcription (Wozniak and Keely, 2005, Sung et al., 2013, Bott et al., 2010, Martino et al., 2009). In order to circumvent these issues, the behaviour of cells in 3D cell culture has been studied via several different strategies. The seeding or encapsulation of cells into biopolymer hydrogels was reported over 30 years ago (Schor et al., 1983) and this methodology remains popular today. The imaging of cells in 3D culture has become more prevalent with the development of more advanced microscopy, such as confocal scanning laser microscopy. Cellular tracking dyes can be conjugated to specific proteins to enable real-time assessment of cell behaviour and protein translation.

Despite these advances, the search for more biomimetic models in which to study cell behaviour at the tissue level has led to the development of organotypic cell culture models, in which the entire environment of the 3D model is focussed on replicating a specific organ. As such, spheroids and organoids are becoming frequently identified terms within the literature (Ranga et al., 2014) as they enable the various cellular and non-cellular components of the target organ to be studied with greater accuracy. These advanced strategies of 3D cell culture recognise the various roles played by each component of a living tissue and attempt to recreate this environment more biomimetically.

2.5.4 Cell migration assessment in REPs

In regenerative endodontic procedures, several histological studies have been reported that are able to demonstrate cell migration into previously devascularised root canals (Albuquerque et al., 2014). These studies are proving pivotal in addressing the current dearth of literature relating to the actual biological tissues that are recreated when REPs are performed clinically. Through histological studies it is now clear that REPs performed in necrotic teeth display different reparative processes than those that have maintained some viable pulpal tissue (Shimizu et al., 2012, Shimizu et al., 2013). Whilst further ex vivo studies will continue to add to these findings, it is currently not clear how tissue scaffolds could influence the regenerative processes being undertaken and how the use of such biomaterials may influence or direct stem cell fate. Due to strict regulatory restrictions, it is exceedingly difficult to develop biomaterials for use in clinical scenarios and as such, clinicians instead often opt to use current medical devices and products with FDA approval (Chrepa et al., 2017).

The use of extracted teeth to model REPs enables the dentine-pulp interface to be studied more closely. However, problems with collection, disinfection and processing of the teeth may arise. Furthermore, the extracted tooth model is low throughput and better suited for the study of optimised tissue scaffolds. As a result, an in vitro model that represents the possible dimensions of an intact root canal system would serve to increase the knowledge relating to tissue scaffold's parameters and the role of the tissue scaffold in facilitating pulp regeneration. At the time of writing, no 3D model or organotypic model specifically for REPs could be identified to study cell migration and cell-ECM interactions in vitro. Whilst some commercially available 3D migration tools were identified e.g. CelluSponge™ (Merck, Dorset, UK), their design did not accurately replicate pulp regeneration.

2.6 Additive Manufacturing Strategies

Additive Manufacturing (AM) is now synonymous with a wide range of CAD/CAM processes, which includes rapid prototyping (RP), 3-dimensional printing (3DP) and solid free-form fabrication (SFF). AM acknowledges that the final object is produced in an additive manner and has been endorsed by the American Society for Testing and Materials (www.astm.org - ASTM International, Pensylvania, USA). AM enables a CAD file to be manufactured through a range of technologies, most of which involve the deposition of successive layers of a chosen material, which provides precise control over product geometry and architecture. The degree of precision and accuracy is dependent upon the technology being used and the materials that are available for each method. A wide range of

AM techniques have been developed and they have previously been classified into five categories based on the technology and material being utilised (Table 1) (Gross et al., 2014).

These processes have developed significantly since 1986 when 'Stereolithography' was patented by Charles Hull (Schubert et al., 2014). This original process, also known as 'Stereolithography Apparatus' (SLA), utilises ultra-violet light to photopolymerise resin monomer into a 3-Dimensional resin polymer. Originally used to print prototypes and models, this technology has revolutionised the production and engineering of components in many disciplines including the automotive and aeronautical industries. AM is expected to grow to become a $6 billion dollar industry by 2021 (Wohler's, 2013). In 2013, medical applications of AM were reported at only 1.2% of the entire industry; however, with greater advances in material science, medical applications are projected to account for 21% of the industry by 2023 (Schubert et al., 2014).

Technology	Principle	Materials	Resolution
Stereolithography Apparatus (SLA)	UV Photopolymerisation	Epoxy/Acrylate based Resins	70-250µm (1-10µm with two photon polymerisation).
Inkjet Printing	Powder-Liquid binding	Photoresins or plaster powder particles.	20-50µm
Selective laser sintering (SLS)	Laser induced fusion of powdered particles.	Metals, resins, ceramic powders, nylon.	1-50µm
Fused-deposition modelling (FDM)	Molten thermoplastic extrusion	Wax, polycarbonate, nylon, ceramics.	50-250µm
Laminated Object Manufacturing (LOM)	Laser cutting of coated sheet.	Coated polymer, paper, metal.	10-100µm

Table 1 Common additive manufacturing technologies and their properties

2.6.1 Additive Manufacturing in Medicine and Dentistry

AM has been investigated for use in a wide range of potential applications and encompasses a wide range of techniques (Table 1). In the medical field, customised prostheses, anatomical models and surgical guides are becoming more and more accessible (Ventola,

2014). One additional AM strategy gaining popularity in tissue engineering is ‘Bioprinting’ (Murphy and Atala, 2014). Bioprinting refers to the production of organic tissues or organs in a process which involves the automated, controlled deposition of cells and ECM in a predefined spatial relationship. Production of patient specific organs could have significant ramifications for the field of organ transplantation, which is currently oversubscribed and results in many deaths each year when a suitable organ donor cannot be located (Cui et al., 2012). Whilst further investigation into the effects of bioprinting on mammalian cells is required, it is clear that these strategies will radically shape the future of healthcare, with a much greater focus on biomimetic, custom-made devices and personalised medicine.

Additive manufacturing processes are rapidly advancing the field of dentistry and appear to be at the forefront of improvements in patient-centred outcomes as well as offering significant economic benefits from digitalising workflow and decreasing personnel costs. Anatomical models, prostheses (dentures and implants) and surgical guides can now be produced and it is therefore clear why concerns about the reduction in demand for dental technicians have been raised for some time (Battersby, 2014). Furthermore, finite element methods (FEM) is an alternative CAD/CAM process that can be used to analyse and assess prostheses to optimize their performance (Chen et al., 2015). Aside from the more global economic benefits of adopting AM, it is also being used to study the impact of scaffold architecture and surface topography on cell phenotype, which presents an additional facet of the benefits of embracing AM technologies (Unadkat et al., 2011).

3 Materials and Methods

3.1 General Materials

3.1.1 Basic Materials

Tissue-culture treated polystyrene culture flasks and plates were purchased from Merck (Dorset, UK). Non-treated (non-adherent) polystyrene tissue culture plates were purchased from StarLab Ltd (Milton Keynes, UK). Dulbecco's Modified Eagles Media (DMEM – GlutaMax), Antibiotics (1% Penicillin-Streptomycin), Fetal Calf Serum (FCS), gelatin from porcine skin (Gel strength 300g Bloom) and *N*-Hydroxysuccinimide (NHS) were purchased from Sigma-Aldrich (Dorset, UK). The carbodiimide, 1-(3-Dimethylaminopropyl)-3-ethylcarbodiimide HCl (EDCI), was purchased from Carbosynth (Berkshire UK). Medical Grade Type I, bovine collagen was purchased from Collagen Solutions (Glasgow, UK) in 3mg/ml and 6mg/ml concentrations. Additional laboratory equipment used was available within the Institute of Aging and Chronic Diseases (IACD) and will be discussed within the text. Where required, cells were fixed using 4% paraformaldehyde available from internal stock made within the IACD. Cells were permeabilized with 1% Triton™ X-100 for molecular biology, a non-ionic surfactant and emulsifier (Sigma-Aldrich, Dorset, UK). Nucleus staining was performed using 4′,6-diamidino-2-phenylindole (DAPI) either in solution, Invitrogen™ DAPI dilactate, or with mountant, ProLong™ Diamond Antifade mountant with DAPI (ThermoFisher Scientific, UK). Actin staining was performed using Invitrogen™ Alexa Fluor™ 647 Phalloidin, a high-affinity F-actin probe (ThermoFisher Scientific, UK).

3.2 Cell lines, Cell Passaging and Cell Counting.

For the purpose of model validation, rapidly dividing and easily cultured cells were utilised. These included immortalised L929 mouse fibroblasts (passage 14-22) (Earle et al., 1943) and MDA-MB-231 human breast adenocarcinoma (triple negative) cells (passage 20-25) (Cailleau et al., 1974) that were available in previous stock frozen within the IACD. Cryovials containing cells were removed from the freezer and placed immediately into a water bath at 37°C and observed closely until defrosted i.e. no visible ice crystals (approximately two minutes). The defrosted dimethyl sulphoxide (DMSO)/cell suspension was quickly added to 5ml of DMEM with 1% Penicillin-Streptomycin in a 15ml centrifuge tube before being centrifuged at 1500RPM for 5 minutes. All media and DMSO were removed from the centrifuged pellet and the cells were resuspended in 10ml of fresh

DMEM, 1% Pen/Strep and subsequently aliquoted into five T75 flasks containing 10ml DMEM 1% Pen/Strep.

3.2.1 Cell passaging

Cells were cultured in an incubator at 37°C with 5% CO_2 and observed daily until sub-confluency (80-90%) was observed using light microscopy. Cells were subsequently passaged by removing excess media and rinsing each flask with 4ml PBS before discarding. Each flask was then washed with 2ml of pre-warmed 1x Trypsin/EDTA solution (0.12% trypsin, 0.02% EDTA) to detach the cells from the fibronectin-treated polystyrene flasks. The flasks were returned to the incubator and visualised every minute until all cells has detached and were in solution (approximately 3 minutes). 4ml of DMEM with 10% FCS and 1% Pen-Strep was subsequently added to each flask before transferring the solution to a 15ml centrifuge tube. Each flask was rinsed with 4ml PBS to ensure that all cells were collected and added to the cell solution in the centrifuge tube. The cells were then centrifuged at 1500RPM for five minutes. The resultant supernatant was carefully removed and the pellet resuspended in 2ml of DMEM/10% FCS/1% Pen-Strep cell media per flask into which the cells were to be split i.e. one flask split into five flasks required 10ml of media (1:5). 2ml of the cell solution was then added to each new T75 flask and an additional 10ml of DMEM/FCS/Pen-Strep cell media was added. Flasks were then labelled and returned to the incubator at 37°C with 5% CO_2/air mixture.

3.2.2 Cell counting using the haemocytometer

Cell counting was performed using a cell haemocytometer and a Biorad TC20™ automated cell counter (Bio-Rad Laboratories Ltd, Hertfordshire, UK). A single T75 flask was removed from the incubator and cells detached from the flask using the same process described above. Briefly, 2ml of pre-warmed trypsin/EDTA solution was added to the flask and incubated for five minutes. 4ml DMEM/FCS/Pen-Strep cell media was added along with 4ml PBS before the resultant cell solution was centrifuged at 1500RPM for five minutes. The supernatant was carefully removed from the pellet and resuspended in 1ml of cell media. 10µl of cell suspension was mixed with 10µl of Trypan Blue Exclusion Dye (ThermoFisher Scientific, UK). The 20µl solution was then transferred to the cleaned haemocytometer with glass cover slip. Cells were systematically counted using a phase contrast microscope and manual tally counter, with blue cells discarded as non-viable. The total cells counted within four squares of the haemocytometer were multiplied by the haemocytometer constant i.e. the volume within one $1mm^2$ ($1 \times 10^{-4}/10{,}000$) and the dilution factor (2), before being divided by the number of $1mm^2$ squares counted (4).

$$\text{Total cells per ml} = \frac{\text{Total cells counted x dilution factor (2) x 10,000}}{\text{Number of Haemocytometer squares counted (4)}}$$

3.3 Design and Production of the 'Culture Button Well' (CBW)

3.3.1 Initial Design Considerations (Culture Plate Measurements)

The production of a root canal analogue was fundamental to this project. A root canal analogue would enable cell migration to be assessed for the specific function of pulp regeneration. Of greatest interest in REPs is the discussion surrounding a "critical apical diameter", which is the hypothetical diameter below which REPs may be an unsuitable management strategy for the immature apex. This concept was first introduced in a seminal dental trauma paper from 1986 (Kling et al., 1986). This paper assessed the influence of clinical factors on spontaneous revascularisation of avulsed permanent central incisors and reported that revascularisation failed to occur when radiographic apex diameter was less than 1mm, compared to diameters greater than 1mm. Extrapolating these findings, several studies have attempted to further investigate this concept, with the suggestion that neovascularisation into the vacant root canal system and subsequent nutrient exchange is compromised with smaller apical diameters (Fang et al., 2018). Whilst more recent studies have reported successful outcomes with apical diameters of less than 0.5mm (Laureys et al., 2013), the apical diameter remains an important parameter that may function as a prognostic factor when deciding upon patient-centred clinical management. In line with current in vitro cell migration strategies an insert was required that would support biomaterial fabrication and cell culture, whilst introducing no detrimental effects upon any cells utilised.

The initial design considerations for an in vitro cell migration model was the standard 6 well tissue culture plate (Figure 1).Whilst Transwell® inserts (Figure 1 Inset) would be an alternative strategy for assessing cell migration into a range of biomaterials, these inserts are not available in sizes that would approximate to the anatomy, or diameter, of a root canal system and so the 'critical apical diameter' could not be assessed. It was also hypothesised that alternative researchers developing pulp regeneration biomaterials would be able to fabricate materials in a range of sizes to match the insert designed. For this reason, an insert was designed and produced for in vitro experimentation using commercially available CAD/CAM strategies and it is henceforth referred to as the 'Culture Button Well' (CBW).

Figure 1 6 well plate for cell culture: *Inset – 48 well Transwell® Insert for cell migration assays*

Depending upon manufacturer, the internal diameter and depth of a 6 well plate is approximately 35mm by 17mm. The upper well of the CBW was therefore designed with an external diameter of 30mm and an internal diameter of 25mm. A maximum height for the CBW was selected as 16mm to enable it to fit into a 6 well plate. From a design perspective, the CBW could be further subdivided into a 3mm upper compartment, or well, and a 12mm lower compartment containing the root canal analogues that would house the biomaterials being investigated. Extra space was created for media within the plates by designing the lower compartment with a square cross-section with a diameter of 18mm. Reducing the width of the lower compartment was also guided by the concept that it may be possible to image the root canal analogues through the side of the CBW, assuming the CBW itself was translucent and that thickness did not exceed approximately 1-2mm. Figure 2 displays initial sketches of potential CBW designs with calculations regarding the outlined parameters

defined above.

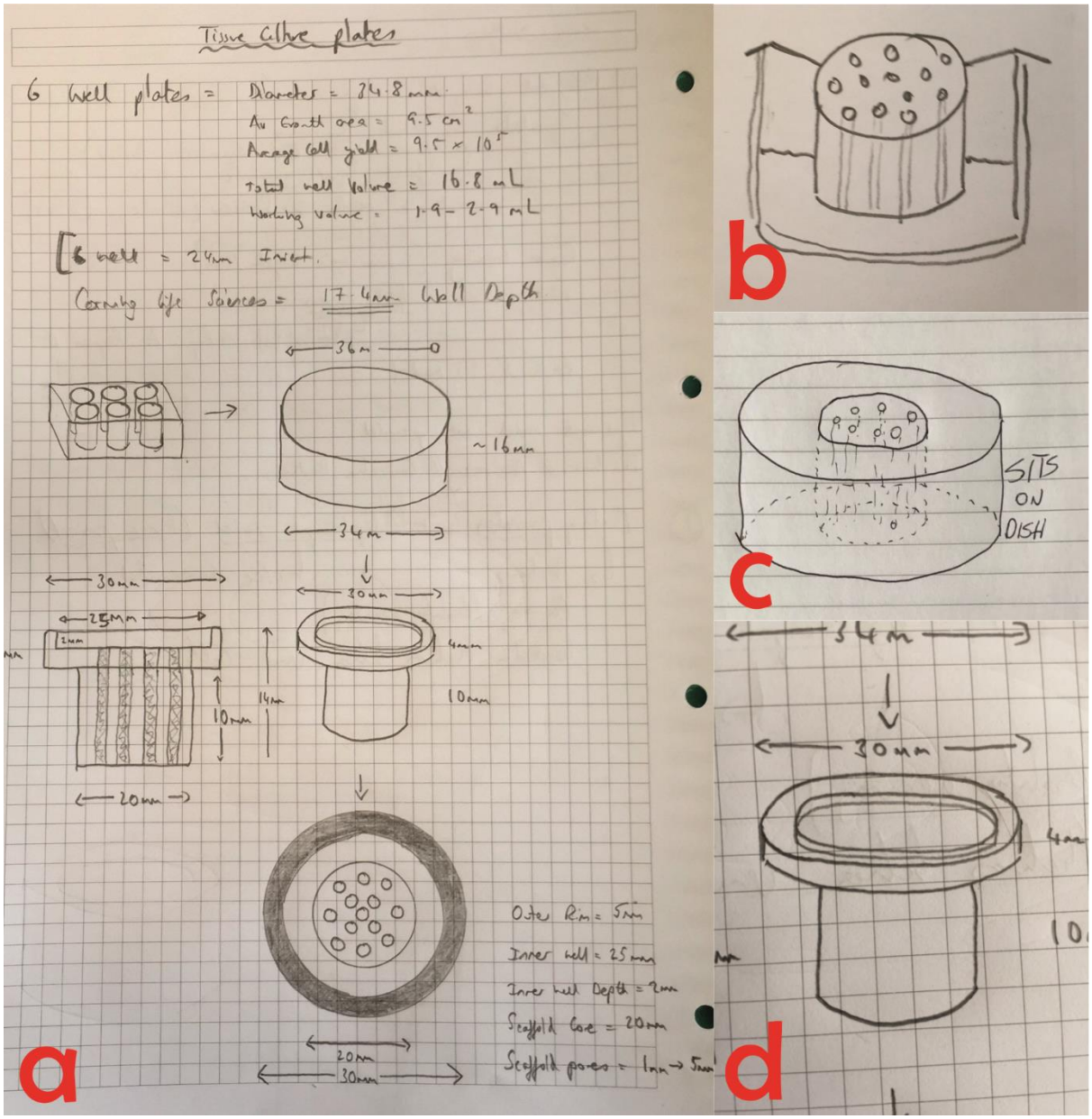

Figure 2 Initial Hand Sketches of possible CBW designs*: a) Formal Graph Pad sketches with measurements; b, c) Early Prototype designs following formulation of the research question; d) Magnified image of preliminary design from image*

3.3.2 Computer Aided Design

Following the initial hand designs (Figure 2) the CBW was subsequently designed using software called 3-Matic™ from Materialise® (Leuven, Belgium). A two day training course took place at Cambridge University in June 2017, with approximately 50% of the course assigned to segmentation skills for computed tomography (CT) and magnetic resonance

imaging (MRI) and the remaining 50% focussing on the design and production of implantable, custom-made medical devices and surgical drill guides. In short, the design process requires a series of shapes ('primitives') to be created and appropriated before merging ('boolean addition') or subtracting ('boolean subtraction') the primitives from each other. Figure 3 shows the design process which essentially started with a flat cylinder (upper compartment - Figure 3a) and cube (lower compartment - Figure 3c). Cylinders representing root canal analogues were created in a range of diameters (1-5mm – Figure 3d shows 2mm diameter) and were subtracted from the lower compartment cube to create space for the resultant biomaterials. Due to the limited cross-sectional space of the lower compartment, larger diameter cylinders 4-5mm were present in smaller numbers (n=4) compared with small diameter cylinders (1-2mm) which could be manufactured in greater numbers (n=20).

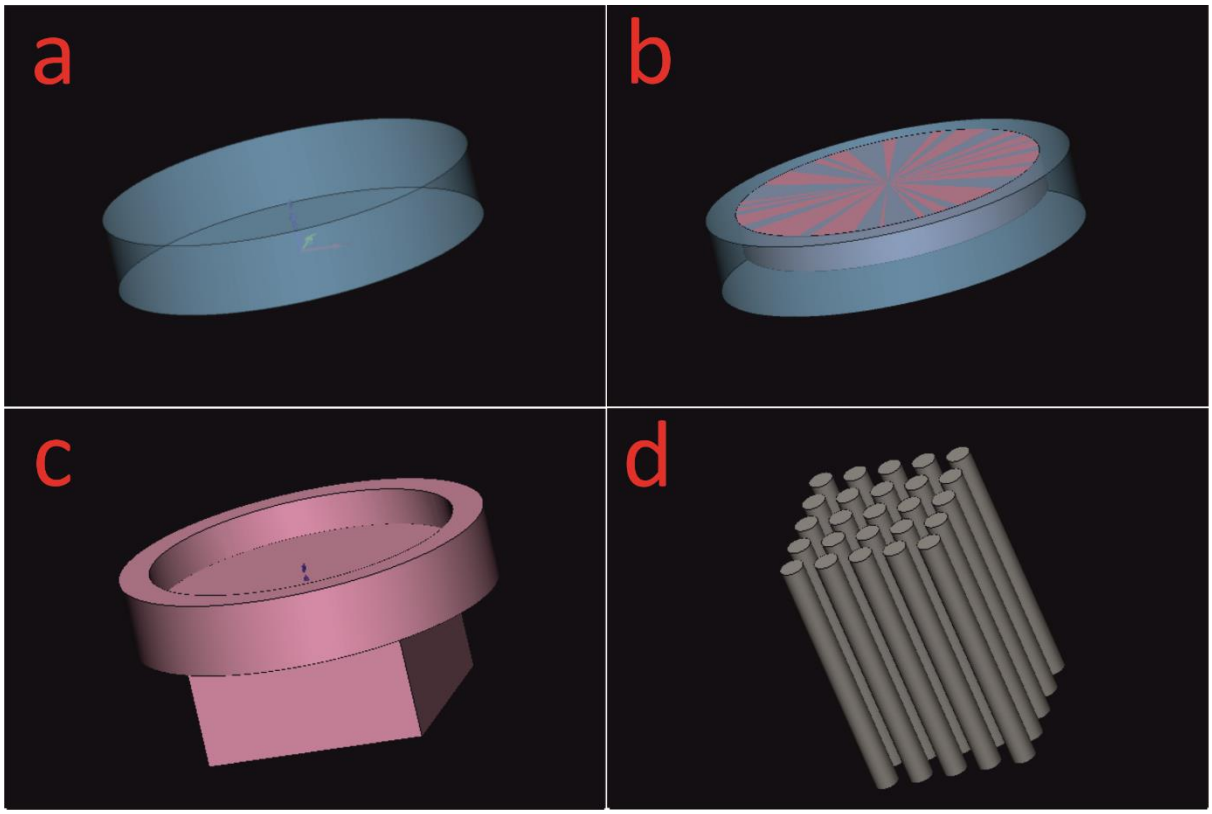

Figure 3 CBW iterative computer aided design using Materialise 3-Matic: *a) upper compartment 30mm blank; b) Superimposed 25mm blank cylinder; c) primitive CBW design with upper cylinder and lower square; d) 5x5 grid of 2mm cylinders which were subsequently subtracted from the blank CBW*

Following the initial design stage, the model was refined, smoothed and annotated using the software's 'Finish' tools to facilitate the orientation and labelling of samples when in vitro.

3.3.3 Additive Manufacturing Strategies

A number of additive manufacturing strategies were investigated. These included stereolithography (SLA), Digital Light Processing (DLP), Selective Laser Sintering (SLS) and MultiJet Printing (MJP). SLA/DLP remain the most widely used, commercially available AM strategies within dentistry. SLA and DLP both use a photo-polymerisable resin monomer, contained within a resin vat. As the monomer is in liquid form, traditionally these technologies require the product to be produced upside-down. The build platform is sequentially lifted from the resin, with each subsequent layer cured to the previous layer by the judicious and meticulous targeting of a single photon of UV light from a laser (Vanderburgh et al., 2017). SLA therefore requires the CAD-controlled laser to "sketch" out the entire layer prior to moving on to the next layer. Comparatively, DLP technology enables an entire layer to be cured at one time through the use of a projector. For this reason, DLP technology can produce an item quicker than SLA. However, this speed can be at the expense of surface finish and part resolution, due to the subsequent scatter of the light from the projection. Post-production for both technologies involve separate wash and cure stages. The removal of excess, uncured monomer by washing in an ultrasonic bath takes place before an extended cure in an ultra-violet light cure box.

Figure 4 First Additively Manufactured Culture Button Well*: The first CBW fabricated using a Form 2® Stereolithography Apparatus (SLA) printer.*

Figure 4 shows the first CBW printed using SLA within the School of Engineering, University of Liverpool. The device had a good quality finish and took approximately four hours to print. Some concerns regarding the presence of uncured resin-monomer remained, along with the slight opacity of the part once cured. For this reason MultiJet printing was investigated with a commercial company, CBM (Swansea, UK). MultiJet printing involves the bottom-up production of the part from a range of powdered materials such as photo-curable resin or casting wax. CBM utilised a ProJet 3500 HD Max from 3D Systems (Rock Hill, South Carolina, U.S.A) to fabricate a CBW from their VisiJet Crystal polymer that is United States Pharmacopeia (USP) class VI, meaning that the material and it's constituents are tested for biocompatibility to determine if any leachates are toxic (Figure 5).

Figure 5 Prototype Culture Button Well fabricated using MultiJet Printing: *The picture part was additively manufactured from a photocurable-resin powder. The internal cylinders were fabricated in a range of diameters and macro-porous internal scaffolds are partially visible within the channels.*

However, the material was opaque and again concerns were raised about the ability to image biomaterials in situ. Furthermore, the high quality surface finish of the MJP CBW came with an equally high price, which restricted the optimisation process of the CBW as fewer "trial" CBWs could be printed and cast aside if inaccurate or subsequently rendered obsolete.

At this time, the Kulzer CaraPrint 4.0 (Figure 6) was investigated and purchased by the School of Dentistry as a 3D printer for model production and splint manufacturing. These

large items with limited surface detail are ideal for DLP technology as an adequate surface finish for a study model or occlusal appliance is easily attainable with DLP. This DLP printer was used to print the CBW in a process that took approximately 25 minutes per build. Multiple CBWs (4-5) could be printed with each build.

This technology was therefore, quick and efficient for the purpose of this study and any possible reductions in surface finish were deemed inconsequential. Despite these improvements in cost and efficiency, DLP presented similar limitations to SLA in terms of uncured monomer and lack of translucency. For this reason, an alternative approach was investigated and utilised, Indirect Additive Manufacturing.

Figure 6 Kulzer CaraPrint 4.0 Digital Light Processing (DLP) Printer

3.3.4 Indirect Additive Manufacturing

To circumvent any issues associated with leachable constituents from additively manufactured parts and to improve the optical properties of the CBW, an indirect AM strategy was considered. Indirect AM involves the CAD/CAM production of a part negative, into which addition cured polyvinylsiloxane (PVS), or polydimethylsiloxane (PDMS) can be cast. In this capacity the AM part is used, indirectly, as a mould for the desired component.

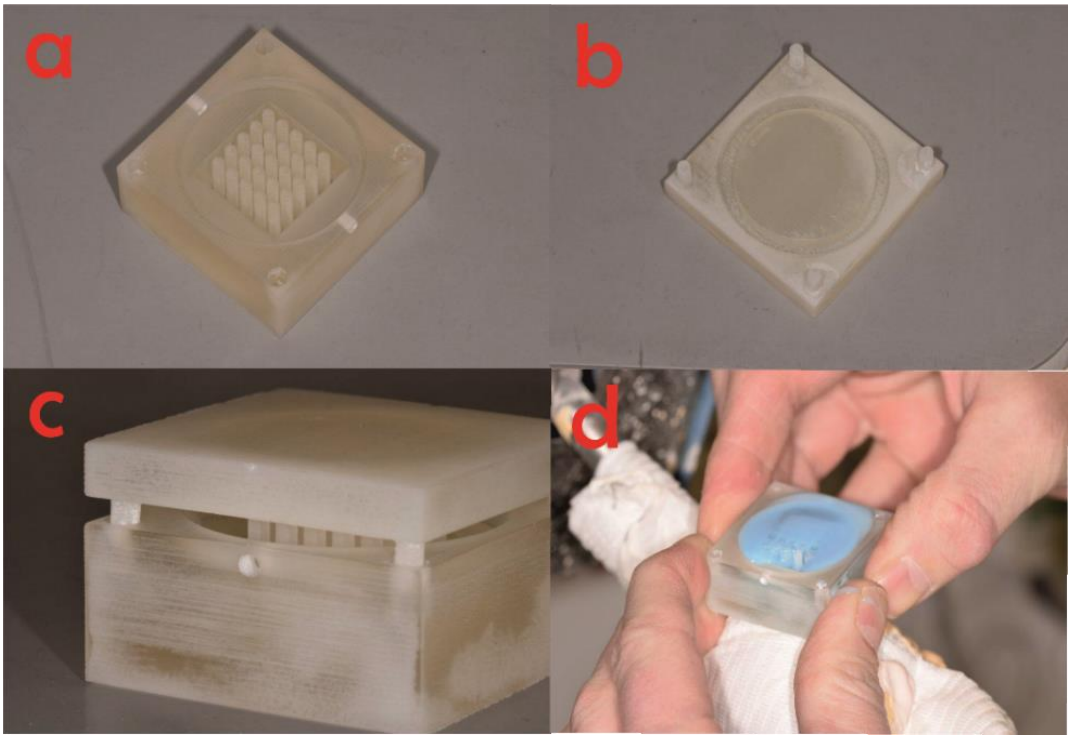

Figure 7 Initial Indirect Additive Manufacturing Prototypes: *a-c) Display the first prototype two part negative designed using multijet printing. a) Lower Negative part b) Upper negative part c) Combined two-part negative d) Addition-cured PVS poured into the lower compartment during material trials and design optimisation*

Materialise 3-Matic™ software was again used to produce a negative of the CBW in a similar manner to that discussed above. During this process the previously designed CBW was essentially deleted from a square blank and then the resultant part separated at appropriate points to allow the cast part to be removed. This iterative design process ran simultaneously with the material considerations discussed in chapter 3.3.5 – Addition-cured PDMS. Initially a two part design was produced (Figure 7). Following printing of this part, a number of PVS/PDMS materials were trialled (Figure 7d), but unfortunately, the large number of parallel cylinders (twenty) and the shear strength of the materials meant that it was difficult to retrieve the cast CBW from the negative without tearing or damaging the CBW. Figure 8 (a-d) documents the iterative process which occurred, including an initial trial of a 3-part negative, in which the lower negative split in two parts (Figure 8d). Despite this modification, tearing of the PVS was evident and for this reason the lower part of the negative was designed in three-parts that approximated together and which were held with cable ties (Figure 9a). Cone shaped locating jigs ensured the three parts fit accurately. The optimised negatives to fabricate the CBW can be seen in Figure 9 including the 3-part lower (Figure 9b).

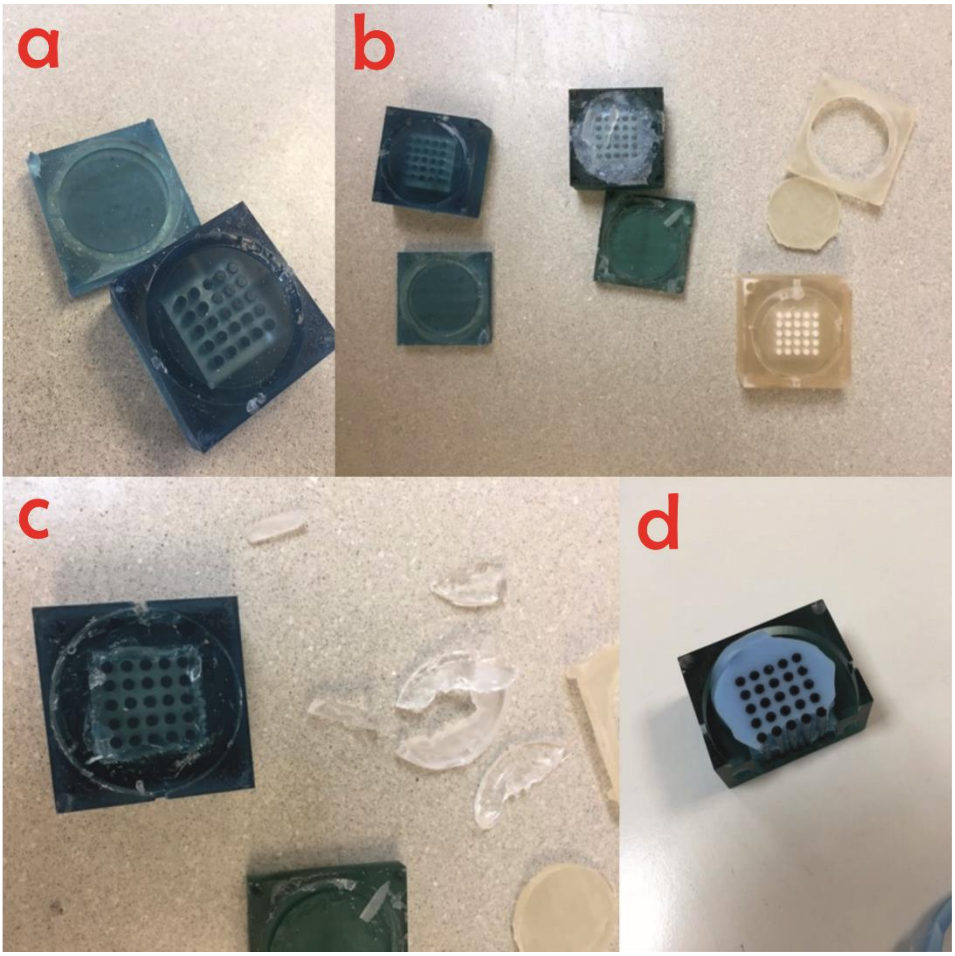

Figure 8 Negative Part Optimisation using various addition cured poly-vinyl siloxane and polydimethylsiloxane: *a) Initial PVS in 2-part negative b) 3 different PVS sample trials within the 2-part negatives c) tearing of the PVS trials with attempted removal d) torn PVS within a modified 3-part negative with 2 lower parts (note: smaller part of lower negative not visible in photo)*

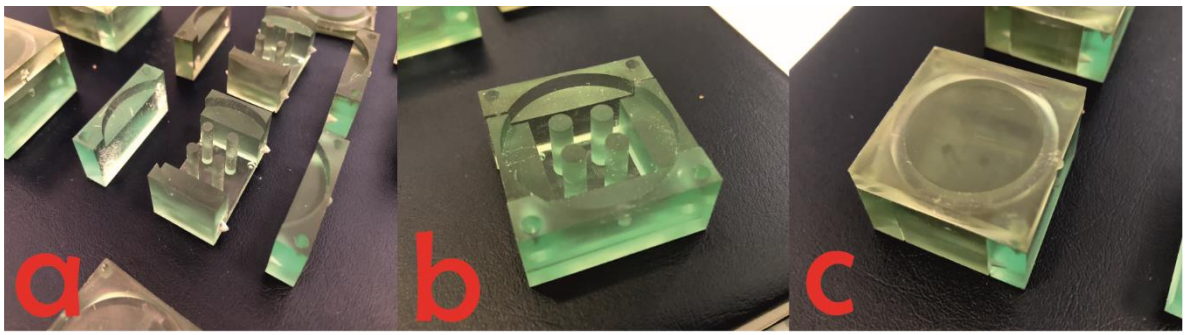

Figure 9 DLP produced CBW Negatives*: a) Lower 3-part negative with locating points visible b) lower 3-part negative approximated together c) completed 4-negative with upper lid to close off the internal chamber*

To simplify the production of the CBWs, each subsequent negative was designed and produced with four cylinders. This reduced the occurrence of tearing of the PDMS upon removal from the mould (Figure 8) and simplified the tissue scaffold production as only four

scaffolds could be produced in each CBW. As the number of cylinders within the CBW increased, it became harder to maintain the media within the upper compartment of the CBW and a greater amount of raw material was used in producing the tissue scaffolds. Four cylinders within each CBW was therefore the optimal number as it enabled CBWs with different diameter cylinders to each hold the same number; it facilitated removal of the cast CBW from the negative mould without tears or damage; and it also reduced the amount of wasted raw materials when experimenting with different ECM-derivatives during the fabrication of the tissue scaffold range.

The finalised CAD/CAM process was as follows:

1. CAD file was loaded onto cara Print 4.0
2. Print plate was cleaned with 99% Isopropanol with a microfiber cloth
3. The print cartridge was filled with light-polymerisable resin
4. Print was commenced
5. Printed components were carefully removed from the print plate using a plastic spatula
6. Components were rinsed thoroughly with 99% Isopropanol to remove excess resin
7. Components were placed in 'Pre-clean' 99% Isopropanol ultrasonic bath for three minutes
8. Components were cleaned with pressurised air
9. Components were placed in 'post-clean' 99% Isopropanol ultrasonic bath for three minutes
10. Components were cleaned with pressurised air
11. Components were placed in Kulzer UV-light cure box for five minutes on the top surface and five minutes on the bottom surface

3.3.5 Addition-cured polydimethylsiloxane (PDMS)

A series of translucent, addition-cured PDMS products were investigated from a number of different sources (Table 2). Whilst the optical properties of the clear PDMS were desirable, the shear strength of the material was important as materials with low-shear strength tended to tear. Initial experiments combined PDMS catalyst and base at appropriate concentrations in line with manufacturer's guidelines.

After a series of materials had been trialled, a product known to our laboratory group was proposed as a possible suitable material. The material had previously been utilised to produce stretch chambers to assess the influence of circadian rhythms on cells (Rogers, 2019). As such, Elastosil® 601, a translucent, pourable, addition cured silicone (Part A and

B) was purchased from Wacker Chemicals Ltd (Bracknell, UK). As no detrimental effects of over-curing were identified, the documented curing times were doubled to ensure curing through the negative was complete.

Initial attempts to allow the material to cure for 24 hours at room temperature resulted in voids as the PDMS was able to leak from small injection vents within the CBW negative that allowed air to re-enter. For this reason, the mould was secured in a small vice and immersed in a water bath at 70ºC for40 minutes until the material was cured. Despite this accelerated cure, CBWs were produced with bubbles due to the mixing process of the constituent PDMS and the possible re-entry of air or water during the curing process. Two strategies were investigated to circumvent these issues. Firstly, to avoid the presence of trapped bubbles incorporated during mixing, the PDMS was placed in a vacuumed-desiccator for twenty minutes prior to pouring. Whilst this method was reasonably successful at excluding bubbles, a second approach involved centrifuging the mixed PDMS prior to pouring, which rapidly produced the most homogenous and air-free mix. The second strategy utilized involved using an oven at 90ºC to further accelerate the curing of the PDMS post-pouring. This strategy reduced the curing time to approximately 20 minutes and served to reduce the risk of PDMS leakage from the mould during curing.

The finalized casting process was as follows:

1. The three part lower negative was secured with cable ties.
2. A light coating of petroleum jelly (Vaseline™) was rubbed onto the external aspect of the cylinders using a micro-brush to facilitate CBW removal post-curing.
3. Elastosil 601 was mixed in a glass beaker at a ratio of 9:1 (A:B)
4. The mixed Elastosil was transferred to a 50ml falcon tube and centrifuged at 1000RPM for two minutes.
5. Upper and lower negatives were loaded with Elastosil and lids positioned carefully upon their lower counterparts.
6. The mould was secured in a table clamp and immediately transferred to an oven set at 90ºC for twenty minutes.
7. The clamp was carefully removed from the oven using oven gloves and cooled under cold running water.
8. The resultant PDMS CBW was removed carefully with a small scalpel and the use of a high-pressure laboratory air-line.
9. The CBW was rinsed with 99% Isopropanol and internal channels gently cleaned with a small microbrush.

Material	Supplier	Reason for rejection
Dow Corning® EI-1184 Optical encapsulant	Univar Ltd (Widness, UK)	Poor shear strength/tearing
Dow Corning® 3140 RTV coating	Univar Ltd (Widnes, UK)	Poor shear strength/tearing
Z-Dupe duplicating silicone	Henry Schein (Gillingham, UK)	Non-transparent
Sylgard™ 186	Univar SC (Tamworth, UK)	Supply restrictions
Elastosil® 601	Wacker Chemicals Ltd (Bracknell, UK)	Chosen material

Table 2 Commericially available silicones trialled during CBW fabrication

3.3.6 Post-Production

Following curing, the CBWs were carefully removed using a high-pressure, laboratory air-line to help separate the PDMS from the mould. Small amounts of flash and excess in the injection vents were removed using a number 15 scalpel (Swann-Morten, Sheffield, UK). The PDMS CBWs were cleaned with a micro-brush and 99% Isopropanol to ensure that no residual resin-monomer or petroleum jelly (Vaseline™) remained.

4 Development and Validation of the Culture Button Well for Regenerative Endodontic Tissue Scaffold Assessment

The following chapter details a number of optimisation processes involved in validating the CBW as a useful in vitro tool to assess cell migration. Due to the range of biomaterials trialled and a number of issues that developed with handling/imaging the scaffolds the research presented does not follow chronological order but serves to detail the key milestones and issues that arose in relation to the CBW design. In brief, this chapter documents the four key aspects associated with validating the CBW, which are: fabricating cylindrical scaffolds in the CBW; material choice and their modifications; imaging considerations; and attempts at inducing migration.

4.1 Fabrication strategies for tissue scaffolds within the CBW

Due to the wide range of potential biomaterials that have been proposed and reported as possible tissue scaffolds in REPs, it was hoped that the CBW could be used to fabricate the scaffold cylinders in situ. This would more closely replicate the use of injectable technology during the clinical regenerative endodontic procedure. As the CBW had been designed with open ended cylinders to house the scaffolds, the scaffolds could subsequently be created using the CBW in an upright or inverted position. Prior to experimentation, the CBWs were boxed, autoclaved and stored appropriately, whilst glass cover slips and the upper component of the CBW negative were cleaned with 99% Isopropanol and sterilised for 10 minutes per side using a UV-steriliser.

4.1.1 The Inverted Fabrication Technique

Using this technique, UV-sterilised 22mm glass coverslips (Agar Scientific, Stansted, UK) were placed into the upper compartment of the CBW and the CBW inverted and reinserted into the upper negative from which the inserts were cast (Figure 10). Any liquid hydrogel could subsequently be administered using pipettes and pipette tips or syringes with small gauge hollow-bore needles attached. UV-sterilised 16mm glass cover slips (Agar Scientific, Stansted, UK) could then be positioned on top to ensure consistent gels were produced and to reduce risk of cross-contamination whilst within the incubator. Figure 11 shows 6mg/ml bovine collagen hydrogels in situ produced using the inverted fabrication technique.

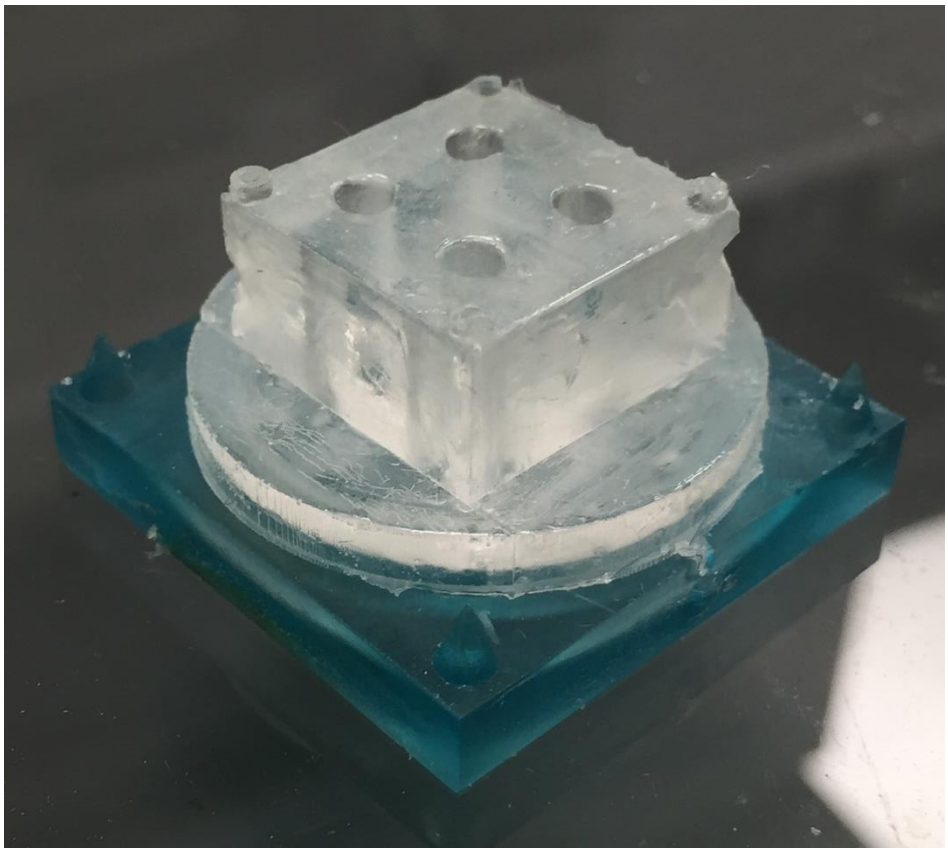

Figure 10 A CBW with 4mm diameter internal cylinders inverted within the upper CBW negative

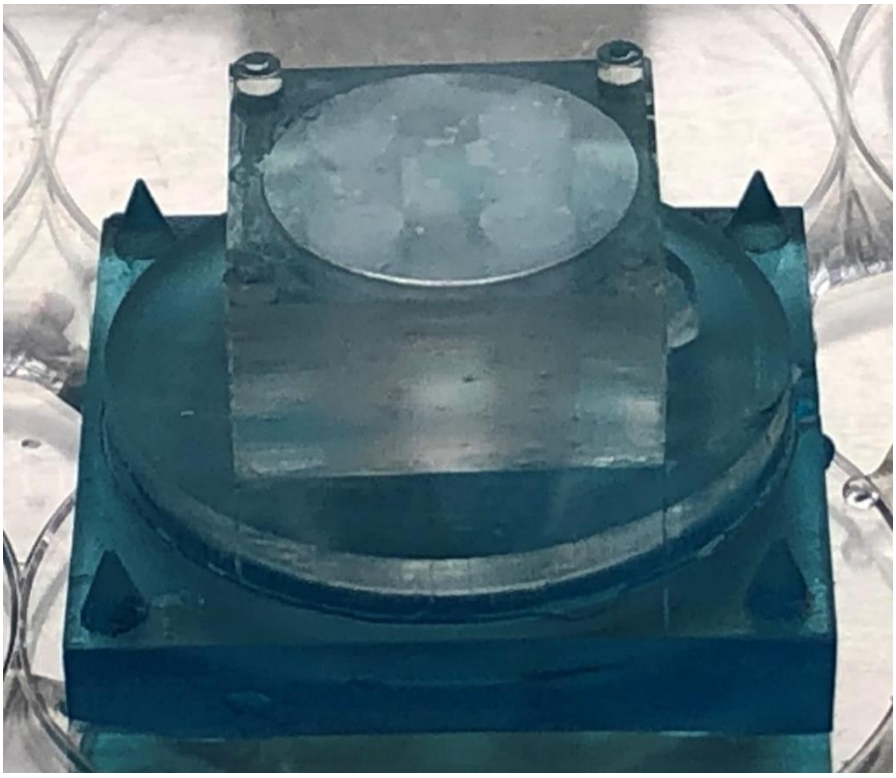

Figure 11 An inverted CBW with 6mg/ml type 1 bovine collagen in situ*: Note - 16mm coverslip to help reduce cross-contamination and to assist with consistent dimensions of the gels*

4.1.2 The upright fabrication technique

This technique is the reverse of the technique described above. It involved the positioning of a sterile 16mm glass cover slip onto the bottom of the CBW, which was initially held in place using a gloved finger. Following pouring of the hydrogel, the surface tension created held the glass cover slip in place and the CBW could be positioned within a 6 well plate. This technique enabled a small layer of excess hydrogel to be poured to link the four cylinders from above. This additional layer (Figure 12) served to maintain the positioning of the hydrogels during extended culture, which on occasions could sag, drain or slip out of the CBW.

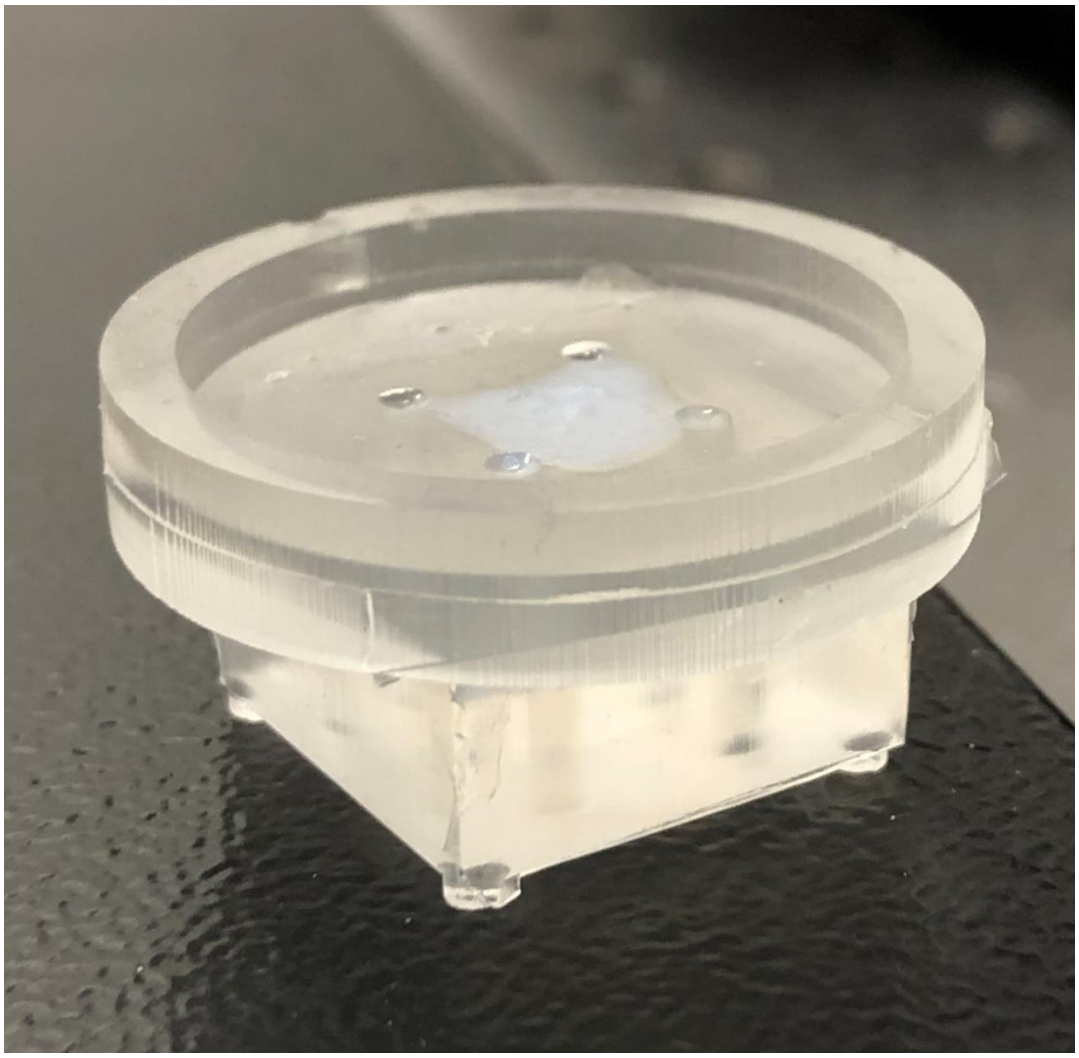

Figure 12 A 2mm diameter CBW with 6mg/ml type 1 bovine collagen: *Note: additional collagen film linking all four cylinders to resist gravitational forces during cross-linking*

4.1.3 Coating of cover slips with Bovine Serum Albumin

In an attempt to avoid the hydrogels from sticking to the glass cover slips, they were soaked in 1% bovine serum albumin over night at 4ºC. These cover slips were subsequently used to seal 6mg/ml collagen into the CBWs. As with previous experiments, the coating of cover slips did not appear to make the collagen cylinders more consistent in their shape, nor did it stop some of the collagen draining out of the CBWs following cover slip removal. As some cylinders had also previously gelled without the BSA coated coverslips, it was decided that optimising the collagen gelation process was the main priority and further coating of the coverslips was not pursued.

4.2 Biological Hydrogels and their challenges

A range of suitable biological hydrogels were sought in an attempt to validate the CBWs as a possible in vitro cell migration tool. Due to the abundance of collagenous proteins in the pulp, collagen and gelatin were the predominant hydrogels investigated. The latter of these, gelatin, has been well documented as a possible biological tissue scaffold (Koshy et al., 2014, Van Vlierberghe et al., 2007) that is cheap to purchase and translucent, making it an ideal matrix for imaging cell migration.

4.2.1 Crosslinking of Gelatin using Carbodiimide and *N*-Hydroxysuccinimide

Gelatin from porcine skin (Merck, Dorset UK) was dissolved in pre-warmed distilled H_2O on a magnetic stirrer at a temperature of 60ºC. Initial trial experiments found concentrations in excess of 20% w/v gelled almost immediately and it was therefore impossible to add the cross-linking solution prior to gelation. Subsequently, 1g of gelatin was added to 10ml dH_2O at 60ºC using a magnetic stirrer. EDCI was dissolved in 5ml of dH_2O to produce a 10mM solution. NHS were added to 5ml dH_2O to produce a 4mM concentration solution. EDCI and NHS was combined and added to the gelatin to produce a 5% Gelatin-EDCI-NHS (XLGel) solution before syringing the solution into the CBW using the 'inverted fabrication technique'. Figure 13 shows a 4mm CBW containing 5% Gelatin-EDCI-NHS hydrogels, the bottom right cylinder of which, has been intentionally extruded with a micro-brush for illustration purposes.

4.2.2 pH-Crosslinked Collagen Hydrogels

In addition to the hydrogels described above, gelatin's parent protein collagen was also studied. As such, medical grade, type I bovine collagen was purchased from Collagen Solutions (Glasgow, UK) in 3mg/ml and 6mg/ml concentrations. This product is cross-linked by increasing the pH with a buffer to the optimal pH of 7.4.

Following optimisation of the mixing ratio (9 parts collagen to 1 part buffer), a consistent gel was produced in a 7ml bijou flask. However, trying to replicate the same consistency within the CBWs met with great difficulty. Frequently, when removing the cover slips from the CBWs after polymerisation in the incubator, the hydrogels would drain out of the CBW. On occasions, some cylinders would polymerise and others would not, further highlighting the challenges of working with biological hydrogels that can display batch variability (Caliari and Burdick, 2016, Antoine et al., 2014). Furthermore, when consistent collagen cylinders were produced, extended culture in media often resulted in notable dimensional changes that resulted in the movement of the gels. Movement, shrinkage or swelling during the incubation period affected the integrity of the gels and the seal created within the CBWs. In these situations, media frequently drained around the gels into the lower compartment which made maintaining growth factor gradients problematic. Due to these challenges, 3mg/ml was quickly abandoned as a possible concentration due to the lack of rigidity of the gels.

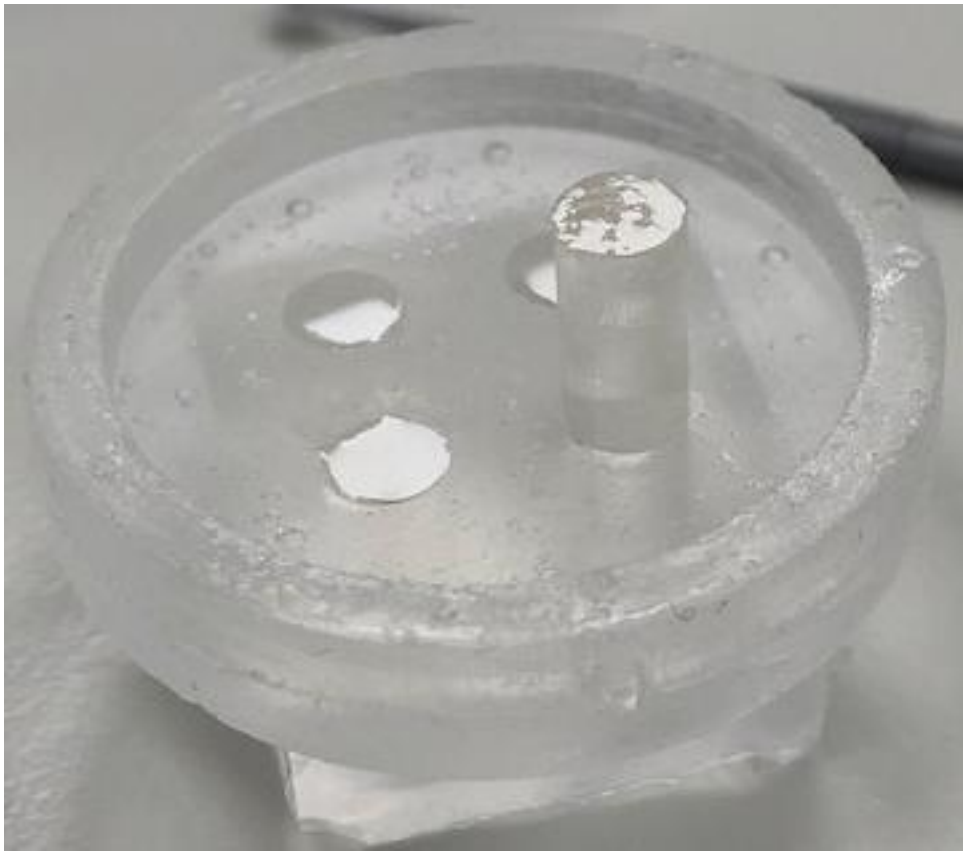

Figure 13 A 4mm CBW with 5% Gelatin cylinders chemically crosslinked with EDCI (10mM) and NHS (4mM) *(Note: The lower right cylinder has been extruded from illustrative purposes).*

4.2.3 UV-Crosslinking of collagen hydrogels

Due to the ongoing challenges with trying to maintain consistent collagen hydrogels in culture, UV-crosslinking was also attempted in addition to using the pH buffer. UV-crosslinking has been reported to polymerise collagen without diminishing the bioactivity of the gel (Davidenko et al., 2016). When compared to chemical cross-linking, UV crosslinking reportedly preserves carboxylic residues that are important attachment sites for integrin-matrix interaction (Davidenko et al., 2016). A ULP-CL1000 machine was used at a range of intensities and time periods. Despite a perceived benefit from investigating this strategy, UV-treated hydrogels did not demonstrate improved structural resilience and a number of possible factors were raised. Firstly, the upright fabrication technique allowed both ends of the cylinder to be irradiated, whilst the inverted fabrication technique could only be irradiated from one aspect due to the presence of the resin negative which may have restricted the penetration of UV. Secondly, the presence of glass coverslips, which remained in situ to protect against contamination, is likely to have reflected a large amount of the UV. Thirdly, it was unclear if the heat generated whilst in the cross-linker may have denatured the collagen. Furthermore, no rheology or chemical assessment was performed on the gels to inform if the UV-crosslinking provided any benefit over pH crosslinking alone. UV-crosslinking is therefore included below for completeness, but the strategy requires much greater investigation and no conclusions can be drawn on the impact that the UV may have had upon the physical and chemical properties of the scaffolds as insufficient data are available at this stage.

4.3 Biocompatibility of the CBW

Previous experimentation with Elastosil 601 within our lab group had concluded that the addition-cured rubber was supportive for cell attachment and growth irrespective of protein/glycoprotein coating e.g. fibronectin (Rogers, 2019). This was confirmed following an experiment using the CBW and Human MDA-MB-231 cells.

4.3.1 Methods

6mg/ml collagen hydrogels were poured using the inverted pour technique into three CBWs with different diameter cylinders (4mm, 3mm and 2mm cylinders) and duplicated using collagen at 3mg/ml. The top right cylinder in each CBW was filled with Matrigel® (Corning Ltd – Life Sciences, UK) at a concentration of 3mg/ml and was intended for comparison as a positive control (See Figure 14). CBWs were placed in a UVP CL-1000 Crosslinker for 20

minutes at 0.45J/cm^2 in an attempt to further cross-link the collagen gels (Davidenko et al., 2016).

2x10^5 MDA-MB-231 cells were seeded onto the upper surface of the CBWs in 400µl cell media and placed in the incubator for 1 hour to attach. Following this time period, the CBWs were gently rinsed with PBS. 1.5ml cell media was placed in the upper compartment and 2ml of cell media with an additional 20ng/ml epidermal growth factor (EGF) was placed in the lower well before returning to the incubator. EGF was selected as chemoattractant for MDA-MB-231 cells, as blockade of EGF receptors (EGFR) expressed on the cells has been shown to inhibit cell proliferation and migration (Hsieh et al., 2013, Prasad, 2009). Media in the upper compartment was changed daily until the end point of 72 hours.

4.3.2 Results

Unfortunately, all of the 3mg/ml collagen along with the 4mm and 2mm diameter 6mg/ml collagen cylinders failed to polymerise adequately and the hydrogel drained out of the CBW when the cover slip was removed and the CBWs reverted to their upright position. Wells A1, A3, B1, B2 and B3 from Figure 14 were therefore removed. Well A2 contained the only CBW that was seeded with cells and subsequently processed. However, by 48 hours it was clear that the collagen cylinders had dramatically reduced in size and length and the media added to the upper compartment was rapidly draining through the collagen cylinders into the lower compartment. At 72 hours the CBW was rinsed with PBS and soaked in 4% paraformaldehyde for 12 hours. This was subsequently removed and cells were permeabilised in 0.1% Triton-X for 20 minutes and stained with DAPI (1 in 10,000) for 1 hour. Following processing, no consistent collagen cylinders remained and imaging of these cylinders was abandoned. Figure 15 shows the resultant confocal microscope image of the top of the CBW (i.e. the surface cells were seeded onto) at the periphery of the single remaining 3mg/ml matrigel cylinder, which was partially intact. This image clearly shows the MDA-MB-231 cells well attached to the CBW that was not coated prior to cell seeding. The left half of the image showing the matrigel cylinder displays limited cell attachment.

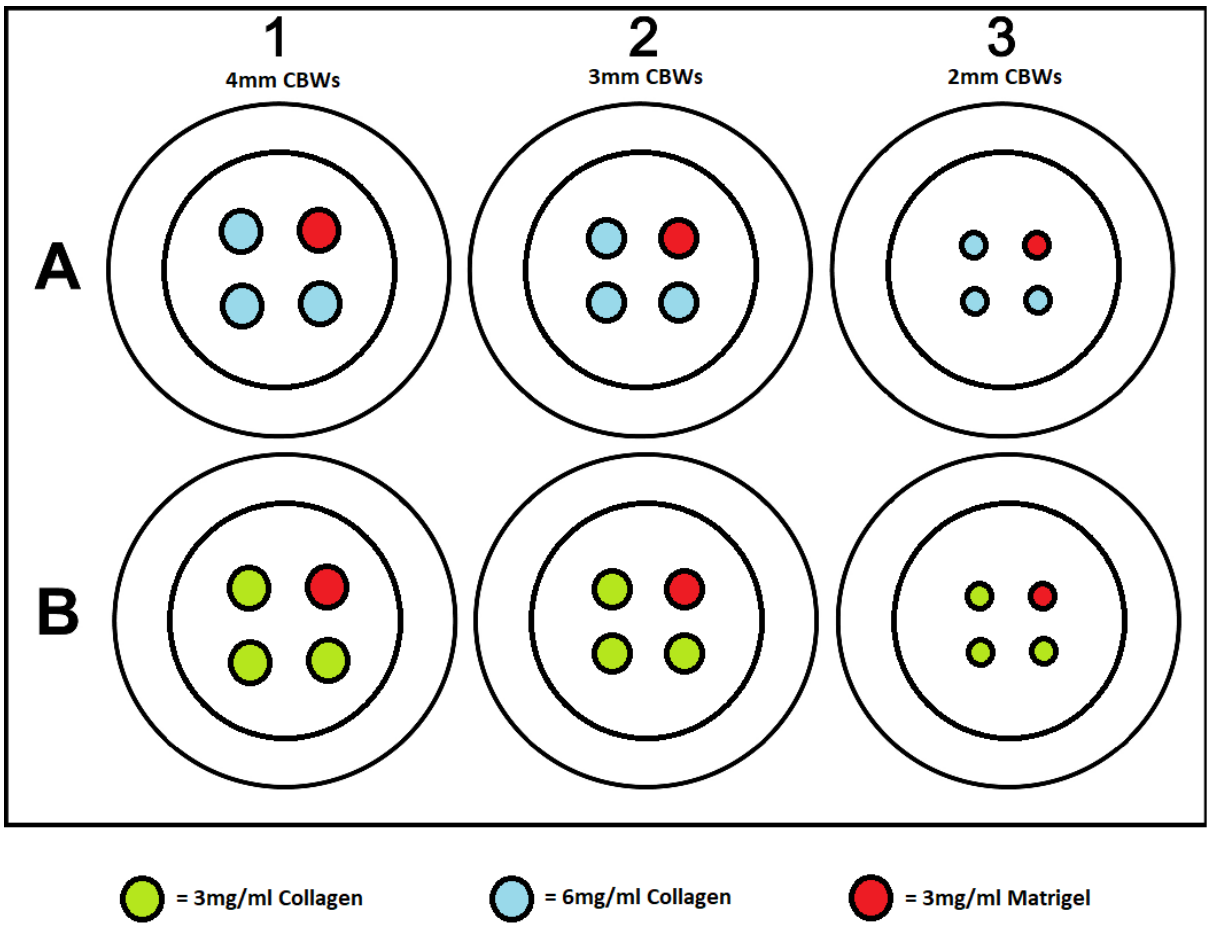

Figure 14 Diagram representing the Collagen/Matrigel CBW experiment. *Only collagen in well A2 polymerised adequately and within this well only the 3mg/ml Matrigel cylinder maintained viability throughout the 72 hour culture period.*

4.3.3 Discussion

It was unclear whether the matrigel cylinder was damaged during processing or whether the cells preferentially attached to the Elastosil 601 material, but no cell migration into the matrigel was noted and limited cell attachment was visualised. As cell attachment to matrigel would be expected, it is more likely that the delicate matrigel cylinder was disturbed during processing. Figure 15 further highlights the difficulties faced imaging the hydrogel cylinders, as the cells visible on the matrigel cylinder are out of focus. The hydrogels frequently changed position in the mould during culture and also displayed a meniscus meaning multi-plane images were required to visualise the surface of the gels. No conclusions could be drawn as to why the gels in well A2 were more consistent than the other wells.

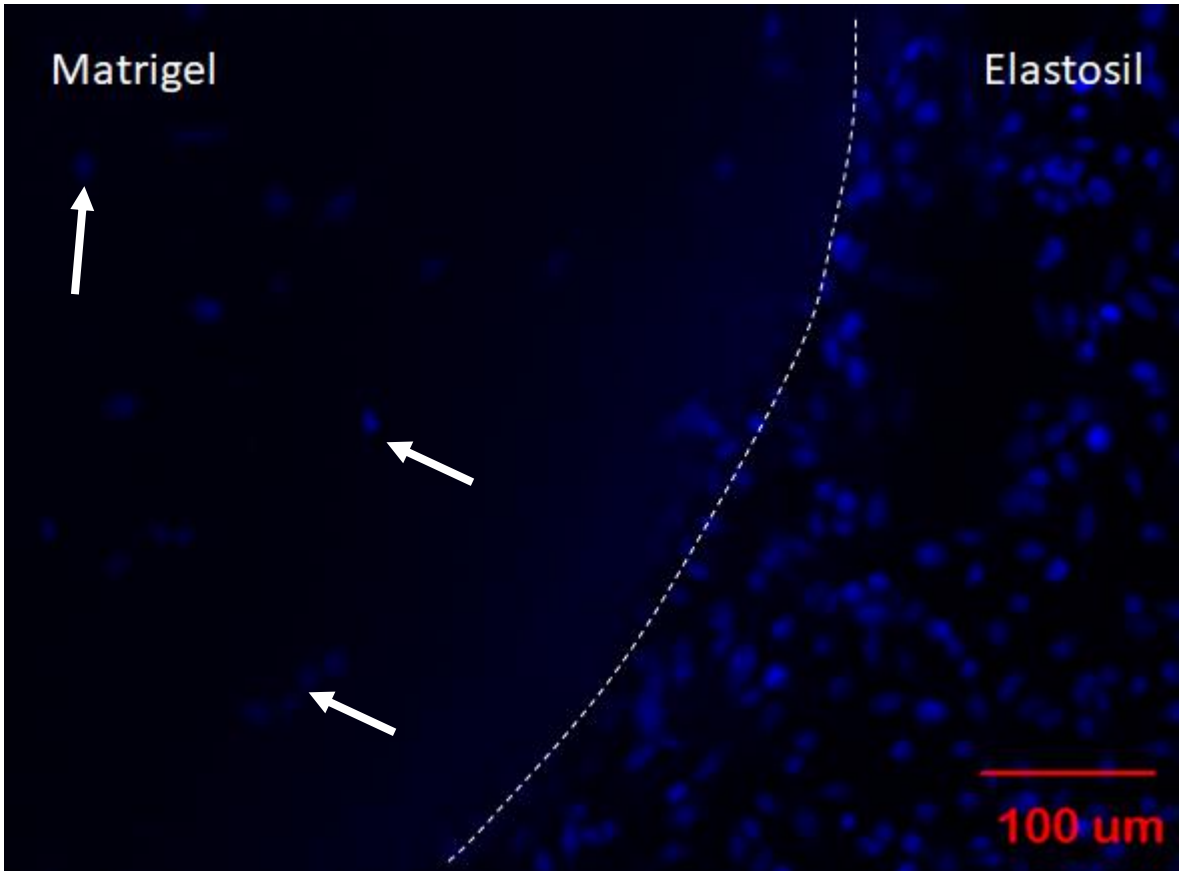

Figure 15 Zeiss i3 Spinning Disk Confocal Image of the upper surface of the 3mg/ml Matrigel cylinder. *The right half of the image displays the MDA-MB-231 cells attached to the Elastosil rubber of the CBW, whilst the left half of the image displays the 3mg/ml Matrigel cylinder. The dashed line represents the boundary between the two materials, with greater cell numbers on the Elastosil Rubber compared to the Matrigel. Arrows to the left of this line show a small number of cells visible compared to the densely populated area to the right of the dashed line.*

4.4 Imaging of hydrogels within the CBW

It was clear from working with both collagen and gelatin, that hydrogels can be produced within the CBW. In addition, the rigidity of the 5% Gelatin/EDCI/NHS cylinders enabled the cylinders to be removed, processed and imaged separately. However, it would be highly desirable for the CBW to be designed so that imaging and live cell imaging could occur without removal of the scaffolds. For this reason, experiments were performed to assess the ability of a spinning disc confocal microscope (Courtesy of Tobias Zech – Institute of translational medicine, Liverpool University) to image scaffolds within the CBW.

4.4.1 6mg/ml collagen scaffolds pre-seeded with fixed MDA-MB-231 within the CBW

In order to assess the design of the CBW on the feasibility of direct imaging of cells, the following experiment was performed: MDA-MB-231 cells were harvested and counted using a biorad TC20™ automated cell counter, with $2x10^6$ cells removed in 448µl of cell media and mixed with 50µl of 37% paraformaldehyde for 7 minutes before centrifuging. Cells were subsequently permeabilised in 0.1% Triton-X solution for 7 minutes and centrifuged before being resuspended in PBS and DAPI (1 in 7500) for 20 minutes before centrifuging. The fixed and stained cells were re-suspended in 240µl of collagen buffer, which was mixed with 1.8ml of type I bovine collagen. This resultant fixed cell-collagen suspension was syringed into 3mm and 4mm CBWs with glass cover slips on each end and incubated for one hour prior to being imaged using the Zeiss i3 spinning disc confocal microscope at 10x magnification.

Figure 16 shows a single slice of the subsequent Z-stack images that were recorded. As the coverslips were not removed from the gels prior to imaging, the collagen gels retained their shape and structure and imaging to a depth greater than 1mm was possible. During imaging, it became apparent that the microscope utilises two stages, a 300µm fine-focus stage that enables Z-stacking over a short distance and a larger, main stage that can enable imaging in the Z-axis to the maximum length of the lens. Whilst it was possible to record multiple 300µm stacks within the gel, it was not possible to combine the smaller 300µm stacks together due to a technical issue with the software that communicates between the two stages. Appendix A (PDF Copy) shows a 300µm stack of the MDA cells pre-seeded within the collagen gels. Whilst no accurately defined length of imaging could be recorded, the ability to successfully image multiple 300µm sections throughout the gel suggested that the predominant factor that would limit the length of cell imaging was the working distance of the microscope lens. As the Zeiss i3 microscope has a working distance of 5mm, two key conclusions were made:

1. The current design of the CBW with 12mm hydrogel cylinders was too long to image in its entirety. Inverting the CBW and imaging both ends would allow for a maximum depth of approximately 10mm, but concerns were raised regarding the splicing together of the two sections when imaged from different ends. As such, with the exception of purchasing a different microscope lens, a maximum length of 5mm would be considered a more realistic length for imaging.
2. With the current design, the distance between the hydrogel and the overlying cover slip must be minimised to ensure that there is no wasted imaging space. Desiccation or swelling of the gels when incubated could result in a large gap between the lens

and the top of the gel. This gap would reduce the total amount of the gel that could be imaged.

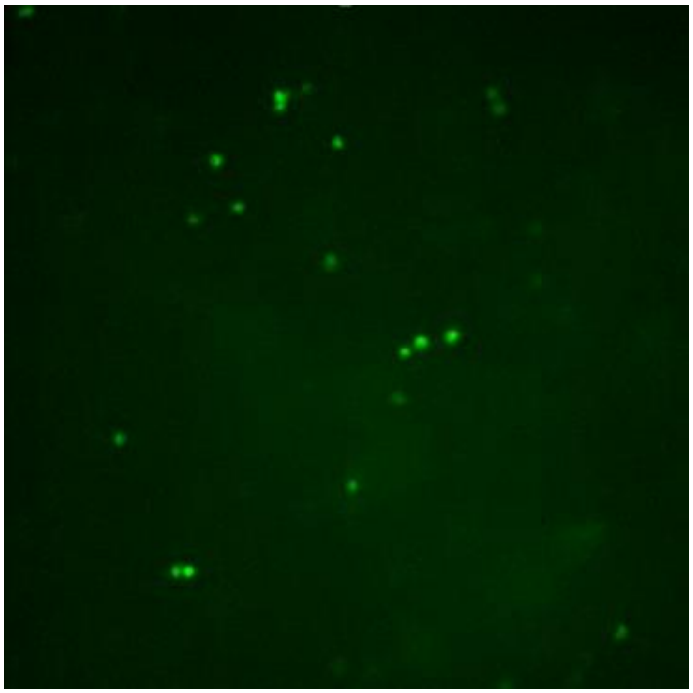

Figure 16 6mg/ml collagen hydrogel containing MDA-MB-231 cells imaged within a 4mm CBW. *(Note: single slice taken from video)*

Following this imaging session and further informal collagen experimentation, a decision was made to only use the 2mm CBWs for future experiments as collagen poured in 4mm and 3mm CBWs rarely had adequate surface tension or support to survive extended culture. The collagen when poured in the larger diameter cylinders would frequently be disrupted during removal of the coverslip and with addition of media.

4.5 Migration Experiment 1 - 6mg/ml collagen hydrogels with L929 Fibroblasts

Following the initial attempts at imaging, it became clear that migration into the collagen hydrogels could be visualised using the imaging strategy outlined above without removal of the gels from the CBW. Whilst some issues were highlighted regarding the length of the gels, an experiment was performed utilising the same 6mg/ml collagen cylinders.

4.5.1.1 Methods

Firstly, four 2mm CBWs were cleaned with 70% Ethanol and autoclaved. Collagen was poured into two CBWs using the upright fabrication technique with the remaining two CBWs poured using the inverted technique. To further investigate the role that UV cross-

linking may have upon the stiffness of the collagen hydrogels, one CBW from each fabrication technique arm were treated with 0.45J/cm^2 UV light for a total of 30 minutes, whilst the remaining two CBWs not treated with UV light were given an additional 30 minutes in the incubator.

CBWs were subsequently transferred to a non-coated 6 well plate and cover slips were removed carefully with sterile tweezers. Cell media was supplemented with 10% FCS, 1% Pen-strep and 2% L-Glutamine for use in the lower compartment, whilst the same combination without FCS was utilised for the upper compartment. 2x10^6 L929 fibroblasts were harvested and counted using the biorad TC20™ automated cell counter and seeded onto the upper compartment of all four CBWs. 20ng/ml of EGF was added to the lower compartments, which along with the FCS was intended to act as the chemoattractant for cell migration. The 6 well plate, which is diagrammatically represented in Figure 17, was transferred to an incubator at 37ºC with 5% CO_2/air mixture. Media was changed at 24 hour intervals until the end point of 72 hours was reached.

At 72 hours, the media was removed and the CBWs were gently rinsed with PBS. Cells were subsequently fixed by adding 4% PFA solution to the upper and lower compartments and left at -4ºC for 12 hours. PFA solution was then carefully removed and 0.1% Triton-X solution was placed in the upper and lower wells for 20 minutes before the CBWs were gently rinsed with PBS. Staining of cells took place by using Invitrogen™ Alexa Fluor™ 647 Phalloidin (Life Technologies Ltd, Paisley, UK) at 1x concentration (25µl 40x solution in 1ml PBS) for 1 hour before gently rinsing with PBS. Finally, the CBWs were soaked with 2ml of PBS containing Invitrogen™ DAPI dilactate (1 in 4000) for 2 hours. Cover slips were repositioned in the upper compartment of the CBWs before imaging took place.

4.5.1.2 Results

At 48 hours, cells were visualised on the bottom of the 6 well plate in wells B2 and B3, whilst wells A2 and A3 did not, suggesting that the collagen seal within the CBWs remained intact for the CBWs poured using the upright fabrication technique. Visually at 72 hours, the collagen hydrogels in well A2 (without UV) seemed the most consistent, but all CBWs underwent initial processing with PFA.

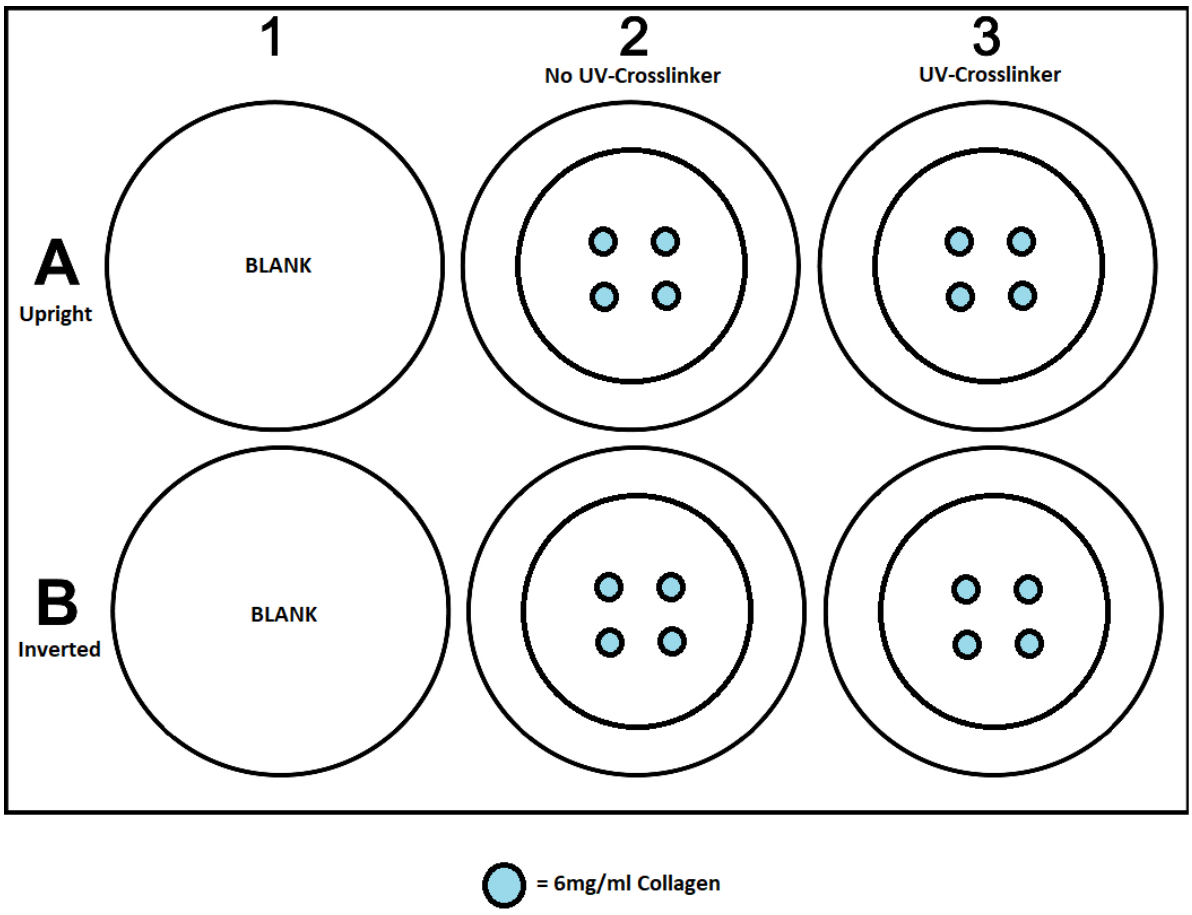

Figure 17 Diagram of 'migration experiment 1'. *2mm CBWs with collagen hydrogels fabricated using the upright (Row A) and Inverted (Row B) techniques. CBWs in column 3 received further UV-Crosslinking.*

Following fixation and staining, it was apparent that CBWs in wells B2 and B3 were incomplete. Due to a large gap between the coverslip and the residual gel, no imaging could be recorded. CBWs from wells A2 and A3 displayed viable cell growth on the upper surface of the collagen hydrogels. Figure 18 shows an orthogonal reconstruction of a Z-stack series of images taken of the top of a collagen hydrogel in well A2. The curvature of the cell plane represents the meniscus formed by the hydrogel following pouring. Despite cell attachment and growth, no migration was evident. Figure 19 shows montage Z-stack images of the upper surfaces of collagen hydrogels from wells A2 and A3. Again, whilst these images demonstrate the concavity created naturally due to the meniscus of the gel, there was no clear migration demonstrated on any of the cylinders imaged.

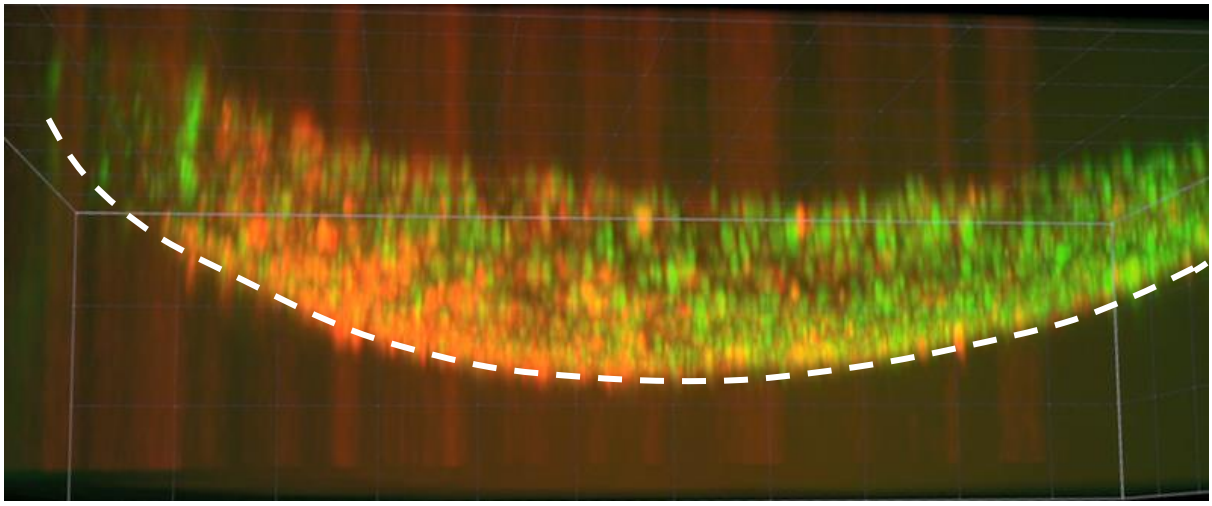

Figure 18 Orthogonal Reconstruction of Z-stack images of the upper surface of a 2mm diameter, collagen hydrogel (Well A2) stained for Actin (Red) and DAPI (Green). *The image has been reconstructed from a series of individual slices to show the top of the collagen hydrogel from a lateral position. Note the evident curvature of the cell plane depicted by the dashed line, which is due to the meniscus created when pouring the collagen hydrogel. This dashed line represents the top of the gel, where cells appear to have attached and proliferated on the superficial surface with no clear migration into the collagen hydrogel seen (below dashed line). The overall depth of gel visualised measures approximately 70 microns. Migration into the gel would be seen as clear cell penetration towards the bottom surface of the image.*

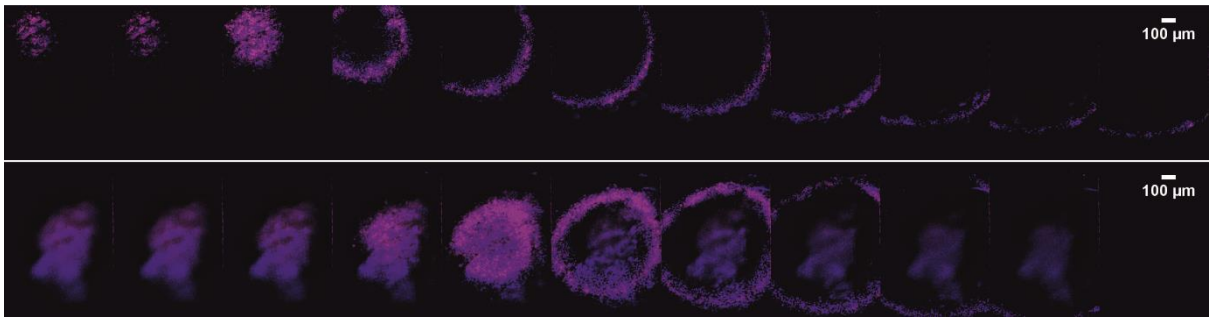

Figure 19 Z-Stack Montage of L929-Fibroblast cells on 6mg/ml collagen hydrogels: *Each montage displays 11 images (Left to Right) of subsequent 5µm slices from the lowest point (Left) to the highest point (right) stained with DAPI (Cyan) and Phalloidin (Magenta). Top = Collagen Gel from well A2. Bottom = Collagen Gel from Well A3.*

4.5.1.3 Discussion

Aside from the continued issues relating to collagen gel consistency and integrity, three further issues were raised following this experiment. Firstly, and most fundamentally, no migration was evident into the collagen gels. Three possible factors could have accounted for this:

1. No growth factor gradient was detectable by the L929 fibroblasts due to the length of collagen cylinders.

2. The collagen hydrogels at 6mg/ml were too stiff for the fibroblasts to invade into or a longer time period in culture would be required.
3. The cell line utilised at passage 14-20 may have lost their capacity to invade.

The issue relating to the length of the collagen gel and a possible lack of chemoattractant gradient seems plausible. As growth factors were added to the lower compartment, unless the chemoattractants were imbibed into the gels and wicked upwards, it is unlikely that the cells would have been able to sense the chemotactic agent present. This issue could be circumvented by pre-mixing chemo-attractant into the gels or by shortening the length of the gels altogether. As previous imaging issues have already highlighted the excessive length of the gels, this finding further reinforces the recommendation that the CBW should be redesigned with a shorter cylinder length to increase the likelihood that chemoattractants will be detected by cells. Furthermore, for revascularisation of the dental pulp to become a predictable strategy it is highly probable that strong chemoattractant profiles will be required. As part of this requirement, the liberation of dentine sequestered growth factors and their effects upon cell proliferation and expression has gained traction in the pulp biology literature (Tomson et al., 2017). With this in mind, the CBW could enable multiple chemoattractant profiles to be investigated in great detail and as such, optimising the length of the cylinders for this purpose seems an important and logical consideration.

To investigate the second issue outline above, a further experiment was performed to assess the ability of L929 fibroblasts to migrate into 6mg/ml collagen, whilst the third issue could be investigated with human primary cells following CBW optimisation.

4.6 L929 Fibroblasts and MDA-MB-231 cell exclusion zone assays with 6mg/ml collagen

In order to assess the ability of the chosen cell lines to invade into the collagen hydrogels, a cell exclusion zone assay was performed utilising L929 fibroblasts and MDA-MB-231 cells. Whilst it is clear that migration and invasion assays associated with monolayer cell cultures are not representative of the complex cell-matrix interactions witnessed in vivo (Baker and Chen, 2012, Duval et al., 2017), these experiments are quick to perform and provide a large amount of information about the speed of migration and possible strategies for optimising the matrix bioactivity. In these experiments, no additional cytokines were added to the collagen matrix, but prior to further experimentation, L929 fibroblasts were transduced with a green fluorescent protein (GFP) to enable imaging of cells in the CBW without requiring fixation and staining.

4.6.1 Viral transduction of L929 fibroblasts with a green fluorescent protein

Stable GFP expression was introduced to the L929 fibroblasts via lentiviral mediated plasmid transduction. The cytomegalovirus-driven plasmid, pGIPz, also expresses puromycin resistance, which allows antibiotic selection of the L929 fibroblasts expressing eGFP. Cells expressing fluorescence can subsequently be imaged and monitored in prolonged culture without additional staining. Firstly, $5x10^4$ L929 fibroblasts were seeded in 6 well plates and allowed to reach subconfluency. 120µl of lentivirus (OriGene, Herford, Germany) was added to 6ml of DMEM into which 3µl of Polybrene® (Hexadimethrine bromide) was added (Polybrene stock 12µg ml^{-1}/working solution 6µg/ml). Polybrene® serves to facilitate the transduction of the virus into the cells by modifying cell surface electrical charge. 1ml of this solution was added to each well and left overnight.

Antibiotic selection for eGFP-expressing cells was performed using puromycin (GibCo, Life Technologies Ltd, Paisley, UK), an aminonucleoside antibiotic that inhibits translation of proteins. Puromycin selection involves the optimisation of the antibiotic concentration, which was performed using the following technique. Firstly, media containing the lentiviral particles were removed from the subconfluent L929 fibroblasts and cells were gently rinsed with PBS. Puromycin stock 500µg/ml was diluted 250x to produce a working solution of 2µg/ml and 2ml of media containing different concentrations of puromycin were added to each well in duplicate (Figure 20) and cells were imaged after 24 hours.

At 24 hours, there was limited expression of GFP and no clear selection for transduced cells was evident. For this reason, the same experiment was repeated with greater concentrations of puromycin. Puromycin was reconstituted from stock to produce a working solution of 2.5µg/ml (5µg in 2ml). Increasing concentrations were trialled and cells imaged after 24 hours (Figure 21). Following 24 hours, a puromycin concentration of 20µg/ml appeared optimal for selection of transduced cells and this concentration was added to all four wells and refreshed with media changes every 48 hours for 7 days. At this point, cells were harvested and combined in a T75 flask with cell media and 20µg/ml until used in the circular invasion assays.

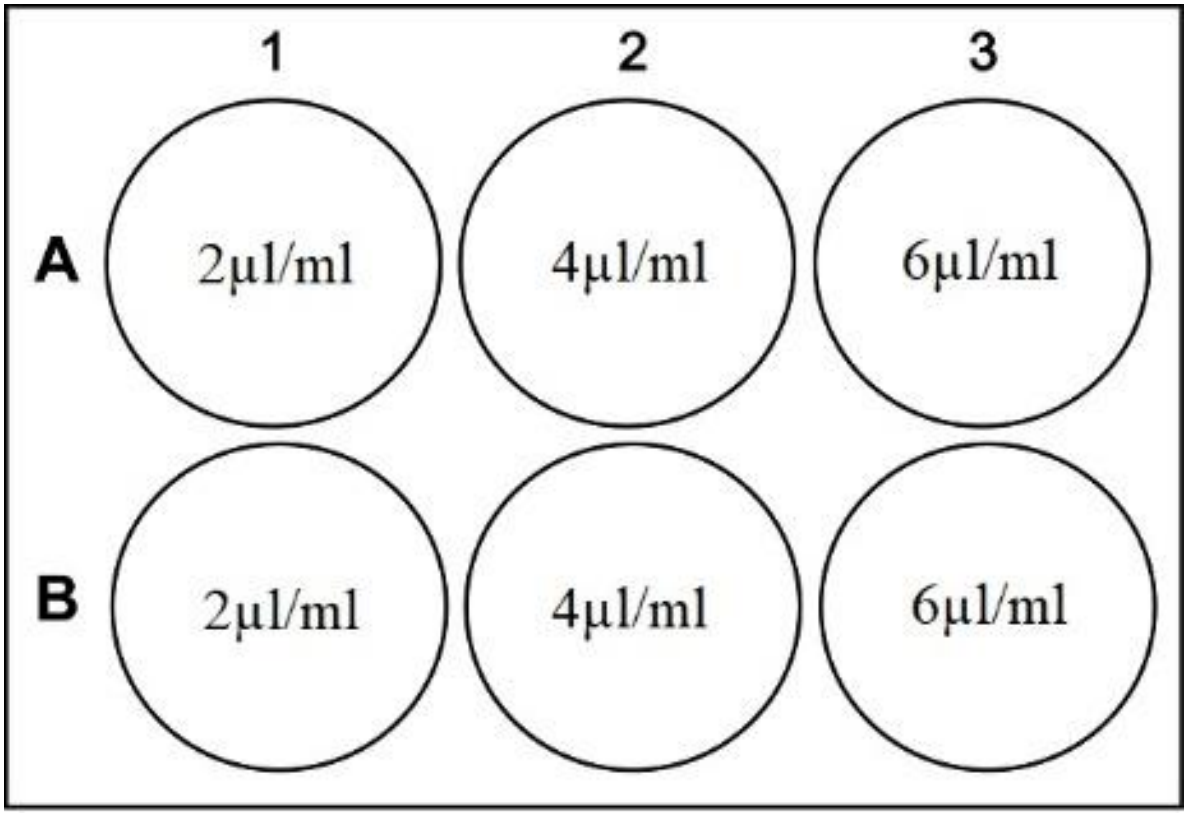

Figure 20 First Puromycin Selection of lenti-virus tranduced L929 fibroblasts

#

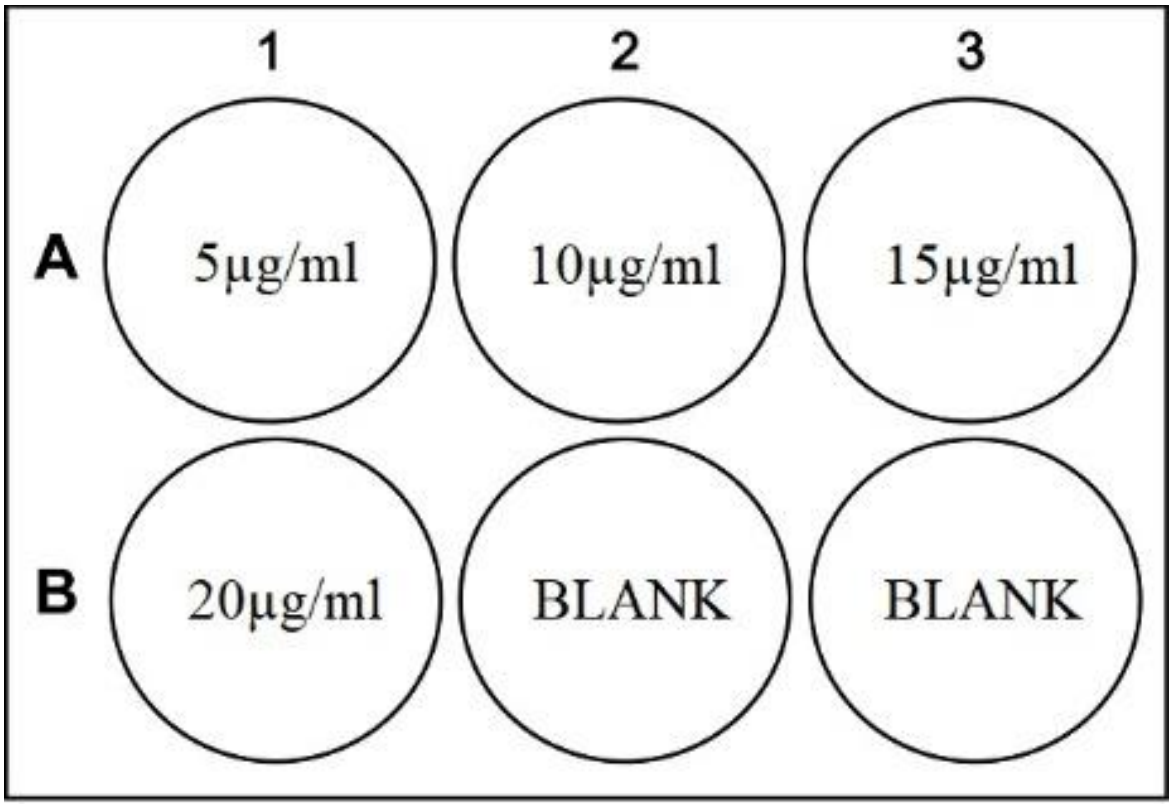

Figure 21 Second Puromycin Selection of lenti-virus tranduced L929 fibroblasts

4.6.2 Cell Exclusion Zone Assays

4.6.2.1 Methods

Cell exclusion zone assays were performed using both cell lines available – GFP-L929 Mouse fibroblasts and triple negative Human Adenocarcinoma Cells (MDA-MB-231). Sterile 2 well, silicone inserts with a defined cell free zone of 500µm (Ibidi GmbH, Gräfelfing, Germany) were positioned in the centre of a 24 well plate using sterile tweezers. $3x10^4$ cells from both cell lines were harvested in 80µl of media and seeded into both chambers of the inserts in duplicate. Cells were incubated overnight in 37°C with 5% CO2/air mixture allowing them to double in number and reach subconfluency. After 24 hours, silicone inserts were removed and the wells gently rinsed with 1ml of sterile PBS. 6mg/ml medical grade, type I, bovine collagen was prepared as per previous experiments using a sterile buffer and 100µl was poured into each well to cover the remaining cell monolayer. Cells were incubated and imaged overnight for 16 hours using the Carl Zeiss ApoTome Inverted Microscope.

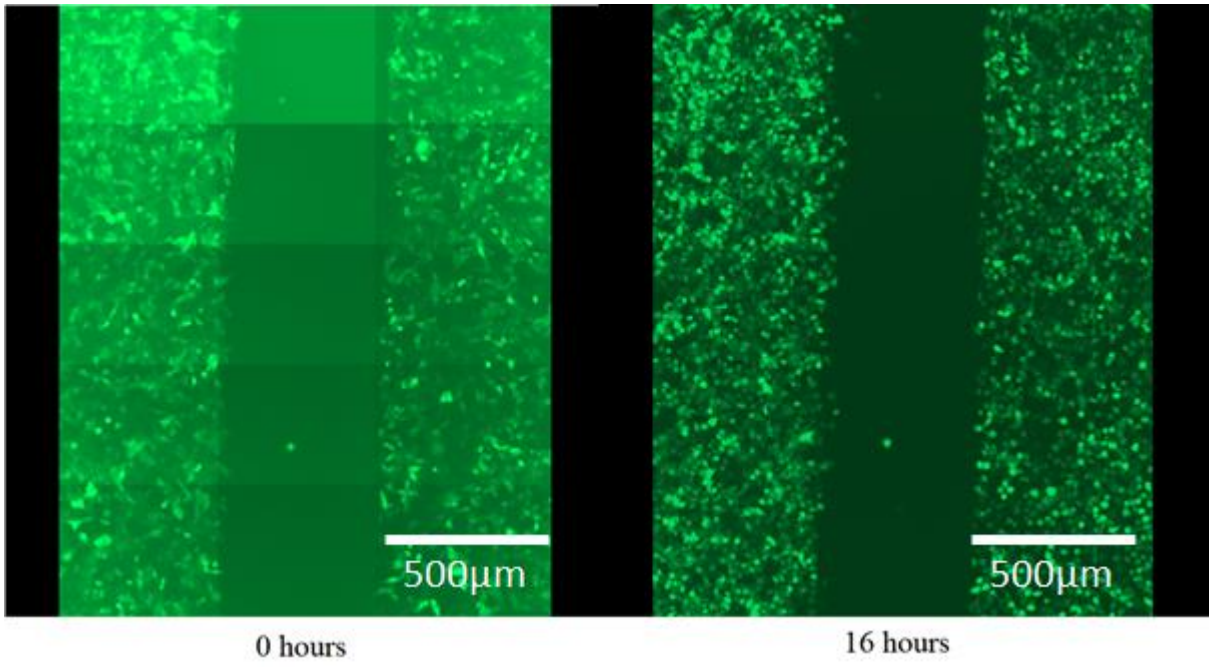

Figure 22 Cell exclusion zone assay with GFP-L929 Fibroblasts coated in 6mg/ml type 1, bovine collagen. *Left - 0 hours. Right - 16 hours.*

4.6.2.2 Results

Figure 22 displays the start (0 hours) and end (16 hours) time points for the migration assay using GFP-L929 fibroblasts. Whilst cell growth and division were evident, no clear invasion into the 6mg/ml collagen was seen. Figure 23 displays a bright field image with equivalent time points for the MDA-MB-231 cell line, which is a known invasive adenocarcinoma cell line (MacDonald et al., 2018, García et al., 2016). Appendix B (GFP-L929) & C (MDA-

MB-231) show the video sequences for the two assays respectively (PDF Copy). Progressive migration is evident from both sides of the 500µm gap, which by the end point of 16 hours had reduced by approximately 50%.

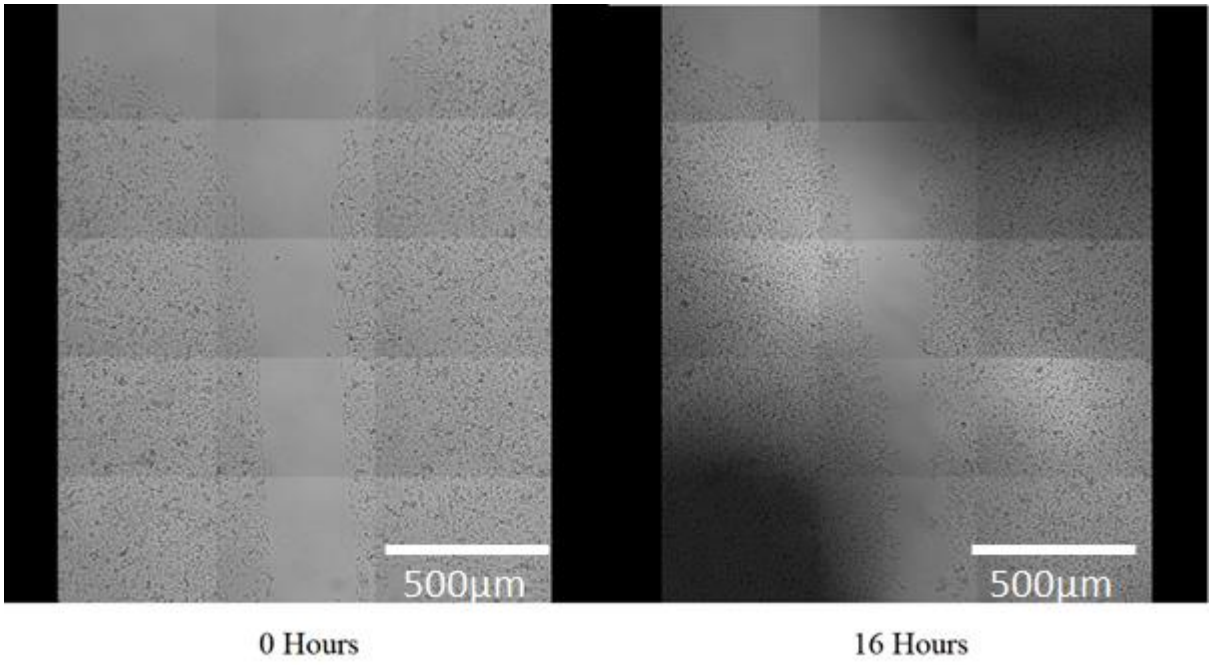

Figure 23 Cell exclusion zone assay with MDA-MB-231 adenocarcinoma cells coated in 6mg/ml, type I, bovine collagen. *Left - 0 hours. Right - 16 hours.*

4.6.2.3 Discussion

Following the cell exclusion zone assays, it was clear that the L929 fibroblasts utilised in 'migration experiment 1' were unable to invade into the stiffer 6mg/ml collagen hydrogels over a 16 hour time period. Therefore, for the purpose of validating the CBW as a 3D migration/invasion tool, the more aggressive MDA-MB-231 cells appeared to represent a more desirable cell line. However, these cells do not represent a relevant cell line encountered in pulp regeneration. Whilst the L929 fibroblasts failed to migrate within migration experiment 1, it could be argued that the addition of chemotactic growth factors in the collagen hydrogels could influence the L929 fibroblasts migration or that primary cells may retain a more migratory phenotype.

Despite the known aggressive nature of the adenocarcinoma cell line, invasion into the 6mg/ml collagen was slow at a rate of approximately 100-150µms in 16 hours. As no attempt was made to characterise the architecture of the collagen hydrogel, it is unclear how the microchannels formed within the 3D collagen meshwork will have restricted or inhibited the speed of cell progression (Paul et al., 2017). The study of scaffold porosity and interconnectivity along with material characteristics such as linear and non-linear elasticity

is an extremely exciting and interesting field for tissue engineering (Doyle et al., 2013). Previously, 3D collagen gel elasticity has been shown to influence the migratory behaviour of cells from lamellipodia-based to lobopodia-based migration, that is mediated by RhoA-ROCK-myosin II activity (Petrie et al., 2012). Further study on the mechanical characteristics of scaffolds and their impact upon cell migration is required.

This slow invasion noted (Trepat et al., 2012) above has highlighted that the previous end point of 72 hours for the CBW migratory experiments is likely to be inadequate when considering the clinical challenge faced with pulp re-vascularisation. A vacant pulp canal space of 12mm, whilst long, would not be considered excessive for complete pulpal regeneration and as such the bioactivity and topography of the tissue scaffolds would likely require modification to facilitate and accelerate cell migration i.e. through the development of macro-porous scaffolds. Unfortunately, extended culture beyond 72 hours with the current collagen formulation in the CBWs was unpredictable, as the gels would often lose position and slip out of the cylinders. This therefore raised three further issues that require consideration when redesigning the second generation CBW. The first consideration relates to maintaining the position of the hydrogels within the CBW for extended cultures. In this regard, redesigning the internal cylinders of the CBW as cones, with a slight taper towards the inferior end may help to retain hydrogels in situ during prolonged culture. The second consideration relates to the tissue scaffolds themselves and how modification of the scaffolds may facilitate cell migration and nutrient exchange. In this regard, fabrication of macro-porous hydrogels would provide internal channels for cell movement and nutrient exchange. Thirdly, the addition of growth factors or growth factor gradients to the hydrogels, may serve to encourage cells to migrate more readily into and through the entire gel.

4.7 Dye-Leakage Trial with Bromophenol Blue and 1% Agarose Hydrogels

To assess the ability of hydrogels within the CBW to maintain the “seal” of the upper compartment, bromophenol blue, a dye with a small molecular weight (669.96g/mol), was added to the top of 1% agarose hydrogels in the CBW. This further served the purpose of assessing how easily growth factors could be added to these hydrogels and how quickly the molecules would be expected to permeate through the gels. It also confirmed that consistent hydrogels can be produced using the inverted fabrication technique described earlier (4.1.1). It is well understood from electrophoresis experiments that the water content and density of the gel will fundamentally affect the degree of dye penetration. For this experiment, 1% agarose hydrogels were produced by mixing 0.5g of agarose powder (GibCo, Life

Technologies Ltd, Paisley, UK) in 50ml of PBS before heating until all powder was dissolved. Gels were syringed into 4mm CBWs and allowed to cool for 20 minutes until fully set.

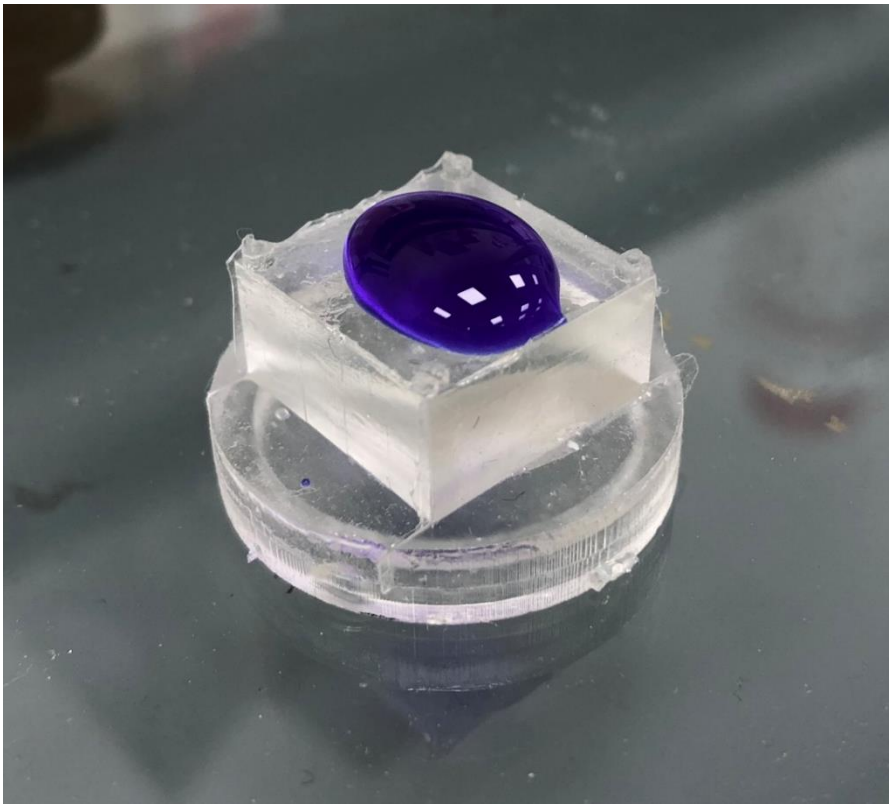

Figure 24 Bromophenol Blue Dye on 1% Agarose Hydrogels in a 4mm CBW

Figure 24 displays 400µl of bromophenol blue dye on a 4mm CBW with 1% agarose gel cylinders (poured using the inverted fabrication technique). 400µl was considered the optimal volume of fluid that could be pipetted onto the CBW in the inverted position, without leakage over the side. This technique and volume could be used to seed cells onto the bottom of the CBW before reverting the CBW and adding growth factors into the upper compartment. This supported the concept that the CBW could be used as a bidirectional in vitro tool. Figure 25 shows 1% agarose hydrogels removed from the CBWs after 3 hours of Bromophenol blue coating. Whilst a fairly crude strategy for introducing growth factor gradients, it presents a different facet for the CBW as a tool that can also investigate different growth factors gradients. It further confirms that well adapted hydrogels will maintain an adequate seal for fluid in the upper compartment. As 1% agarose appeared significantly stiffer than the 6mg/ml collagen trialled, this further suggested that alternative stiffer biomaterials may be more suited for model validation within the current CBW design limitations.

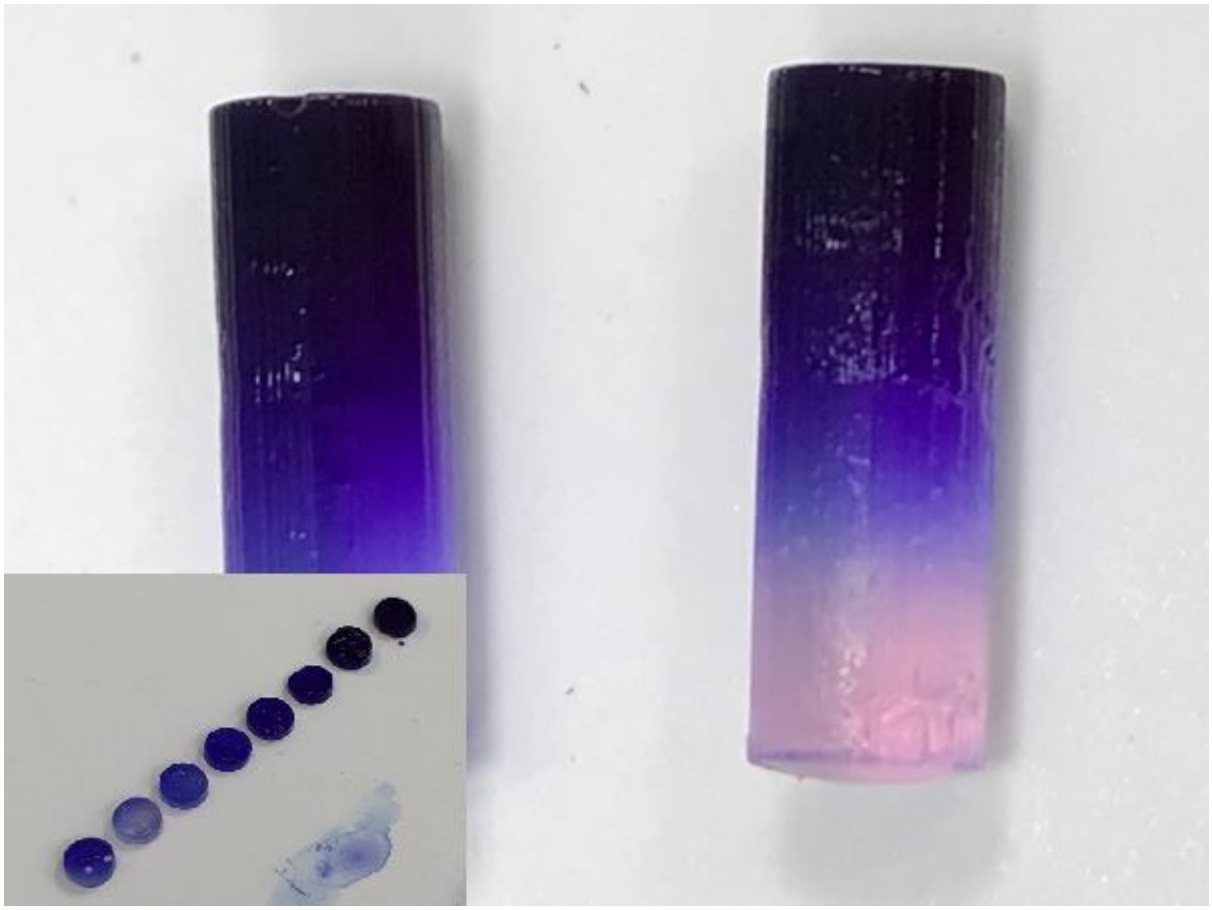

Figure 25 1% Agarose Hydrogels (Seen in Figure 24) removed after 3 hours of bromophenol blue application to the top surface of the gel. *Inset bottom left shows the 12mm gels sliced (~1mm) demonstrating penetration of bromophenol blue through the entire gel).*

4.8 L929 Mouse fibroblasts cultured on EDCI-NHS crosslinked gelatin cryogels

4.8.1 Cryogelation of carbodiimide-crosslinked gelatin as a potential tissue scaffold for the CBW

In an attempt to improve the degree of migration into the tissue scaffolds being investigated, macro-porous hydrogels were investigated. Whilst numerous strategies are available for producing porosity in hydrogels, cryogelation or ice templating was the first to be trialled in this study. The process of cryogelation involves the rapid cooling of an aqueous solution to temperatures below zero. During this process, ice-crystals form within the semi-frozen solution, which concentrates the solutes into a smaller volume referred to as the non-frozen liquid micro-phase (NFLMP) (Van Vlierberghe, 2016, Van Vlierberghe et al., 2011).

Subsequent sublimation of the solvent in these frozen gels removes water to leave a porous and interconnected scaffold structure. When these hydrogel constituents are treated with appropriate crosslinking agents, the NFLMP maintains its highly macroporous structure that can be used in a range of biomedical applications. Since gelatin undergoes a very rapid physical gelation process upon cooling, it has been reported that a true "cryotropic" gelation, i.e. one where ice crystals form within the solution prior to physical gelation, is impossible with concentrations of 10% w/v and above (Van Vlierberghe, 2016). 5% w/v gelatin was subsequently used in the following experiments, with chemical crosslinkers EDCI and NHS added to the solution prior to freezing.

4.8.2 Methods

4.8.2.1 Cryogelation and Sublimation of 5% Gelatin-EDCI-NHS hydrogels.

A 5% Gelatin-EDCI-NHS (EDCI - 10mM/NHS - 4mM) solution was produced (section 4.2.1). The solution was immediately pipetted using pre-warmed pipette tips into the following receptacles:

- 3 x 50mm Petri dishes (4ml in each)
- 600µl of solution syringed into a 4mm button well

Following pouring, the samples were immediately transferred to the following freezers for cryogelation:

- 2 x 50mm Petri dishes inserted in a -20°C freezer
- 1 x 50mm Petri dish inserted in a -80°C freezer
- 600µl of solution syringed into a 4mm button well and inserted in a -80°C freezer

After 36 hours in their respective freezers, the samples were removed on dry ice in an ice box and inserted into a freeze dryer for 24 hours. Sublimation was confirmed by visual assessment. Samples were then soaked overnight in 300ml of dH_2O per sample at 37°C with 5% CO_2/air to remove unreacted, water soluble cross-linker. Scaffolds were subjected to 10 minutes of UV irradiation and ozone in a class II biosafety cabinet. Samples were subsequently rinsed with PBS before being placed in 100mm petri dishes (larger petri-dishes were required due to swollen state of gel) and soaked in cell media (DMEM/10%FCS/1%Pen-Strep) for 48 hours at 37°C with 5% CO2/air mixture.

4.8.2.2 Culture of L929 Mouse fibroblasts on EDCI/NHS crosslinked 5% Gelatin Cryogels – "Pizza Slices"

The two 5% circular samples that underwent cryogelation at -20°C were then each sectioned into 6 evenly portioned slices and transferred to non-treated, polystyrene 6-well culture plates (6-Well, CytoOne® plate, non-treated – StarLab, UK). Each scaffold was assigned to its own 6 well plate with one "slice" per well. L929 mouse fibroblasts at passage 16 were seeded onto each slice at a density of 0.3×10^6. 2ml of cell media was added to each well (DMEM/10% FCS/1% Pen-Step) and cells incubated at 37°C with 5% CO_2 for a total of 7 days. Two slices from each plate were fixed at days 1, 3 and 7. Media was carefully changed with small pipettes at day 3 for the 7 day samples only. For fixation, samples were transferred to a new 6-well plate at the pre-designated time points. Samples were rinsed for five minutes in 1x histology PBS before a one hour soak in 4% PFA. After which, samples were rinsed twice for five minutes with 1x histology PBS. Samples were then stored in the fridge until staining.

Following fixation of all samples on day 7, the samples were stained and mounted on glass slides and visualised using the Carl Zeiss ApoTome Inverted Microscope. Images were recorded using the Z-stacking function on the Carl Zeiss Zen software and post processing of images was performed using Fiji – an open source platform for biological image analysis (Schindelin et al., 2012). Samples were inspected under the microscope and three central areas of the gels were imaged. Staining was performed by removing all PBS and rinsing for five minutes with 1x histology PBS. Cells were permeabilised with 0.5% Triton™ X-100 for 15 minutes before being rinsed twice with 1x histology PBS for eight minutes. Alexa Fluor® 488 phalloidin stain (ThermoFisher Scientific, UK) was mixed with 1x Histology PBS at a ratio of 1:250 (60ul:14940ul) and samples were soaked for 30 minutes in 2ml of stain at 4°C followed by three, five minute rinses with 1x histology PBS. Finally samples were mounted on labelled glass slides and covered with ProLong™ Diamond Antifade mountant with DAPI (ThermoFisher Scientific, UK) and a glass cover slip before being stored at -4°C in a dark microscope slide holder before imaging.

4.8.3 Results

Due in part to the large dimensions of the cryogels and amount of time and data required to image the gels, it was not feasible to image the entire cryogel samples. Furthermore, as cells were seeded centrally, cell growth was not evident on all areas of the gels. The 50mm petri-dish cryogel sample produced by inserting EDCI-NHS crosslinked gelatin into a -80°C freezer along with the 4mm CBW samples subsequently dissolved when rehydrated overnight in dH_2O at 37°C. Autofluorescence was detected from the remaining gelatin

cryogels which was more noticeable using the Cyan filter on the ApoTome i.e. when imaging for DAPI Nucleus staining. Figure 26 displays confocal microscope images of L929 fibroblasts cultured on the 5% gelatin cryogel slices at time points of 24, 72 and 168 hours. Whilst increased cell growth and proliferation is visible by day 7, it is not clear why minimal cell growth was visible by day 3. Figure 27 shows confocal images of the duplicate 5% gelatin cryogel samples with L929 cells fixed the same time intervals of 24, 72 and 168 hours. A more conventional pattern of cell proliferation and expansion is visible compared to Figure 26. Rows 3 and 4 of Figure 27 represent two slices 70µm apart in the Z axis. Figure 28 presents an additional region of the day 7 cryogel pictured in Figure 27.

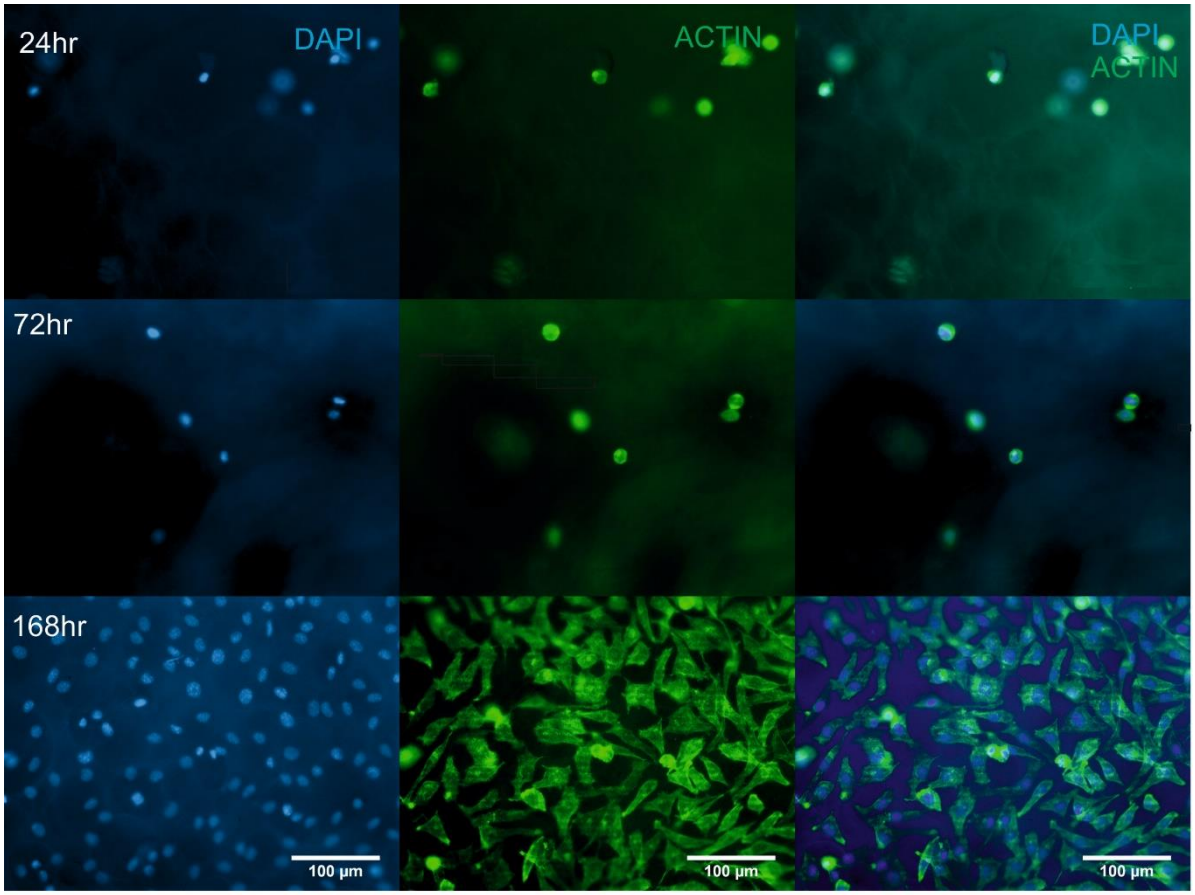

Figure 26 L929 Mouse Fibroblasts cultured on 5% gelatin-EDCI-NHS cryogels. *Montage confocal microscope images taken of the top of the gels representing time points 24 hours, 72 hours and 168 hours from the first samples. Left column – DAPI stain. Middle – Actin Stain (Alexa Fluor® 488 phalloidin). Right – DAPI/Actin stain. An increase in cell number and cell growth is evident between time points – 24 and 168 hour. Furthermore, cell spreading is evident in the bottom right image, which shows the presence of numerous projections (lamellipodia) formed by the stained actin cytoskeleton.*

4.8.4 Discussion

Firstly, the crosslinked gelatin scaffolds that underwent cryogelation at -80°C dissolved upon rehydration with dH_2O at 37°C. This suggests that these gels were inadequately crosslinked, which is interesting because the gels were produced from the same mixture as the cryogels that were subsequently seeded with fibroblasts that underwent cryogelation at -20°C. One possible consideration relates to the low concentrations of EDCI and NHS that were utilised. The minimum quantity of EDCI required for cross-linking has been defined in the literature, which is similar to the molarity used within these experiments (Van Vlierberghe, 2016). The lowest concentration was utilised to increase the working time of the EDCI-Gelatin mixture to avoid chemical crosslinking prior to casting in the appropriate dimensions. It is therefore possible that the rapid freezing process associated with cryogelation at -80°C reduced the activity of the crosslinking process to such a level that the gels were unstable at 37°C. Furthermore, it is highly likely that the stable cryogels produced at the higher temperatures of -20°C had cross-linked prior to freezing and as such these cryogels are likely to display different topographical arrangements than cryogels that are cross-linked after freezing. In fact, it is possible that the subsequent cryogels, displayed large pores that were poorly interconnected, as the ice crystals form within previously gelled hydrogel (Plieva et al., 2006), rather than in the unfrozen solution. A poorly interconnected gel would impede cell migration.

The process of 'ice templating' during the cryogelation process refers to the process of using frozen water crystals to template the subsequent architecture of the cryogel (Bencherif et al., 2013). The frozen solvent serves to compress the gelatin and crosslinker into smaller areas known as the non-frozen liquid microphase in a process also referred to as cryoconcentration. The greater concentration of crosslinker and solute serves to accelerate the cross-linking reaction. Therefore, rapid freezing, such as that associated with freezing at -80°C, will also reduce the overall size of the ice crystals formed and will thus increase the area of the NFLMP resulting in fewer cross-links. Furthermore, the water-soluble cross-linkers, may remain confined to the frozen solvent phase and as such may have a reduced effect upon the adjacent gel. It has been known for many years that the freezing protocol influences the resultant porosity of a scaffold (O'Brien et al., 2004) and further investigation regarding the type of freezing protocol and its effect upon the architecture and stability of the cryogel is planned.

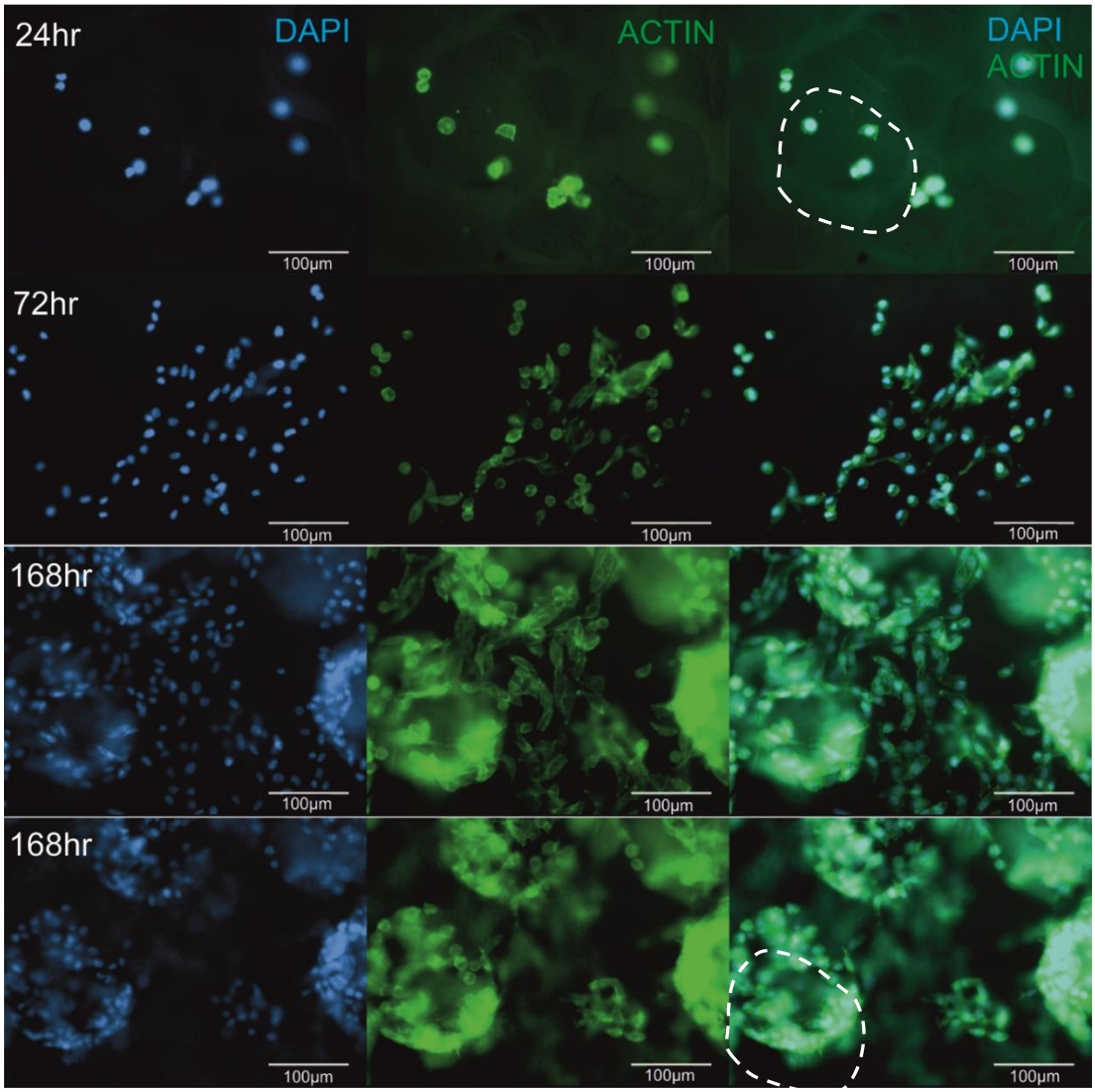

Figure 27 L929 Mouse Fibroblasts culture on 5% gelatin-EDCI-NHS cryogels. *Montage confocal microscope images representing time points 24 hours, 72 hours and 168 hours from the duplicate samples. Left column – DAPI stain. Middle – Actin Stain (Alexa Fluor® 488 phalloidin). Right – Merged DAPI/Actin stain. Note lines 3 and 4 above (168 hours) represent different slices of the same image 70 microns apart in the Z-axis, demonstrating attachment of fibroblasts on the top surface of the gel and also deeper into the cryogel pore structure. Pore structure outline has been demarcated with the dashed white line in the top right and bottom montage.*

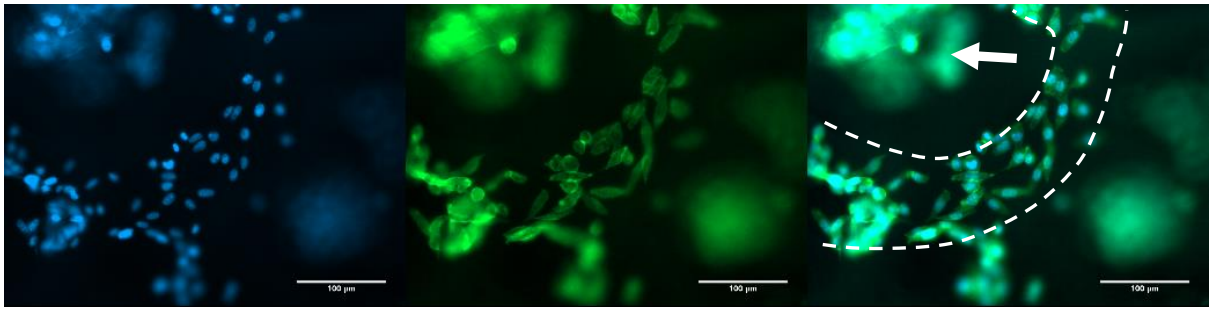

Figure 28 L929 mouse fibroblasts cultured on 5% gelatin-EDCI-NHS cryogels. *A confocal image of L929 fibroblasts within the pore structure of a 5% gelatin cryogel at day 7. Left - DAPI. Middle - Actin stain (Alexa*

Fluor® 488 phalloidin). Right - Merged DAPI/Actin. Note: cells out of focus (Arrow) at the top left of each image suggests cell survival at multiple positions (also demonstrated in figure 27) within the gel. The linear nature of the cells (outlined by white dashed line in right image) in focus demonstrates cell proliferation within a crease or pore of the cyrogel.

The images shown in section 4.8.3 show L929 fibroblasts cultured on 5% Gelatin-EDCI-NHS cryogels. Whilst no accurate µCT images were available to accurately calculate the pore sizes produced, the confocal images clearly demonstrate a macroporous structure to the cryogels, with pore sizes visible in the region of 150-175µm. This suggests that macroporous structures can be produced using chemically crosslinked gelatin despite the presence of chemical cross-linker prior to freezing. The interconnectivity of these macropores within the gels however, remains unknown.

As the experiment progressed, handling of the gelatin cryogels became more challenging due possibly to the imbibition of fluid into the gels and also the breakdown of the ECM by cellular enzymes. L929 cell growth on the sample fixed at day 3 in Figure 26 was minimal. It is possible that this slice was damaged during processing, because the duplicated image in Figure 27 displayed a much greater number of cells with greater spread in line with what would be expected following three days in culture. Rows 3 and 4 from Figure 27 represent different slices of the same cryogel section. These images clearly show co-localisation of cells within the porous structure of the cryogel along with a distribution through the gel of approximately 70-80µm. This suggests that macro-porous gels may offer cells an easier pathway for migration when compared to conventional hydrogels with a nanoporous structure. With regards to the clinical requirements for REPs, rapid speed of migration is desirable, allowing cells to penetrate further into the root canals, as well as offering greater space for nutrient exchange. Whilst these images are a selective representation of the entire cryogels, the large dimensions meant imaging of the entire cryogel was not appropriate for these initial pilot investigations into material production and suitability. The images selected clearly show fibroblast attachment, proliferation and migration into the macroporous cryogels and support previous work within the literature that EDCI-NHS crosslinked gelatin is a suitable substrate for tissue engineering purposes (Cammarata et al., 2015, Lai, 2010, Liang et al., 2004, Sung et al., 1999, Ulubayram et al., 2002, Van Vlierberghe, 2016, Yang et al., 2018). The production strategy utilised appears to be non-cytotoxic and enables cell attachment and proliferation.

The process of ‘freezing after gelation’ has been suggested as a less effective strategy for producing macroporous gels, as the interconnectivity between pores is said to be compromised (Plieva et al., 2006). Despite this, Figure 28**Figure 28** shows cells occupying a linear section of the cryogel, which may represent channels present between pores of the

gels. Whilst no attempt was made to assess the rate of gelation when EDCI and NHS was added to the gelatin, as discussed above, it was clear that the freezing cycle did influence subsequent crosslinking. An alternative strategy that should be investigated, involves the rehydration of lyophilised gelatin cryogels with EDCI-NHS solution (Van Vlierberghe, 2016). Using this strategy, no chemical cross-linking would occur prior to freezing, ensuring that the cross-linking process would have limited impact upon the resultant cryogel structure. In this instance, the freezing cycle utilised could be investigated more predictably.

Finally, it should be noted that chemically-crosslinked gelatin cryogels fabricated using the above strategy, produces a scaffold with defined dimensions and does not represent injectable biomaterial technology. As such, these materials offer perceived advantages in relation to their macroporosity, but this may reduce their ability to contour to the often aberrant and irregular anatomy of the root canal space of an immature tooth.

4.9 Gelatin cryogels fabricated within the CBWs

4.9.1 10% Gelatin Cryogels fabricated within the CBWs

In order to investigate the effects of different freezing cycles upon scaffold porosity, a 10% w/v gelatin solution was produced and the solution was pipetted into a range of CBWs and either inserted into a freezer for 48 hours at -20ºC or snap-frozen with liquid nitrogen. Samples were subsequently transferred into a freezedryer for 48 hours. After 48 hours, samples were removed and visually inspected to ensure the full lyophilisation process had occurred. Figure 29 displays the initial 10% gelatin cryogel trials following lyophilisation. These samples were cast within the CBWs prior to freezing and lyophilisation. No detrimental effects upon the CBW inserts, nor the resin negative were noted from freezing, including with liquid nitrogen, suggesting that the insert could withstand cryogenic treatment.

In addition, several plain cryogel samples were re-produced as above and sent for assessment with µCT after lyophilising and before rehydrating. Unfortunately, as no contrast was added to the solution prior to imaging, the assisting Professor R. Van ‘t Hof was unable to extract useful images for comparison between different freezing cycles. Further investigation of the structure produced via different cryogelation protocols is planned (see section 5.5).

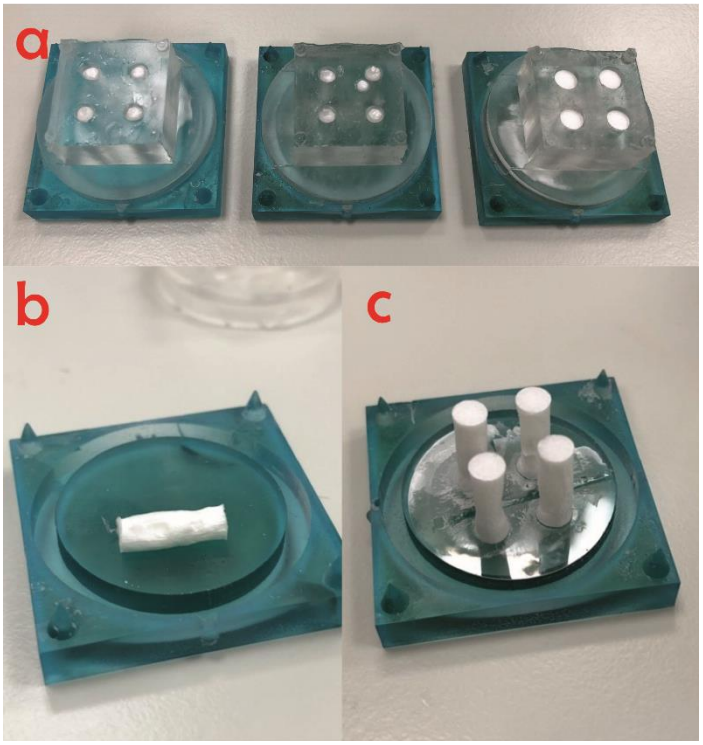

Figure 29 First trials of 10% gelatin cryogels in the CBW: *A) Gelatin cryogels in situ within the CBWs following lyophilisation B) A single 4mm diameter 10% gelation cryogel removed from the CBW after lyophilisation C) 4mm 10% lyophilised gelatin cryogels following careful removal of the CBW insert note: glass cover slip used during the inverted fabrication technique is still attached to the cryogels*

4.9.2 5% Gelatin-EDCI-NHS cryogels fabricated within the CBWs

In order to determine if macroporous gels influenced the degree of migration, a 5% gelatin-EDCI-NHS solution was produced as previously reported (section 4.2.1). The solution was pipetted into a range of 2mm, 3mm and 4mm diameter CBWs using the inverted fabrication technique. CBWs were subsequently frozen in a -20ºC freezer. As discussed in section 4.8, trials of different freezing cycles using liquid nitrogen and dry ice were also performed and were intended to assess whether the resultant cryogels exhibited different topographical arrangement of pores and pore sizes in comparison to the cryogels frozen at -20ºC. As discussed, the absence of contrast from these samples meant the µCT images were not interpretable. Furthermore, the ability to snap-freeze the gelatin-EDCI-NHS solution with liquid nitrogen may enable the solvent to be frozen prior to physical gelation or chemical crosslinking of the gelatin with the EDCI/NHS. It was proposed that this may again influence the topography and porosimetry of the resultant cryogels. Figure 30 displays a variety of production methods utilised to freeze, lyophilise and rehydrate the 5% cryogel samples.

Interestingly, Figure 30e displays a range of individual cryogels post-rehydration in distilled water. Whilst some cryogels closely resembled the cylinders in which they were poured, some cryogels dissolved, some poorly/partially rehydrated and some retained a cross-linked gelatinous component that was grossly different to the cylindrical form pre-rehydration. The majority of the cryogels also displayed a white central core, which suggests that water penetration into the central aspects of the gels was poor. Once again, this may relate to the fact that cross-linker was added to the gelatin solution prior to freezing. However, it was hoped that the liquid nitrogen samples, which can be immediately snap-frozen after being poured would have reduced the effect of any added EDCI-NHS upon the resultant cryogel structure. This did not appear to be the case and the current experiments have raised further questions relating to the type of freezing cycle; the concentration of EDCI/NHS; and the presence or absence of cross-linker prior to freezing on the structure of the cryogels produced.

As some gels did survive, an attempt was made to reposition gels within the CBWs. These CBWs were reverted to their upright position and inserted in a 6 well plate with PBS. However, even gels which appeared to fit adequately within the CBW cylinders still tended to slip out of the bottom of the CBWs when PBS was added to the upper compartments and incubated overnight. As the reliability and validity of any future experiments relies upon the ability of the biomaterials to maintain fluid within the upper compartment, movement of the scaffolds whilst incubated or in culture is undesirable as any cells seeded on the upper compartment could quickly dehydrate or leak into the lower compartment.

Despite the issues above, these attempted experiments highlighted a number of findings. Positive findings were:

1. The CBW can be used to pour hydrogels and fabricate cryogels in situ.
2. The Elastosil 601 used to fabricate the inserts can tolerate sub-zero temperatures to that of liquid nitrogen (-178ºc) without detrimental effects.
3. Prior to rehydrating, the lyophilised 5% gelatin-EDCI-NHS constructs appears macroporous with relatively little dimensional change.
4. Rehydration in distilled water alone did produce some cryogels that were consistent with comparable dimensions to their pre-lyophilised state.

As with all research, a range of additional questions were raised that require further investigation:

1. Why did some cryogels dissolve or poorly rehydrate with gross dimensional changes?

2. How does the addition of cross-linker prior to freezing affect the resultant structure and porosimetry?
3. Does the use of different freezing cycles influence the efficacy of the added carbodiimide cross-linker?
4. Is it possible to fabricate cylindrical hydrogels/cryogels that will hold adequately within the CBW whilst in culture?

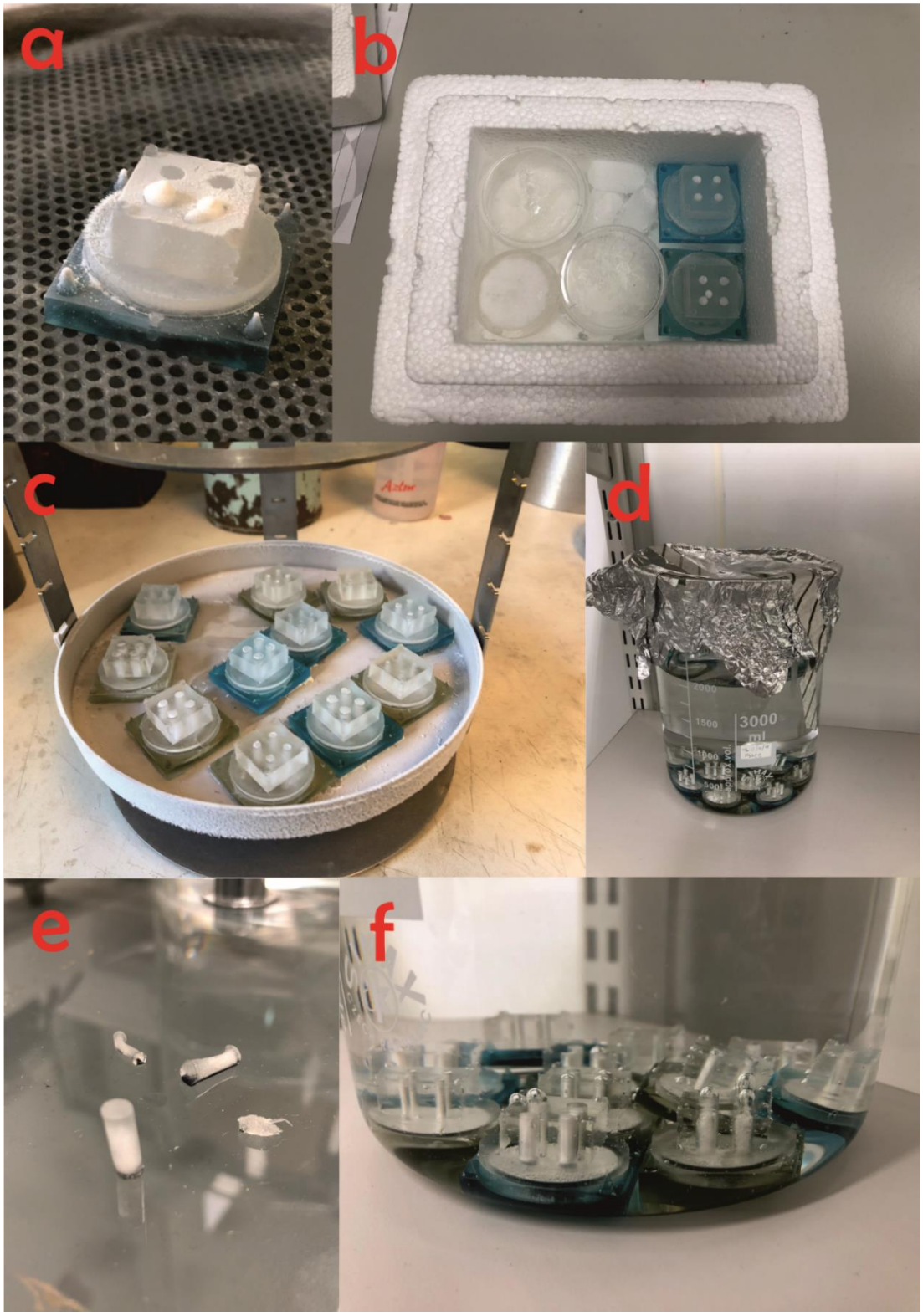

Figure 30 First trials of 5% Gelatin-EDCI-NHS Cryogels: *5% Gelatin-EDCI-NHS solution was used in a range of CBW diameters utilising the inverted fabrication technique a) Close up of the CBW and cryogels immediately post-liquid nitrogen freezing b) Icebox containing dry-ice with CBWs and petri dishes on top for freezing c) Multiple CBWs within the freezedryer component prior to lyophilisation d & f) Lyophilised samples re-hydrated in 2L of dH_2O whilst within the CBWs e) 4 different individual gelatin cryogels removed from the CBWs following 24 hours in dH_2O showing a range of resultant gel qualities and structures.*

5 Discussion

The work above describes the design and fabrication of the CBW, a laboratory insert suitable for cell culture. The research presented details the optimisation and validation processes that have been attempted, some areas of which will be discussed further in the 'future research' section. Pulp regeneration represents a small branch of tissue engineering, which is a vast research field that requires great understanding of cell biology, behaviour and interactions. Studying these topics in situ can be extremely challenging and as such, a well-designed laboratory model could greatly enhance the collective knowledge for the medical and dental research communities. The aim of this study was therefore to produce a laboratory model specific to pulp regeneration that would enable the further study of the above factors, which require specific attention within the field of REPs.

5.1 The Culture Button Well

5.1.1 Design overview

The initial design for the CBW was intended to produce an additively manufactured, in vitro insert for cell culture experiments. Adoption of CAD/CAM technology allows for precise control over all of the insert dimensions and enabled a product to be additively manufactured using commercially available 3D printers using a range of different technologies and materials. The initial design parameters used from 6-well culture plate dimensions produced an insert that fitted nicely into a 6-well plate with adequate space for media and pipette tips. Space was provided for circulation of media in the lower chamber through the addition of small feet. The CBW was designed to support vertically orientated tissue scaffolds that could bidirectional as this would more accurately replicate the tooth, which could be maxillary (i.e. cells above the root canal) or mandibular (i.e. cells below).

5.1.2 Internal cylindrical design and the 'critical apical diameter'

Internal cylindrical voids were created within the insert for the placement of the biomaterial tissue scaffold being investigated. The diameters of these cylinders were selected from a radiographic study that recorded the apical diameters of avulsed immature teeth (Kling et al., 1986). In this study, apices of varying diameters (<1mm to >4.1mm) were reported along with the percentage of spontaneous revascularisation. Of the 82 cases that were reported to have an apex of less than 1mm, no revascularisation was reported. This study contributed to the notion that there was a 'critical apical diameter' below which revascularisation may be compromised; presumably due to space for angiogenesis. However, regeneration using inductive biomaterials presents a different challenge and subsequent studies have shown the

diameter may not be as critical as first thought (Laureys et al., 2013, Fang et al., 2018). Despite these reported successful outcomes, larger apices tend to be associated with shorter roots and as such they may benefit more from regenerative procedures. Anecdotally, larger apices also present a greater clinical challenge as they are more difficult to manage using conventional root-end barrier apexification. As such, diameters ranging from 2-5mm were designed with a maximum number of 20 cylinders and a minimum of 4, diameter dependent.

5.1.3 Indirect Additive Manufacturing and Casting

A number of commercially available AM strategies were trialled. Following the printing of a successful prototype, the biological requirements of the insert were reassessed. Resin polymer based stereolithography and digital light processing systems are predominantly methacrylate based and as such any leachates can have detrimental effects upon cells in culture. These resins were also coloured or slightly opaque, making the pouring and imaging of tissue scaffolds more challenging. A decision to cast the CBW from a translucent addition-silicone was made and the resultant inserts were transparent and autoclaveable, making them reusable. Cells were able to survive prolonged culture on the inserts and there did not appear to be any detrimental effects to the cells. As hydrogels were used for model validation, the translucent design also ensured that no bubbles were incorporated into the cylinders when injected into the CBW. Bubbles or gaps within the scaffolds would frequently have drastic effects upon the positioning of the scaffolds and the ability of the CBW to support fluid in the upper compartment.

The design of a CBW negative did however create some problems due to the large number of internal cylindrical voids originally planned (n = 20). As the cylinders had long parallel walls, the polyvinylsiloxane and polydimethylsiloxane trialled would frequently tear on removal. For the process of optimisation and validation, the number of internal cylinders was reduced to four per insert and these could be easily cast and removed from the moulds.

5.1.4 Validation of the model

The fourth primary objective was to validate the model using a range of tissue scaffolds. Model validation refers to a series of steps that assesses the model's ability to produce data that is reliable, reproducible and robust (Butler, 2014). Validation therefore enables researchers to understand the variation that may result from using the model prior to conducting experiments to test a specific research question. Fundamentally, without appropriate model validation, researchers are unable to conclude that the results they recorded occurred as a result of their experiment and not as a result of the model itself. Unfortunately, at present the CBW has not been validated for use as an in vitro migration

assay tool. Despite this, the research detailed above has highlighted a series of design amendments that may enable validation of future CBW iterations.

5.2 Experimental findings and modifications

5.2.1 General findings

The experimentation conducted and presented represents a series of optimisation experiments that were ultimately unable to fully validate the CBW model in its current form, but there are multiple important findings and results that have resulted in a series of recommendations for future research. A large amount of time was invested on scaffold fabrication and material trials, which ran concomitantly with cell culture training and basic laboratory skills. A number of different materials and fabrication techniques were investigated to fully understand the design requirements for the CBW 2.0. In its current format, the CBW can be used to fabricate a range of consistent hydrogels and cryogels. However, issues arose with prolonged incubation and cell culture.

The CBW itself is fabricated from the addition-cured rubber, Elastosil 601, which has been shown to be a suitable material for an in vitro cell culture insert. This rubber can withstand autoclaving, and it can also be subjected to a range of freezing protocols including dry ice and liquid nitrogen, which can be used for cryogelation. No dimensional changes were noted with prolonged incubation at 37ºC, but this was not the case for the tested tissue scaffolds, which were prone to imbibition and syneresis.

5.2.2 Controlling the scaffold position

The most persistent issue that affected this entire research project, was control over the position and consistency of the hydrogels and cryogels whilst within the CBW. Initial experiments with 10% gelatin and chemically crosslinked gelatin, produced perfectly cylindrical hydrogels. Chemical crosslinking with EDCI/NHS was required as the sol-gel transition temperature of gelatin is below 37ºC. When cross-linked, gelatin maintained a consistent shape and structure. However, the gels frequently slipped through the bottom of the CBW to rest against the floor of the culture plate, this opened gaps around the gel which led to the draining of the fluid in the upper compartment. This problem was also evident when gelatin cryogels were produced with the CBW. Stiffer cryogel samples may represent more ideal handling properties for handling and processing, as they can be removed for processing and imaging, but they may also fail to represent the dental pulp in terms of mechanical characteristics. Failure to match the physical characteristics of the gels with that of dental pulp may influence the resultant cell phenotype and the ultimate tissue that is

produced. Further gel/scaffold rheology would be an appropriate strategy for optimising gel stiffness.

When collagen was used, the lack of consistency became more problematic, as the pH-crosslinked collagen was not rigid enough to support itself within the CBW. As a result, these hydrogels would repeatedly drain from the CBW when cover slips were removed, even when cross-linking was demonstrated within a bijou flask. Other literature has also reported significant dimensional change of collagen gels following cross-linking (Timpson et al., 2011). After a brief attempt to stiffen the hydrogels with UV-irradiation, the 4mm and 3mm CBWs were abandoned in favour of the 2mm cylinders in which the 6mg/ml collagen did remain. It is possible that removal of the overlying coverslip was catastrophically disturbing the delicate collagen gel cross-linked structure. BSA coating of the cover slips also failed to improve the outcome. Any successful collagen hydrogels were often short-lived as prolonged incubation in cell media would lead to dimensional changes in the gels, which often resulted in part if not all of the gel draining into the lower compartment.

One method that did help to maintain the collagen gel structure and held the cell media in the upper well, was to add a thin layer of surplus collagen to connect the four collagen cylinders (Figure 12). Whilst this strategy helped to hold the gels in situ, it also adds to the length of the gel and increases the length of the subsequent hydrogel through which the cells will be required to migrate.

In an additional material experiment, 5% EDCI-NHS-gelatin cryogels demonstrated good L929 fibroblast cell growth at 7 days with evidence of co-localisation within pore structures. It is possible that the macroporosity of these gels is desirable for pulp regeneration as there will be less resistance to cell migration and nutrient exchange. Pore size has also been shown to influence cell behaviour, with smaller pores associated with cell growth and larger pores associated with greater extracellular matrix secretion (Annabi et al., 2010). When fabricated within the CBW these gels maintained a good shape and consistency, but as discussed earlier, the cryogels tended to slip out of the CBW when media was added to the upper compartment.

When compared to Transwell® inserts, there was no track-etched membrane positioned at the lower end of the CBW to support the hydrogels and this contributed to the issues highlighted above. To circumvent all of these issues, the CBW 2.0 should be redesigned with cone shaped internal voids, as opposed to cylinders. The taper of the cones could be tuned to ensure that hydrogels and cryogels are adequately supported during prolonged culture, but a fairly modest taper of 5-10% is likely to be sufficient to prevent slippage of the gels out of the CBW.

5.2.3 Growth factor gradients

A simple application of bromophenol blue to 1% agarose gels within the CBW has also shown that the CBW may be used to produce hydrogels with a molecular gradient (**Figure 25**). This may be extremely beneficial for pulp regeneration, whereby the gradient may serve to increase the depth and speed of cell migration. If growth factor gradients were included and the speed of migration could be enhanced, then it is logical to assume that angiogenesis could also be influenced through the controlled placement of pro-angiogenic growth factors. Aside from the crude method of soaking the hydrogel in growth factor that was performed above, alternative methods such as electrophoresis or fluorescent-labelling of cytokines could be more precise strategies for producing and assessing growth factor gradients within the CBW hydrogels.

5.2.4 Imaging considerations

Cell-seeded hydrogels within the CBW were imaged using a spinning disc confocal laser scanning microscope (Figure 16). Whilst the precise measurement into the gel was unclear due to technical issues with the microscope, the working depth of the microscope lens was considered the limiting factor. As a glass cover slip was placed over the CBW prior to imaging, any space between the gel and the cover slip served to reduce the possible depth of imaging into the scaffolds. This was particularly problematic when collagen was used, as the collagen tended to drain out of the bottom of the CBW during extended culture. As no clear migration was demonstrated with collagen hydrogels, an imaging distance of 12mm is currently excessive. Shortening the length of the internal cylinders to 5mm would enable the entire gel to be imaged with the current lens. This would also serve to shorten the distance between the top and bottom of the CBW, so that cells may be more likely to respond to the growth factors being used as chemoattractants. It is also possible that cells seeded on top of the hydrogel cylinders were too far from the epidermal growth factor and fetal bovine serum that was being used as chemoattractant.

5.2.5 Upper compartment volume

The upper compartment of the CBW was initially designed to hold 1.5ml of cell media. However, with extended culture, this media volume was insufficient as it was imbibed into the gels, evaporated off and also drained into the lower compartment. Loss of media into the lower compartment was more problematic when the consistency or adaptation of the tissue scaffolds were compromised. Furthermore, if excess media were added, the convexity of the fluid surface could reach the lid of the tissue culture plate, predisposing to cross-contamination and infection. It is possible that the current media volume would be adequate

when the CBW was redesigned with tapered internal cones as gels are less likely to move and media is subsequently less likely to drain. However, as the length of the gels is being reduced to assist with imaging, it seems logical to use this reduction in height to increase the volume of the upper reservoir.

5.2.6 CBW Validation

Whilst model validation was not demonstrated within this work, some of the initial processes that may be used are discussed below. As multiple fabrication methods were involved, the first part of model validation, would be to ensure that CBWs are accurately produced within a respectable standard deviation. SEM or µCT would be reasonable techniques to consider for this purpose. As AM strategies develop, it is highly likely that indirect AM strategies will no longer be required. Removing the second production stage and relying solely on CAD/CAM technology should further enhance the accuracy of the CBWs that are produced.

Once the accuracy of the model has been confirmed, the next stage is to validate the model as a suitable tool to study hydrogels. To simplify this process, the use of a pre-validated and commercially available hydrogel peptide such as Puramatrix™ would ensure no further variation is incorporated as a result of the test material. Finally, once placement and imaging of a validated hydrogel had been demonstrated further biocompatibility testing could be performed using multiple cell lines to ensure no change in cell behaviour or survival is identified as a result of the CBW material.

5.3 Recommendations for the redesign of the CBW 2.0

- Decrease the height of the internal tissue scaffold channels from 12mm to 5mm.
- Increase the height of the upper reservoir from 3mm to 6mm.
- Design the internal channels with a taper of 5-10% to help support the resultant tissue scaffold.

5.4 Future research using the CBW 2.0

Acknowledging the design recommendations outlined above and with further optimisation it is hoped that the stability of tissue scaffolds within the CBW can be controlled and this will help provide further information on a range of different topics in regenerative endodontics. Currently there is no specific in vitro model for pulp regeneration reported in the literature. Future research topics include:

- Comparative assessment of biomaterials - It would be realistic to repeat the above cell migration experiments using a range of stable hydrogels and cryogels, with

comparative assessment of the depth and speed of cell migration using a known invasive cell line such as the triple negative, human breast adenocarcinoma line (MDA-MB-231) used above.

- Comparative assessment of different progenitor cells and co-cultures – Successful vasculogenesis/angiogenesis relies upon the complex interaction of several cells including fibroblasts, endothelial cells and progenitor cells. A range of different cells could be trialled with the optimised scaffold to assess cell behaviour including gene expression and protein translation. The use of primary cells such as pulp fibroblasts and DPSCs would be a logical step in the development of a pulp regeneration migration tool.
- Assessment of cryotreatment protocol on scaffold porosity and interconnectivity – By incorporating contrast into the hydrogel solution, µCT could be used to comparatively assess the effect of freezing protocol on the pore size and the interconnectivity of gels.
- The effect of different chemoattractant profiles on cell migration – It has been reported that dentine conditioning with different irrigants, medicaments and cements during -clinical treatment releases different dentine-sequestered growth factors. Once a stable biomaterial has been chosen, it is hoped the effect of different combinations of these sequestered growth factors could be studied.
- Assessment of alternative biological processes such as mineralisation.

6 Conclusions

The present study details the design and fabrication of an in vitro model that is specific for pulp regeneration called the ‘Culture Button Well’. As an additively manufactured insert, the geometry of the internal voids can be modified to replicate a range of possible root canal configurations that may present for regenerative endodontic procedures. The CBW can be used to fabricate hydrogels and cryogels in situ, and cell imaging can be performed without removal of the tissue scaffolds from the CBW. The CBW may be suitable for the assessment of growth factor gradients on cell migration as well as enabling the study of more complex ECM-cell interactions by modifying scaffold chemical and mechanical characteristics. Further design recommendations have been made and further optimisation required.

7 Appendix

Appendix A – Supplemental video of a 300µm Z-Stack of a 4mm diameter, 6mg/ml collagen hydrogel containing MDA-MB-231.

Appendix B – Supplemental video of a Cell exclusion zone assay with GFP-L929 fibroblasts over a 16 hour duration.

Appendix C - Supplemental video of a Cell exclusion zone assay with MDA-MB-231 adenocarcinoma cells over a 16 hour duration.

8 References

ABERCROMBIE, M., HEAYSMAN, J. E. & PEGRUM, S. M. 1970. The locomotion of fibroblasts in culture. I. Movements of the leading edge. *Exp Cell Res,* 59**,** 393-8.

ALBUQUERQUE, M. T., VALERA, M. C., NAKASHIMA, M., NOR, J. E. & BOTTINO, M. C. 2014. Tissue-engineering-based strategies for regenerative endodontics. *J Dent Res,* 93**,** 1222-31.

ALQAHTANI, Q., ZAKY, S. H., PATIL, A., BENIASH, E., RAY, H. & SFEIR, C. 2018. Decellularized Swine Dental Pulp Tissue for Regenerative Root Canal Therapy. *J Dent Res,* 97**,** 1460-67.

ALTHUMAIRY, R. I., TEIXEIRA, F. B. & DIOGENES, A. 2014. Effect of dentin conditioning with intracanal medicaments on survival of stem cells of apical papilla. *J Endod,* 40**,** 521-5.

ANDREASEN, F. M. 2001. Pulpal healing following acute dental trauma: clinical and radiographic review. *Pract Proced Aesthet Dent,* 13**,** 315-22.

ANDREASEN, F. M. & PEDERSEN, B. V. 1985. Prognosis of luxated permanent teeth--the development of pulp necrosis. *Endod Dent Traumatol,* 1**,** 207-20.

ANDREASEN, J. O., BORUM, M. K., JACOBSEN, H. L. & ANDREASEN, F. M. 1995. Replantation of 400 avulsed permanent incisors. 1. Diagnosis of healing complications. *Endod Dent Traumatol,* 11**,** 51-8.

ANDREASEN, J. O., FARIK, B. & MUNKSGAARD, E. C. 2002. Long-term calcium hydroxide as a root canal dressing may increase risk of root fracture. *Dent Traumatol,* 18**,** 134-7.

ANNABI, N., NICHOL, J. W., ZHONG, X., JI, C., KOSHY, S., KHADEMHOSSEINI, A. & DEHGHANI, F. 2010. Controlling the porosity and microarchitecture of hydrogels for tissue engineering. *Tissue engineering. Part B, Reviews,* 16**,** 371-83.

ANTOINE, E. E., VLACHOS, P. P. & RYLANDER, M. N. 2014. Review of collagen I hydrogels for bioengineered tissue microenvironments: characterization of mechanics, structure, and transport. *Tissue engineering. Part B, Reviews,* 20**,** 683-96.

BAKER, B. M. & CHEN, C. S. 2012. Deconstructing the third dimension: how 3D culture microenvironments alter cellular cues. *J Cell Sci,* 125**,** 3015-24.

BATTERSBY, J. 2014. *Is CAD/CAM the end for dental labs? BDJ Team, 1.* [Online]. Available: https://doi.org/10.1038/bdjteam.2014.63 [Accessed 14 Nov. 2019].

BENCHERIF, S. A., BRASCHLER, T. M. & RENAUD, P. 2013. Advances in the design of macroporous polymer scaffolds for potential applications in dentistry. *J Periodontal Implant Sci,* 43**,** 251-61.

BERKHOFF, J. A., CHEN, P. B., TEIXEIRA, F. B. & DIOGENES, A. 2014. Evaluation of triple antibiotic paste removal by different irrigation procedures. *J Endod,* 40**,** 1172-7.
BORIE, E., OLIVÍ, D. G., ORSI, I. A., GARLET, K., WEBER, B., BELTRÁN, V. & FUENTES, R. 2015. Platelet-rich fibrin application in dentistry: a literature review. *Int J Clin Exp Med,* 8**,** 7922-9.
BOSE, R., NUMMIKOSKI, P. & HARGREAVES, K. 2009. A retrospective evaluation of radiographic outcomes in immature teeth with necrotic root canal systems treated with regenerative endodontic procedures. *J Endod,* 35**,** 1343-9.
BOTT, K., UPTON, Z., SCHROBBACK, K., EHRBAR, M., HUBBELL, J. A., LUTOLF, M. P. & RIZZI, S. C. 2010. The effect of matrix characteristics on fibroblast proliferation in 3D gels. *Biomaterials,* 31**,** 8454-64.
BOYDEN, S. 1962. The chemotactic effect of mixtures of antibody and antigen on polymorphonuclear leucocytes. *J Exp Med,* 115**,** 453-66.
BUTLER, J. M. 2014. *Validation Overview* [Online]. National Institute of Standards and Technology. Available: https://www.nist.gov/system/files/documents/forensics/01_ValidationWebinar-Butler-Aug2014.pdf [Accessed 24 March 2020].
CAILLEAU, R., YOUNG, R., OLIVE, M. & REEVES, W. J., JR. 1974. Breast tumor cell lines from pleural effusions. *J Natl Cancer Inst,* 53**,** 661-74.
CALIARI, S. R. & BURDICK, J. A. 2016. A practical guide to hydrogels for cell culture. *Nature methods,* 13**,** 405-14.
CAMMARATA, C. R., HUGHES, M. E. & OFNER, C. M., 3RD 2015. Carbodiimide induced cross-linking, ligand addition, and degradation in gelatin. *Mol Pharm,* 12**,** 783-93.
CAPLAN, A. I. 1991. Mesenchymal stem cells. *J Orthop Res,* 9**,** 641-50.
CARMELIET, P. & JAIN, R. K. 2000. Angiogenesis in cancer and other diseases. *Nature,* 407**,** 249-57.
CAVALCANTI, B. N., ZEITLIN, B. D. & NOR, J. E. 2013. A hydrogel scaffold that maintains viability and supports differentiation of dental pulp stem cells. *Dent Mater,* 29**,** 97-102.
CHAN, B. P. & LEONG, K. W. 2008. Scaffolding in tissue engineering: general approaches and tissue-specific considerations. *Eur Spine J,* 17 Suppl 4**,** 467-79.
CHEN, J., AHMAD, R., SUENAGA, H., LI, W., SASAKI, K., SWAIN, M. & LI, Q. 2015. Shape Optimization for Additive Manufacturing of Removable Partial Dentures--A New Paradigm for Prosthetic CAD/CAM. *PLoS One,* 10**,** e0132552.
CHEN, W. T. 1979. Induction of spreading during fibroblast movement. *J Cell Biol,* 81**,** 684-91.
CHREPA, V., AUSTAH, O. & DIOGENES, A. 2017. Evaluation of a Commercially Available Hyaluronic Acid Hydrogel (Restylane) as

Injectable Scaffold for Dental Pulp Regeneration: An In Vitro Evaluation. *J Endod,* 43**,** 257-62.
CHUENSOMBAT, S., KHEMALEELAKUL, S., CHATTIPAKORN, S. & SRISUWAN, T. 2013. Cytotoxic effects and antibacterial efficacy of a 3-antibiotic combination: an in vitro study. *J Endod,* 39**,** 813-9.
CUI, X., BOLAND, T., D'LIMA, D. D. & LOTZ, M. K. 2012. Thermal inkjet printing in tissue engineering and regenerative medicine. *Recent Pat Drug Deliv Formul,* 6**,** 149-55.
DAVIDENKO, N., BAX, D. V., SCHUSTER, C. F., FARNDALE, R. W., HAMAIA, S. W., BEST, S. M. & CAMERON, R. E. 2016. Optimisation of UV irradiation as a binding site conserving method for crosslinking collagen-based scaffolds. *J Mater Sci Mater Med,* 27**,** 14.
DE CHEVIGNY, C., DAO, T. T., BASRANI, B. R., MARQUIS, V., FARZANEH, M., ABITBOL, S. & FRIEDMAN, S. 2008. Treatment outcome in endodontics: the Toronto study--phase 4: initial treatment. *J Endod,* 34**,** 258-63.
DERBY, B. 2012. Printing and prototyping of tissues and scaffolds. *Science,* 338**,** 921-6.
DEVREOTES, P. & HORWITZ, A. R. 2015. Signaling networks that regulate cell migration. *Cold Spring Harb Perspect Biol,* 7**,** a005959.
DHANDAYUTHAPANI, B., YOSHIDA, Y., MAEKAWA, T. & KUMAR, D. S. 2011. Polymeric scaffolds in tissue engineering application: a review. *Int J Polym Sci,* 2011.
DIOGENES, A., HENRY, M. A., TEIXEIRA, F. B. & HARGREAVES, K. M. 2013. An update on clinical regenerative endodontics. *Endod Topics,* 28**,** 2-23.
DOMINICI, M., LE BLANC, K., MUELLER, I., SLAPER-CORTENBACH, I., MARINI, F., KRAUSE, D., DEANS, R., KEATING, A., PROCKOP, D. & HORWITZ, E. 2006. Minimal criteria for defining multipotent mesenchymal stromal cells. The International Society for Cellular Therapy position statement. *Cytotherapy,* 8**,** 315-7.
DOYLE, A. D., PETRIE, R. J., KUTYS, M. L. & YAMADA, K. M. 2013. Dimensions in cell migration. *Curr Opin Cell Biol,* 25**,** 642-9.
DRUECKE, D., LANGER, S., LAMME, E., PIEPER, J., UGARKOVIC, M., STEINAU, H. U. & HOMANN, H. H. 2004. Neovascularization of poly(ether ester) block-copolymer scaffolds in vivo: long-term investigations using intravital fluorescent microscopy. *J Biomed Mater Res A,* 68**,** 10-8.
DUAN, B., WANG, M., ZHOU, W. Y., CHEUNG, W. L., LI, Z. Y. & LU, W. W. 2010. Three-dimensional nanocomposite scaffolds fabricated via selective laser sintering for bone tissue engineering. *Acta Biomaterialia,* 6**,** 4495-4505.
DUNCAN, H. F., KOBAYASHI, Y. & SHIMIZU, E. 2018. Growth Factors and Cell Homing in Dental Tissue Regeneration. *Curr Oral Health Rep,* 5**,** 276-85.

DUVAL, K., GROVER, H., HAN, L.-H., MOU, Y., PEGORARO, A. F., FREDBERG, J. & CHEN, Z. 2017. Modeling Physiological Events in 2D vs. 3D Cell Culture. *Physiology (Bethesda, Md.),* 32**,** 266-77.

EARLE, W. R., SCHILLING, E. L., STARK, T. H., STRAUS, N. P., BROWN, M. F. & SHELTON, E. 1943. Production of Malignancy in Vitro. IV. The Mouse Fibroblast Cultures and Changes Seen in the Living Cells. *J Natl Cancer Inst,* 4**,** 165-212.

EBELESEDER, K. A., FRIEHS, S., RUDA, C., PERTL, C., GLOCKNER, K. & HULLA, H. 1998. A study of replanted permanent teeth in different age groups. *Endod Dent Traumatol,* 14**,** 274-8.

EL-MELIGY, O. A. & AVERY, D. R. 2006. Comparison of mineral trioxide aggregate and calcium hydroxide as pulpotomy agents in young permanent teeth (apexogenesis). *Pediatr Dent,* 28**,** 399-404.

ENGLER, A. J., SEN, S., SWEENEY, H. L. & DISCHER, D. E. 2006. Matrix elasticity directs stem cell lineage specification. *Cell,* 126**,** 677-89.

ESSNER, M. D., JAVED, A. & ELEAZER, P. D. 2011. Effect of sodium hypochlorite on human pulp cells: an in vitro study. *Oral Surg Oral Med Oral Pathol Oral Radiol Endod,* 112**,** 662-6.

FANG, Y., WANG, X., ZHU, J., SU, C., YANG, Y. & MENG, L. 2018. Influence of Apical Diameter on the Outcome of Regenerative Endodontic Treatment in Teeth with Pulp Necrosis: A Review. *J Endod,* 44**,** 414-31.

FARZANEH, M., ABITBOL, S., LAWRENCE, H. P. & FRIEDMAN, S. 2004. Treatment outcome in endodontics-the Toronto Study. Phase II: initial treatment. *J Endod,* 30**,** 302-9.

FORSBERG, C. M. & TEDESTAM, G. 1990. Traumatic injuries to teeth in Swedish children living in an urban area. *Swed Dent J,* 14**,** 115-22.

FRANTZ, C., STEWART, K. M. & WEAVER, V. M. 2010. The extracellular matrix at a glance. *Journal of Cell Science,* 123**,** 4195.

GALLER, K. M., D'SOUZA, R. N., FEDERLIN, M., CAVENDER, A. C., HARTGERINK, J. D., HECKER, S. & SCHMALZ, G. 2011. Dentin conditioning codetermines cell fate in regenerative endodontics. *J Endod,* 37**,** 1536-41.

GALLER, K. M., KRASTL, G., SIMON, S., VAN GORP, G., MESCHI, N., VAHEDI, B. & LAMBRECHTS, P. 2016. European Society of Endodontology position statement: Revitalization procedures. *Int Endod J,* 49**,** 717-23.

GARCÍA, E., RAGAZZINI, C., YU, X., CUESTA-GARCÍA, E., BERNARDINO DE LA SERNA, J., ZECH, T., SARRIÓ, D., MACHESKY, L. M. & ANTÓN, I. M. 2016. WIP and WICH/WIRE co-ordinately control invadopodium formation and maturation in human breast cancer cell invasion. *Sci Rep,* 6**,** 23590.

GERRITSEN, A. E., ALLEN, P. F., WITTER, D. J., BRONKHORST, E. M. & CREUGERS, N. H. 2010. Tooth loss and oral health-related quality of life: a systematic review and meta-analysis. *Health Qual Life Outcomes,* 8**,** 126.

GOLDBERG, M., KULKARNI, A. B., YOUNG, M. & BOSKEY, A. 2011. Dentin: structure, composition and mineralization. *Front Biosci (Elite Ed),* 3**,** 711-35.

GOLDBERG, M. & SMITH, A. J. 2004. Cells and Extracellular Matrices of Dentin and Pulp: A biological basis for repair and tissue engineering. *Crit Rev Oral Biol Med,* 15**,** 13-27.

GORDON, M. K. & HAHN, R. A. 2010. Collagens. *Cell Tissue Res,* 339**,** 247-57.

GRONTHOS, S., MANKANI, M., BRAHIM, J., ROBEY, P. G. & SHI, S. 2000. Postnatal human dental pulp stem cells (DPSCs) in vitro and in vivo. *Proc Natl Acad Sci U S A,* 97**,** 13625-30.

GROSS, B. C., ERKAL, J. L., LOCKWOOD, S. Y., CHEN, C. & SPENCE, D. M. 2014. Evaluation of 3D printing and its potential impact on biotechnology and the chemical sciences. *Anal Chem,* 86**,** 3240-53.

GUILAK, F., COHEN, D. M., ESTES, B. T., GIMBLE, J. M., LIEDTKE, W. & CHEN, C. S. 2009. Control of stem cell fate by physical interactions with the extracellular matrix. *Cell Stem Cell,* 5**,** 17-26.

HAMEDY, R., SHAKIBA, B., PAK, J. G., BARBIZAM, J. V., OGAWA, R. S. & WHITE, S. N. 2016. Prevalence of root canal treatment and periapical radiolucency in elders: a systematic review. *Gerodontology,* 33**,** 116-27.

HARLAMB, S. C. 2016. Management of incompletely developed teeth requiring root canal treatment. *Aust Dent J,* 61 Suppl 1**,** 95-106.

HEITHERSAY, G. S. 1975. Calcium hydroxide in the treatment of pulpless teeth with associated pathology. *J Br Endod Soc,* 8**,** 74-93.

HOLLISTER, S. J. 2005. Porous scaffold design for tissue engineering. *Nat Mater,* 4**,** 518-24.

HSIEH, C. Y., TSAI, P. C., TSENG, C. H., CHEN, Y. L., CHANG, L. S. & LIN, S. R. 2013. Inhibition of EGF/EGFR activation with naphtho[1,2-b]furan-4,5-dione blocks migration and invasion of MDA-MB-231 cells. *Toxicol In Vitro,* 27**,** 1-10.

HUANG, C.-C., NARAYANAN, R., WARSHAWSKY, N. & RAVINDRAN, S. 2018. Dual ECM Biomimetic Scaffolds for Dental Pulp Regenerative Applications. *Front Physiol,* 9**,** 495.

HUANG, G. T., SONOYAMA, W., CHEN, J. & PARK, S. H. 2006. In vitro characterization of human dental pulp cells: various isolation methods and culturing environments. *Cell Tissue Res,* 324**,** 225-36.

HUANG, G. T., SONOYAMA, W., LIU, Y., LIU, H., WANG, S. & SHI, S. 2008. The hidden treasure in apical papilla: the potential role in pulp/dentin regeneration and bioroot engineering. *J Endod,* 34**,** 645-51.

HUANG, G. T. J., GRONTHOS, S. & SHI, S. 2009. Mesenchymal stem cells derived from dental tissues vs. those from other sources: their biology and role in regenerative medicine. *J Dent Res,* 88**,** 792-806.

HUTTENLOCHER, A. & HORWITZ, A. R. 2011. Integrins in cell migration. *Cold Spring Harbor perspectives in biology,* 3**,** a005074-a005074.

IKADA, Y. (ed.) 2006. *Tissue Engineering: Fundamentals and Applications,* Oxford, U.K.: Elsevier Ltd.

IWAYA, S. I., IKAWA, M. & KUBOTA, M. 2001. Revascularization of an immature permanent tooth with apical periodontitis and sinus tract. *Dent Traumatol,* 17**,** 185-7.

JAIN, R. K., AU, P., TAM, J., DUDA, D. G. & FUKUMURA, D. 2005. Engineering vascularized tissue. *Nat Biotechnol,* 23**,** 821-3.

JAIPAN, P., NGUYEN, A. & NARAYAN, R. J. 2017. Gelatin-based hydrogels for biomedical applications. *MRS Communications,* 7**,** 416-26.

JEERUPHAN, T., JANTARAT, J., YANPISET, K., SUWANNAPAN, L., KHEWSAWAI, P. & HARGREAVES, K. M. 2012. Mahidol study 1: comparison of radiographic and survival outcomes of immature teeth treated with either regenerative endodontic or apexification methods: a retrospective study. *J Endod,* 38**,** 1330-6.

JONKER, A. M., LÖWIK, D. W. P. M. & VAN HEST, J. C. M. 2012. Peptide- and Protein-Based Hydrogels. *Chem Mater,* 24**,** 759-73.

JUSTUS, C. R., LEFFLER, N., RUIZ-ECHEVARRIA, M. & YANG, L. V. 2014. In vitro cell migration and invasion assays. *J Vis Exp***,** 51046.

KAM, Y., GUESS, C., ESTRADA, L., WEIDOW, B. & QUARANTA, V. 2008. A novel circular invasion assay mimics in vivo invasive behavior of cancer cell lines and distinguishes single-cell motility in vitro. *BMC cancer,* 8**,** 198.

KARAGEORGIOU, V. & KAPLAN, D. 2005. Porosity of 3D biomaterial scaffolds and osteogenesis. *Biomaterials,* 26**,** 5474-91.

KAWASHIMA, N. 2012. Characterisation of dental pulp stem cells: a new horizon for tissue regeneration? *Arch Oral Biol,* 57**,** 1439-58.

KEREKES, K., HEIDE, S. & JACOBSEN, I. 1980. Follow-up examination of endodontic treatment in traumatized juvenile incisors. *J Endod,* 6**,** 744-8.

KISIDAY, J., JIN, M., KURZ, B., HUNG, H., SEMINO, C., ZHANG, S. & GRODZINSKY, A. J. 2002. Self-assembling peptide hydrogel fosters chondrocyte extracellular matrix production and cell division: implications for cartilage tissue repair. *Proc Natl Acad Sci U S A,* 99**,** 9996-10001.

KLING, M., CVEK, M. & MEJARE, I. 1986. Rate and predictability of pulp revascularization in therapeutically reimplanted permanent incisors. *Endod Dent Traumatol,* 2**,** 83-9.

KOSHY, S. T., FERRANTE, T. C., LEWIN, S. A. & MOONEY, D. J. 2014. Injectable, porous, and cell-responsive gelatin cryogels. *Biomaterials,* 35**,** 2477-87.

KRAMER, N., WALZL, A., UNGER, C., ROSNER, M., KRUPITZA, G., HENGSTSCHLAGER, M. & DOLZNIG, H. 2013. In vitro cell migration and invasion assays. *Mutat Res,* 752**,** 10-24.

KRASNER, P. & RANKOW, H. J. 1995. New philosophy for the treatment of avulsed teeth. *Oral Surg Oral Med Oral Pathol Oral Radiol Endod,* 79**,** 616-23.

KREGER, S. T., BELL, B. J., BAILEY, J., STITES, E., KUSKE, J., WAISNER, B. & VOYTIK-HARBIN, S. L. 2010. Polymerization and matrix physical properties as important design considerations for soluble collagen formulations. *Biopolymers,* 93**,** 690-707.

KUBOKI, Y., TAKITA, H., KOBAYASHI, D., TSURUGA, E., INOUE, M., MURATA, M., NAGAI, N., DOHI, Y. & OHGUSHI, H. 1998. BMP-induced osteogenesis on the surface of hydroxyapatite with geometrically feasible and nonfeasible structures: topology of osteogenesis. *J Biomed Mater Res,* 39**,** 190-9.

LAI, J. Y. 2010. Biocompatibility of chemically cross-linked gelatin hydrogels for ophthalmic use. *J Mater Sci Mater Med,* 21**,** 1899-911.

LANGER, R. & VACANTI, J. P. 1993. Tissue engineering. *Science,* 260**,** 920-6.

LAUREYS, W. G., CUVELIER, C. A., DERMAUT, L. R. & DE PAUW, G. A. 2013. The critical apical diameter to obtain regeneration of the pulp tissue after tooth transplantation, replantation, or regenerative endodontic treatment. *J Endod,* 39**,** 759-63.

LEBLEU, V. S., MACDONALD, B. & KALLURI, R. 2007. Structure and function of basement membranes. *Exp Biol Med (Maywood),* 232**,** 1121-9.

LI, J., CELIZ, A. D., YANG, J., YANG, Q., WAMALA, I., WHYTE, W., SEO, B. R., VASILYEV, N. V., VLASSAK, J. J., SUO, Z. & MOONEY, D. J. 2017. Tough adhesives for diverse wet surfaces. *Science,* 357**,** 378-81.

LI, Q., REED, D. A., MIN, L., GOPINATHAN, G., LI, S., DANGARIA, S. J., LI, L., GENG, Y., GALANG, M.-T., GAJENDRAREDDY, P., ZHOU, Y., LUAN, X. & DIEKWISCH, T. G. H. 2014. Lyophilized platelet-rich fibrin (PRF) promotes craniofacial bone regeneration through Runx2. *Int J Mol Sci* 15**,** 8509-25.

LI, Y.-H. & ZHU, C. 1999. A modified Boyden chamber assay for tumor cell transendothelial migration in vitro. *Clin Exp Metastas,* 17**,** 423-29.

LIANG, C. C., PARK, A. Y. & GUAN, J. L. 2007. In vitro scratch assay: a convenient and inexpensive method for analysis of cell migration in vitro. *Nat Protoc,* 2**,** 329-33.

LIANG, H.-C., CHANG, W.-H., LIANG, H.-F., LEE, M.-H. & SUNG, H.-W. 2004. Crosslinking structures of gelatin hydrogels crosslinked with genipin or a water-soluble carbodiimide. *J Appl Polym,* 91**,** 4017-26.

LIN, P., MA, S., WANG, X. & ZHOU, F. 2015. Molecularly Engineered Dual-Crosslinked Hydrogel with Ultrahigh Mechanical Strength, Toughness, and Good Self-Recovery. *Adv Mater,* 27**,** 2054-59.

LINDE, A. 1985. The extracellular matrix of the dental pulp and dentin. *J Dent Res,* 64 Spec No**,** 523-9.

LIU, H., GRONTHOS, S. & SHI, S. 2006. Dental pulp stem cells. *Methods Enzymol,* 419**,** 99-113.
LOH, Q. L. & CHOONG, C. 2013. Three-dimensional scaffolds for tissue engineering applications: role of porosity and pore size. *Tissue Eng Part B Rev,* 19**,** 485-502.
LOVETT, M., LEE, K., EDWARDS, A. & KAPLAN, D. L. 2009. Vascularization strategies for tissue engineering. *Tissue Eng Part B Rev,* 15**,** 353-70.
MA, S., YU, B., PEI, X. & ZHOU, F. 2016. Structural hydrogels. *Polymer,* 98**,** 516-35.
MACDONALD, E., BROWN, L., SELVAIS, A., LIU, H., WARING, T., NEWMAN, D., BITHELL, J., GRIMES, D., URBE, S., CLAGUE, M. J. & ZECH, T. 2018. HRS-WASH axis governs actin-mediated endosomal recycling and cell invasion. *J Cell Biol,* 217**,** 2549-64.
MACKIE, I. C., BENTLEY, E. M. & WORTHINGTON, H. V. 1988. The closure of open apices in non-vital immature incisor teeth. *Br Dent J,* 165**,** 169-73.
MARSHALL, J. 2011. Transwell(R) invasion assays. *Methods Mol Biol,* 769**,** 97-110.
MARTINO, M. M., MOCHIZUKI, M., ROTHENFLUH, D. A., REMPEL, S. A., HUBBELL, J. A. & BARKER, T. H. 2009. Controlling integrin specificity and stem cell differentiation in 2D and 3D environments through regulation of fibronectin domain stability. *Biomaterials,* 30**,** 1089-97.
MEHDIZADEH, H., SUMO, S., BAYRAK, E. S., BREY, E. M. & CINAR, A. 2013. Three-dimensional modeling of angiogenesis in porous biomaterial scaffolds. *Biomaterials,* 34**,** 2875-87.
MILLER, E. K., LEE, J. Y., TAWIL, P. Z., TEIXEIRA, F. B. & VANN, W. F., JR. 2012. Emerging therapies for the management of traumatized immature permanent incisors. *Pediatr Dent,* 34**,** 66-9.
MURPHY, C. M., HAUGH, M. G. & O'BRIEN, F. J. 2010. The effect of mean pore size on cell attachment, proliferation and migration in collagen-glycosaminoglycan scaffolds for bone tissue engineering. *Biomaterials,* 31**,** 461-6.
MURPHY, C. M. & O'BRIEN, F. J. 2010. Understanding the effect of mean pore size on cell activity in collagen-glycosaminoglycan scaffolds. *Cell Adh Migr,* 4**,** 377-81.
MURPHY, S. V. & ATALA, A. 2014. 3D bioprinting of tissues and organs. *Nat Biotechnol,* 32**,** 773-85.
MURRAY, P. E. 2018. Platelet-Rich Plasma and Platelet-Rich Fibrin Can Induce Apical Closure More Frequently Than Blood-Clot Revascularization for the Regeneration of Immature Permanent Teeth: A Meta-Analysis of Clinical Efficacy. *Front Bioeng Biotech* 6**,** 139.
MURRAY, P. E., GARCIA-GODOY, F. & HARGREAVES, K. M. 2007. Regenerative endodontics: a review of current status and a call for action. *J Endod,* 33**,** 377-90.

NAGANO, M. H., D.; KOSHIKAWA, N.; AKIZAWA, T.; SEIKI, M. 2012. Turnover of Focal Adhesions and Cancer Cell Migration. *Int J Cell Biol,* 2012**,** 310616.

NAGAOKA, S., MIYAZAKI, Y., LIU, H. J., IWAMOTO, Y., KITANO, M. & KAWAGOE, M. 1995. Bacterial invasion into dentinal tubules of human vital and nonvital teeth. *J Endod,* 21**,** 70-3.

NAIK, B., KARUNAKAR, P., JAYADEV, M. & MARSHAL, V. R. 2013. Role of Platelet rich fibrin in wound healing: A critical review. *J Conserv Dent,* 16**,** 284-93.

NAIR, P. N., DUNCAN, H. F., PITT FORD, T. R. & LUDER, H. U. 2008. Histological, ultrastructural and quantitative investigations on the response of healthy human pulps to experimental capping with mineral trioxide aggregate: a randomized controlled trial. *Int Endod J,* 41**,** 128-50.

NAKASHIMA, M. & IOHARA, K. 2014. Mobilized dental pulp stem cells for pulp regeneration: initiation of clinical trial. *J Endod,* 40**,** S26-32.

NAKAYAMA, H., IOHARA, K., HAYASHI, Y., OKUWA, Y., KURITA, K. & NAKASHIMA, M. 2017. Enhanced regeneration potential of mobilized dental pulp stem cells from immature teeth. *Oral Dis,* 23**,** 620-8.

NG, Y. L., MANN, V. & GULABIVALA, K. 2011. A prospective study of the factors affecting outcomes of nonsurgical root canal treatment: part 1: periapical health. *Int Endod J,* 44**,** 583-609.

NG, Y. L., MANN, V., RAHBARAN, S., LEWSEY, J. & GULABIVALA, K. 2008. Outcome of primary root canal treatment: systematic review of the literature -- Part 2. Influence of clinical factors. *Int Endod J,* 41**,** 6-31.

NOSRAT, A., KOLAHDOUZAN, A., KHATIBI, A. H., VERMA, P., JAMSHIDI, D., NEVINS, A. J. & TORABINEJAD, M. 2019. Clinical, Radiographic, and Histologic Outcome of Regenerative Endodontic Treatment in Human Teeth Using a Novel Collagen-hydroxyapatite Scaffold. *J Endod,* 45**,** 136-43.

NOVOSEL, E. C., KLEINHANS, C. & KLUGER, P. J. 2011. Vascularization is the key challenge in tissue engineering. *Adv Drug Deliv Rev,* 63**,** 300-11.

NYGAARD-OSTBY, B. & HJORTDAL, O. 1971. Tissue formation in the root canal following pulp removal. *Scand J Dent Res,* 79**,** 333-49.

O'BRIEN, F. J. 2011. Biomaterials & scaffolds for tissue engineering. *Mater Today,* 14**,** 88-95.

O'BRIEN, F. J., HARLEY, B. A., WALLER, M. A., YANNAS, I. V., GIBSON, L. J. & PRENDERGAST, P. J. 2007. The effect of pore size on permeability and cell attachment in collagen scaffolds for tissue engineering. *Technol Health Care,* 15**,** 3-17.

O'BRIEN, F. J., HARLEY, B. A., YANNAS, I. V. & GIBSON, L. 2004. Influence of freezing rate on pore structure in freeze-dried collagen-GAG scaffolds. *Biomaterials,* 25**,** 1077-86.

OU, K. L., CHANG, C. C., CHANG, W. J., LIN, C. T., CHANG, K. J. & HUANG, H. M. 2009. Effect of damping properties on fracture resistance of root filled premolar teeth: a dynamic finite element analysis. *Int Endod J,* 42**,** 694-704.

PAK, J. G., FAYAZI, S. & WHITE, S. N. 2012. Prevalence of periapical radiolucency and root canal treatment: a systematic review of cross-sectional studies. *J Endod,* 38**,** 1170-6.

PARSONS, J. T., HORWITZ, A. R. & SCHWARTZ, M. A. 2010. Cell adhesion: integrating cytoskeletal dynamics and cellular tension. *Nat Rev Mol Cell Biol,* 11**,** 633-43.

PASHLEY, D. H. 1996. Dynamics of the pulpo-dentin complex. *Crit Rev Oral Biol Med,* 7**,** 104-33.

PAUL, C. D., MISTRIOTIS, P. & KONSTANTOPOULOS, K. 2017. Cancer cell motility: lessons from migration in confined spaces. *Nat Rev Cancer,* 17**,** 131-40.

PEK, Y. S., WAN, A. C. & YING, J. Y. 2010. The effect of matrix stiffness on mesenchymal stem cell differentiation in a 3D thixotropic gel. *Biomaterials,* 31**,** 385-91.

PEPPAS, N. A., BURES, P., LEOBANDUNG, W. & ICHIKAWA, H. 2000. Hydrogels in pharmaceutical formulations. *Eur J Pharm Biopharm* 50**,** 27-46.

PETRIE, R. J., GAVARA, N., CHADWICK, R. S. & YAMADA, K. M. 2012. Nonpolarized signaling reveals two distinct modes of 3D cell migration. *J Cell Biol,* 197**,** 439-55.

PETRIE, R. J. & YAMADA, K. M. 2012. At the leading edge of three-dimensional cell migration. *J Cell Sci,* 125**,** 5917.

PIVA, E., SILVA, A. F. & NOR, J. E. 2014. Functionalized scaffolds to control dental pulp stem cell fate. *J Endod,* 40**,** S33-40.

PLIEVA, F., HUITING, X., GALAEV, I. Y., BERGENSTÅHL, B. & MATTIASSON, B. 2006. Macroporous elastic polyacrylamide gels prepared at subzero temperatures: control of porous structure. *J Mater Chem,* 16**,** 4065-73.

POLLARD, T. D. & BORISY, G. G. 2003. Cellular motility driven by assembly and disassembly of actin filaments. *Cell,* 112**,** 453-65.

PRASAD, N. K. 2009. SHIP2 phosphoinositol phosphatase positively regulates EGFR-Akt pathway, CXCR4 expression, and cell migration in MDA-MB-231 breast cancer cells. *Int J Oncol,* 34**,** 97-105.

RAFTER, M. 2005. Apexification: a review. *Dent Traumatol,* 21**,** 1-8.

RANGA, A., GJOREVSKI, N. & LUTOLF, M. P. 2014. Drug discovery through stem cell-based organoid models. *Adv Drug Deliv Rev,* 69-70**,** 19-28.

RICAPITO, N. G., GHOBRIL, C., ZHANG, H., GRINSTAFF, M. W. & PUTNAM, D. 2016. Synthetic Biomaterials from Metabolically Derived Synthons. *Chem Rev,* 116**,** 2664-704.

ROGERS, E. H. 2019. Exploring the potential of the physio-mechanical environment and circadian timing in adult progenitor cell differentiation. University of Liverpool.
ROUWKEMA, J., RIVRON, N. C. & VAN BLITTERSWIJK, C. A. 2008. Vascularization in tissue engineering. *Trends Biotechnol,* 26**,** 434-41.
RUPAREL, N. B., TEIXEIRA, F. B., FERRAZ, C. C. & DIOGENES, A. 2012. Direct effect of intracanal medicaments on survival of stem cells of the apical papilla. *J Endod,* 38**,** 1372-5.
SABERIANPOUR, S., HEIDARZADEH, M., GERANMAYEH, M. H., HOSSEINKHANI, H., RAHBARGHAZI, R. & NOURI, M. 2018. Tissue engineering strategies for the induction of angiogenesis using biomaterials. *J Biol Eng,* 12**,** 36.
SALEHRABI, R. & ROTSTEIN, I. 2004. Endodontic treatment outcomes in a large patient population in the USA: an epidemiological study. *J Endod,* 30**,** 846-50.
SCHINDELIN, J., ARGANDA-CARRERAS, I., FRISE, E., KAYNIG, V., LONGAIR, M., PIETZSCH, T., PREIBISCH, S., RUEDEN, C., SAALFELD, S., SCHMID, B., TINEVEZ, J. Y., WHITE, D. J., HARTENSTEIN, V., ELICEIRI, K., TOMANCAK, P. & CARDONA, A. 2012. Fiji: an open-source platform for biological-image analysis. *Nat Methods,* 9**,** 676-82.
SCHOR, S. L., ALLEN, T. D. & WINN, B. 1983. Lymphocyte migration into three-dimensional collagen matrices: a quantitative study. *J Cell Biol,* 96**,** 1089-96.
SCHUBERT, C., VAN LANGEVELD, M. C. & DONOSO, L. A. 2014. Innovations in 3D printing: a 3D overview from optics to organs. *Br J Ophthalmol,* 98**,** 159-61.
SHARPE, P. T. 2016. Dental mesenchymal stem cells. *Development,* 143**,** 2273.
SHIMIZU, E., JONG, G., PARTRIDGE, N., ROSENBERG, P. A. & LIN, L. M. 2012. Histologic observation of a human immature permanent tooth with irreversible pulpitis after revascularization/regeneration procedure. *J Endod,* 38**,** 1293-7.
SHIMIZU, E., RICUCCI, D., ALBERT, J., ALOBAID, A. S., GIBBS, J. L., HUANG, G. T. & LIN, L. M. 2013. Clinical, radiographic, and histological observation of a human immature permanent tooth with chronic apical abscess after revitalization treatment. *J Endod,* 39**,** 1078-83.
SHIVASHANKAR, V. Y., JOHNS, D. A., VIDYANATH, S. & KUMAR, M. R. 2012. Platelet Rich Fibrin in the revitalization of tooth with necrotic pulp and open apex. *J Conserv Dent,* 15**,** 395-98.
SLOAN, A. J. 2015. Chapter 29 - Biology of the Dentin-Pulp Complex. *In:* VISHWAKARMA, A., SHARPE, P., SHI, S. & RAMALINGAM, M. (eds.) *Stem Cell Biology and Tissue Engineering in Dental Sciences.* Boston: Academic Press.

SMITH, A. J., CASSIDY, N., PERRY, H., BEGUE-KIRN, C., RUCH, J. V. & LESOT, H. 1995. Reactionary dentinogenesis. *Int J Dev Biol,* 39**,** 273-80.

STORY, B. J., WAGNER, W. R., GAISSER, D. M., COOK, S. D. & RUST-DAWICKI, A. M. 1998. In vivo performance of a modified CSTi dental implant coating. *Int J Oral Maxillofac Implants,* 13**,** 749-57.

SUNG, H.-W., HUANG, D.-M., CHANG, W.-H., HUANG, R.-N. & HSU, J.-C. 1999. Evaluation of gelatin hydrogel crosslinked with various crosslinking agents as bioadhesives: In vitro study. *J Biomed Mater Res* 46**,** 520-30.

SUNG, K. E., SU, X., BERTHIER, E., PEHLKE, C., FRIEDL, A. & BEEBE, D. J. 2013. Understanding the impact of 2D and 3D fibroblast cultures on in vitro breast cancer models. *PLoS One,* 8**,** e76373.

SURENDRAN, S. & SIVAMURTHY, G. 2015. Current Applications and Future Prospects of Stem Cells in Dentistry. *Dent Update,* 42**,** 556-8, 560-1.

TAHA, N. A. & ABDELKHADER, S. Z. 2018. Outcome of full pulpotomy using Biodentine in adult patients with symptoms indicative of irreversible pulpitis. *Int Endod J,* 51**,** 819-28.

THIBODEAU, B., TEIXEIRA, F., YAMAUCHI, M., CAPLAN, D. J. & TROPE, M. 2007. Pulp revascularization of immature dog teeth with apical periodontitis. *J Endod,* 33**,** 680-9.

TIMPSON, P., MCGHEE, E. J., ERAMI, Z., NOBIS, M., QUINN, J. A., EDWARD, M. & ANDERSON, K. I. 2011. Organotypic collagen I assay: a malleable platform to assess cell behaviour in a 3-dimensional context. *J Vis Exp***,** e3089.

TOMSON, P. L., LUMLEY, P. J., SMITH, A. J. & COOPER, P. R. 2017. Growth factor release from dentine matrix by pulp-capping agents promotes pulp tissue repair-associated events. *Int Endod J,* 50**,** 281-92.

TREPAT, X., CHEN, Z. & JACOBSON, K. 2012. Cell migration. *Compr Physiol,* 2**,** 2369-92.

TREVINO, E. G., PATWARDHAN, A. N., HENRY, M. A., PERRY, G., DYBDAL-HARGREAVES, N., HARGREAVES, K. M. & DIOGENES, A. 2011. Effect of irrigants on the survival of human stem cells of the apical papilla in a platelet-rich plasma scaffold in human root tips. *J Endod,* 37**,** 1109-15.

TROPE, M. 2010. Treatment of the immature tooth with a non-vital pulp and apical periodontitis. *Dent Clin North Am,* 54**,** 313-24.

ULUBAYRAM, K., AKSU, E., GURHAN, S. I., SERBETCI, K. & HASIRCI, N. 2002. Cytotoxicity evaluation of gelatin sponges prepared with different cross-linking agents. *J Biomater Sci Polym Ed,* 13**,** 1203-19.

UNADKAT, H. V., HULSMAN, M., CORNELISSEN, K., PAPENBURG, B. J., TRUCKENMULLER, R. K., CARPENTER, A. E., WESSLING, M., POST, G. F., UETZ, M., REINDERS, M. J., STAMATIALIS, D., VAN BLITTERSWIJK, C. A. & DE BOER, J. 2011. An algorithm-

based topographical biomaterials library to instruct cell fate. *Proc Natl Acad Sci U S A,* 108**,** 16565-70.
VAN VLIERBERGHE, S. 2016. Crosslinking strategies for porous gelatin scaffolds. *J Mater Sci,* 51**,** 4349-57.
VAN VLIERBERGHE, S., CNUDDE, V., DUBRUEL, P., MASSCHAELE, B., COSIJNS, A., PAEPE, I. D., JACOBS, P. J., HOOREBEKE, L. V., REMON, J. P. & SCHACHT, E. 2007. Porous gelatin hydrogels: 1. Cryogenic formation and structure analysis. *Biomacromolecules,* 8**,** 331-7.
VAN VLIERBERGHE, S., DUBRUEL, P. & SCHACHT, E. 2011. Biopolymer-based hydrogels as scaffolds for tissue engineering applications: a review. *Biomacromolecules,* 12**,** 1387-408.
VANDERBURGH, J., STERLING, J. A. & GUELCHER, S. A. 2017. 3D Printing of Tissue Engineered Constructs for In Vitro Modeling of Disease Progression and Drug Screening. *Ann Biomed Eng,* 45**,** 164-79.
VELNAR, T., BAILEY, T. & SMRKOLJ, V. 2009. The wound healing process: an overview of the cellular and molecular mechanisms. *J Int Med Res,* 37**,** 1528-42.
VENTOLA, C. L. 2014. Medical Applications for 3D Printing: Current and Projected Uses. *P&T,* 39**,** 704-11.
VERNIEKS, A. A. & MESSER, L. B. 1978. Calcium hydroxide induced healing of periapical lesions: a study of 78 non-vital teeth. *J Br Endod Soc,* 11**,** 61-9.
VICENTE-MANZANARES, M., WEBB, D. J. & HORWITZ, A. R. 2005. Cell migration at a glance. *J Cell Sci,* 118**,** 4917-9.
WANG, X., THIBODEAU, B., TROPE, M., LIN, L. M. & HUANG, G. T. J. 2010. Histologic Characterization of Regenerated Tissues in Canal Space after the Revitalization/Revascularization Procedure of Immature Dog Teeth with Apical Periodontitis. *J Endod,* 36**,** 56-63.
WATT, R. G., STEELE, J. G., TREASURE, E. T., WHITE, D. A., PITTS, N. B. & MURRAY, J. J. 2013. Adult Dental Health Survey 2009: implications of findings for clinical practice and oral health policy. *Br Dent J,* 214**,** 71-5.
WHITE, D., PITTS, N., STEELE, J., SADLER, K. & CHADWICK, B. 2011. 2: Disease and related disorders – a report from the Adult Dental Health Survey 2009
WITHERSPOON, D. E. & HAM, K. 2001. One-visit apexification: technique for inducing root-end barrier formation in apical closures. *Pract Proced Aesthet Dent,* 13**,** 455-60; quiz 462.
WITHERSPOON, D. E., SMALL, J. C., REGAN, J. D. & NUNN, M. 2008. Retrospective analysis of open apex teeth obturated with mineral trioxide aggregate. *J Endod,* 34**,** 1171-6.
WOHLER'S. 2013. *Wohlers Report 2013 Reveals Continued Growth in 3D Printing and Additive Manufacturing* [Online]. Wohler's Associates. Available: https://wohlersassociates.com/press59.html [Accessed 20/6 2017].

WOODFIELD, T. B. F., MALDA, J., DE WIJN, J., PÉTERS, F., RIESLE, J. & VAN BLITTERSWIJK, C. A. 2004. Design of porous scaffolds for cartilage tissue engineering using a three-dimensional fiber-deposition technique. *Biomaterials,* 25**,** 4149-61.

WOZNIAK, M. A. & KEELY, P. J. 2005. Use of three-dimensional collagen gels to study mechanotransduction in T47D breast epithelial cells. *Biol Proced Online,* 7**,** 144-61.

YAMAUCHI, N., NAGAOKA, H., YAMAUCHI, S., TEIXEIRA, F. B., MIGUEZ, P. & YAMAUCHI, M. 2011a. Immunohistological Characterization of Newly Formed Tissues after Regenerative Procedure in Immature Dog Teeth. *J Endod,* 37**,** 1636-41.

YAMAUCHI, N., YAMAUCHI, S., NAGAOKA, H., DUGGAN, D., ZHONG, S., LEE, S. M., TEIXEIRA, F. B. & YAMAUCHI, M. 2011b. Tissue Engineering Strategies for Immature Teeth with Apical Periodontitis. *J Endod,* 37**,** 390-97.

YANG, G., XIAO, Z., LONG, H., MA, K., ZHANG, J., REN, X. & ZHANG, J. 2018. Assessment of the characteristics and biocompatibility of gelatin sponge scaffolds prepared by various crosslinking methods. *Sci Rep,* 8**,** 1616.

YASSEN, G. H., CHU, T. M., ECKERT, G. & PLATT, J. A. 2013. Effect of medicaments used in endodontic regeneration technique on the chemical structure of human immature radicular dentin: an in vitro study. *J Endod,* 39**,** 269-73.